Cosmochrony: A Structurally Constrained Pre-Geometric Framework for Emergent Physics

Jérôme Beau[1*]

[1*]Independent Researcher, France.

Corresponding author(s). E-mail(s): jerome.beau@cosmochrony.org;

Abstract

Cosmochrony is a pre-geometric relational framework in which time, spacetime geometry, and physical observables emerge from the irreversible relaxation of a single underlying substrate, denoted χ. The framework adopts a principle of ontological minimalism, postulating no fundamental spacetime, metric, or quantum structure. Instead, effective geometric, dynamical, and quantum descriptions arise only through coarse-grained, generally non-injective projections of admissible χ configurations.

Within this approach, temporal ordering is identified with intrinsic monotonic relaxation, while spatial relations and curvature emerge as effective summaries of relational and spectral correlations. Bounded-response regimes naturally arise from saturation of relational relaxation fluxes, leading to Born–Infeld-like effective dynamics without introducing additional fundamental fields. In this context, the speed of light and Planck's constant are interpreted as complementary bounds on projectability and resolvability, rather than as primitive constants.

Matter, inertia, and electric charge are described as stable or metastable invariants of the χ relaxation dynamics, associated with localized excitations and topological constraints of the projected description. Quantum indeterminacy, entanglement, and violations of Bell inequalities are interpreted as structural consequences of non-injective projection, without invoking superluminal influences or fundamental wavefunction collapse.

At macroscopic scales, gravitation is treated as a collective effect of inhibited relaxation, recovering general-relativistic phenomenology in appropriate regimes. At galactic and cosmological scales, the same saturation mechanism provides an effective interpretation of flat galaxy rotation curves and environment-dependent Hubble parameter inference, without invoking dark matter particles or a fundamental dark energy component.

Cosmochrony is presented as a unifying structural framework rather than a complete replacement for established physical theories. Its primary role is to clarify how time, geometry, quantum phenomena, and large-scale cosmological behavior

may consistently emerge from a common pre-geometric relational substrate, and to organize a set of testable effective predictions developed in companion works.

Keywords: Pre-geometric substrate, emergent spacetime, relational dynamics, Born–Infeld dynamics, spectral geometry, quantum non-injectivity

Contents

Part I
Foundations

This part establishes the conceptual and ontological foundations of the Cosmochrony framework. Its purpose is to state explicitly the minimal assumptions from which all subsequent developments follow, without presupposing spacetime, geometry, or quantization as fundamental primitives.

We introduce the pre-geometric relational substrate χ, clarify its ontological status, and define the structural principles governing its admissible configurations. Central notions such as non-injective projection, bounded relaxation, intrinsic ordering, and effective projectability are defined in a canonical manner and will be used throughout the document without repetition.

Effective geometric, dynamical, and temporal descriptions are shown to arise only within restricted projective regimes. This part therefore serves as the reference layer for all later physical interpretations, formal developments, and phenomenological applications.

1 Introduction and Motivation

Modern fundamental physics is built upon two highly successful yet conceptually distinct frameworks: quantum mechanics and general relativity [1, 2]. Quantum theory accurately describes microscopic phenomena, while general relativity provides a geometric account of gravitation and spacetime dynamics at macroscopic and cosmological scales. Despite their empirical success, these theories rely on incompatible foundational assumptions and resist unification within a single coherent conceptual framework [3–5].

A central difficulty underlying this tension concerns the status of spacetime itself. In general relativity, spacetime geometry is dynamical and responds to matter, yet it remains the arena within which all physical processes are formulated. In quantum theory, time is treated as an external parameter, while spatial locality is assumed as a primitive input. These roles are difficult to reconcile in regimes where spacetime itself is expected to emerge or lose operational meaning, such as near cosmological origins or in strongly quantum gravitational settings.

It is important to emphasize that this tension does not, by itself, require spacetime to have a temporal origin. Scenarios in which spacetime is eternal, cyclic, or undergoes conformal transitions remain logically and physically consistent. The difficulty addressed here is therefore not the existence of spacetime, but the explanatory sufficiency of spacetime-based descriptions for accounting for their own structural properties.

Any attempt to account for the emergence, persistence, or breakdown of spacetime descriptions faces a conceptual constraint: spacetime cannot, on its own, provide a complete account of the conditions under which its notions of time, causality, locality, and dynamics become meaningful. Descriptions that presuppose temporal evolution, spatial propagation, or geometric structure are necessarily limited when used to explain how such notions arise or cease to apply. This suggests that spacetime, even if taken as fundamental or eternal, may not be explanatorily self-sufficient.

A closely related motivation concerns a broad class of phenomena commonly described as emerging from the vacuum. In contemporary quantum field theories, effects such as zero-point energies, vacuum fluctuations, virtual processes, and renormalized self-energies are routinely invoked to account for observable phenomena. While these constructs are operationally successful, they raise a conceptual tension similar to that encountered for spacetime itself.

If physical observables are defined entirely within spacetime-based descriptions, then entities attributed to the vacuum cannot originate from observable degrees of freedom alone. Their explanatory role therefore implicitly points toward a deeper level of description, one that is not itself accessible as a physical observable.

From this standpoint, the vacuum should not be regarded as a physically populated medium, but as a manifestation of structural limitations of the effective description. Apparent vacuum-related phenomena then signal the presence of unresolved degrees of freedom associated with a non-observable, infra-physical, and pre-geometric level of description.

This observation reinforces the need for a framework in which both spacetime structure and vacuum-related effects arise as effective concepts, emerging from the same underlying constraints. The question is therefore not what fills the vacuum, but what structural conditions render such effective descriptions necessary in the first place.

From this perspective, the problem of unification is not merely one of combining dynamical laws within spacetime, but of identifying at least one additional level of description from which spacetime, causality, and dynamical evolution can appear as effective concepts. Such a level need not provide an ultimate origin of physical reality. Its role is more modest: to supply the minimal structural conditions required for spacetime-based descriptions to be applicable at all.

The framework developed in this work, referred to as *Cosmochrony*[1], is motivated by this requirement. It explores whether the emergence of spacetime geometry, gravitation, and quantum phenomena can be understood as consequences of deeper structural constraints, without assuming spacetime itself to be explanatorily complete. At this stage, no specific realization of such a structure is assumed.

The present introduction is therefore concerned exclusively with the *necessity* of a pre-geometric level of description. The definition of the underlying entity, its ontological status, and the minimal assumptions governing its admissible descriptions are introduced systematically in Section 2.

Cosmochrony does not aim to replace the Standard Model or general relativity in their empirically validated domains, nor does it claim to provide a final unification of quantum theory and gravitation. It offers an exploratory and internally coherent framework designed to clarify why notions such as time, geometry, gravitation, and quantum correlations may require a common explanatory level beyond spacetime-based descriptions.

1.1 The Unification Problem

Quantum mechanics and general relativity differ not only in their mathematical formalisms but also in their foundational concepts. Quantum theory is intrinsically probabilistic, relies on a fixed causal structure, and treats time as an external parameter [1, 6]. General relativity describes gravitation as the dynamics of spacetime geometry itself, with time acquiring a coordinate-dependent and observer-relative status [2, 3].

This conceptual mismatch becomes acute in regimes where both quantum effects and strong gravitational fields are relevant, such as near spacetime singularities or in the early universe [7, 8]. Direct attempts to quantize gravity encounter persistent difficulties, including the problem of time, non-renormalizability, and the absence of a preferred background structure. These difficulties suggest that the tension may reflect a deeper incompatibility in the assumed ontological status of time and geometry.

Several major research programs have sought to address these challenges. Quantum field theory in curved spacetime accounts for particle creation and vacuum effects but retains a classical spacetime background [4]. Canonical and covariant approaches to quantum gravity attempt to quantize spacetime geometry itself, often at the cost of substantial mathematical complexity and interpretational ambiguity. String theory introduces extended fundamental objects and higher-dimensional structures, offering deep mathematical unification but leading to a large space of possible low-energy realizations [5]. While internally rich, these approaches face ongoing challenges concerning

[1] From $\kappa\acute{o}\sigma\mu o\varsigma$ and $\chi\rho\acute{o}\nu o\varsigma$, denoting a framework in which cosmic structure and temporal ordering are treated as emergent.

empirical testability and the physical interpretation of their fundamental degrees of freedom.

These limitations motivate the exploration of alternative perspectives in which spacetime geometry, matter, and quantum behavior emerge from a common underlying mechanism operating at a pre-geometric level.

1.2 Minimalism as a Guiding Principle

The framework developed in this work adopts minimalism as a guiding principle. Rather than introducing multiple fundamental fields, additional dimensions, or independent quantization rules, we explore whether a single continuous fundamental entity can account for temporal ordering, spatial relations, and quantum features within a unified relational dynamics.

The quantity χ is not interpreted as a conventional matter field, nor as a component of spacetime geometry. It represents a pre-geometric substrate whose irreversible relaxation underlies the emergence of both duration and separation. In this view, time and space are not independent primitives but complementary aspects of a single dynamical process. Effective geometric and quantum descriptions arise only through coarse-grained, generally non-injective projections of the underlying χ-configurations.

1.3 Time, Irreversibility, and Cosmological Expansion

A central motivation for the Cosmochrony framework is the close connection between time, irreversibility, and cosmological expansion. In standard cosmology, expansion is described kinematically through the scale factor, while the arrow of time is typically attributed to boundary conditions or entropy growth [7–9].

In Cosmochrony, the monotonic relaxation of χ provides a unified origin for both phenomena. Irreversibility follows directly from the intrinsic directionality of the relaxation process, while cosmological expansion is interpreted as its large-scale geometric manifestation in the effective, projected description. Expansion does not require an externally imposed energy component but arises as an emergent consequence of the underlying pre-geometric dynamics. In the effective description, this manifestation is encoded geometrically as a large-scale compensatory response to sustained relational relaxation.

1.4 Conceptual Context and Related Approaches

The idea that spacetime geometry and gravitation may be emergent has been explored in a variety of contemporary theoretical frameworks. Several approaches interpret the spacetime metric as an effective description arising from deeper geometric, informational, or dynamical structures, and recast gravitation as a collective phenomenon [10, 11]. Cosmochrony belongs to this broad conceptual lineage while adopting a deliberately minimalist ontological stance: a single pre-geometric relational substrate χ, whose irreversible relaxation governs the emergence of physical observables.

Like Loop Quantum Gravity (LQG), Cosmochrony holds that spacetime geometry is not fundamental [5]. However, the two frameworks operate at distinct explanatory levels. LQG provides a quantized description of geometry once a spacetime structure is

already assumed, encoding areas and volumes through spin networks and holonomies. Related ideas have also appeared in modern holographic approaches formulated in asymptotically flat spacetimes, such as celestial holography, where scattering amplitudes are reorganized as conformal correlators on the celestial sphere [12]. These approaches reformulate or quantize geometric degrees of freedom, but do not address the origin of spacetime geometry itself.

Beyond frameworks centered on the quantization or reformulation of geometry, several recent proposals have emphasized that specific physical entities or processes may not admit a fully spacetime-embedded description. In particular, arguments based on null worldlines in relativistic kinematics have motivated interpretations in which photons are described as experiencing no proper time between emission and absorption, leading to conceptual models in which light is treated as effectively atemporal or as residing outside the standard spacetime description [13]. Other approaches have similarly explored descriptions in which physical objects are interpreted as stable modal or vibrational structures of an underlying substrate, with spacetime notions emerging only at an effective level.

While these perspectives share with Cosmochrony the motivation to question the fundamental status of spacetime and time, they differ at a structural level. In Cosmochrony, the pre-geometric substrate is neither static nor timeless in a kinematic sense. Instead, it is characterized by an intrinsic and irreversible relaxation process, from which temporal ordering and dynamical notions arise only at the level of effective, projected descriptions. The emphasis is therefore not placed on the atemporality of specific entities, nor on the postulation of an underlying field or substrate with prescribed dynamics, but on the finite projectability and bounded relaxation of relational structure.

Cosmochrony thus addresses an earlier and more primitive explanatory level. It neither quantizes geometry nor posits timeless physical entities as fundamental. Rather, it seeks to explain how geometric and temporal notions themselves arise as effective, coarse-grained descriptions of underlying χ-configurations. The emergence of spacetime is mediated by a non-injective projection from the pre-geometric substrate to effective observables, allowing geometric, dynamical, and quantum features to appear only once specific relational and spectral conditions are met. From this perspective, Cosmochrony does not compete with LQG or related frameworks but conceptually precedes them, aiming to account for the physical origin of the geometric and temporal degrees of freedom that may subsequently be treated within spacetime-based or quantized descriptions.

1.5 Scope and Limitations

The aim of this work is exploratory rather than definitive. Cosmochrony does not seek to replace established theories within their empirically validated domains, but to offer a coherent reinterpretation that may clarify persistent conceptual difficulties concerning time, geometry, and quantization. Emphasis is placed on internal consistency, conceptual clarity, and qualitative contact with observable phenomena, while openly acknowledging open questions and limitations.

1.6 Structure of the Paper

The paper is organized in five parts. Part I introduces the χ substrate, its minimal structural properties, and its ontological status (Section 2). Part II develops the effective dynamics of χ (Section 3), the emergence of particle-like excitations (Section 4), and the projection fiber with gauge emergence (Section 5). Part III addresses gravity as a collective effect (Section 6) and cosmological implications (Section 7). Part IV presents the unified treatment of quantum phenomena, entanglement, and the relation to quantum formalism (Section 8). Part V collects radiation and quantization (Section 9), the spectral mass spectrum (Section 10), testable predictions (Section 11), and the discussion with conclusion (Section 12). Appendices A–G provide mathematical foundations, conceptual extensions, cosmological and numerical supplements, and a glossary of notation.

2 The χ Substrate: Definition, Properties, and Ontology

This section introduces the single fundamental entity at the core of Cosmochrony: the pre-geometric relational substrate χ. We identify the minimal structural properties required for effective descriptions of spacetime, dynamics, and physical observables to arise in appropriate regimes, and we clarify the ontological status of χ and its relation to emergent physical quantities.

No spacetime manifold, metric structure, or background geometry is assumed. Geometric and dynamical notions are recovered only through non-injective, coarse-grained projections of χ configurations once suitable stability conditions are met. This minimality principle, referred to as a regime of *ontological poverty*, is adopted as a foundational constraint.

2.1 Definition of the χ Field

We define the existence of a single pre-geometric relational substrate, denoted χ, which constitutes the primitive ontological basis of physical reality. The quantity χ is not defined on a pre-existing spacetime manifold and does not presuppose any metric, causal, or geometric structure. Spacetime notions arise only as effective descriptions of the relational, spectral, and dynamical properties of χ configurations.

Ontologically, χ is not a scalar order parameter and does not possess local values. Scalar order parameters arise only at the effective level, as coarse-grained descriptors of projected χ configurations once a geometric regime is established. Dimensional quantities associated with length, duration, or mass arise only when χ configurations admit a stable geometric interpretation. The monotonic ordering intrinsic to χ configurations gives rise, upon projection, to what is operationally perceived as temporal flow.

Temporal ordering and spatial separation are not fundamental primitives but arise respectively from the intrinsic ordering of χ configurations and from their relational structure once a quasi-stable geometric regime is reached. Effective time corresponds to ordering, while space corresponds to relational structure.

The analogy with thermodynamic order parameters applies only at the effective level: χ itself is not an order parameter but gives rise to effective order parameters once projected. The substrate χ therefore provides the minimal ontological basis from which time, space, inertial mass, gravitation, and quantum phenomena jointly emerge as harmonics of a single irreversible relaxation process.

Further interpretative clarifications and the fully relational formulation of χ are provided in Appendix C.1 and Appendix F.1.

2.2 The Geometric Effective Description of χ Dynamics

Effective Observables from χ Correlations

Quantities conventionally described in geometric terms—such as time intervals, spatial separation, and causal ordering—arise as effective summaries of relational patterns within the χ substrate, accessed only through projected, coarse-grained representations. The configurations σ represent internal relational states of χ and are defined without

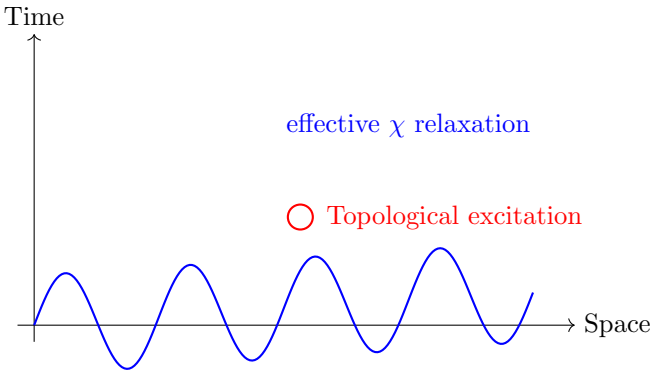

Fig. 1 Conceptual representation of Cosmochrony. An effective spacetime depiction of the projected scalar description of χ, used for visualization purposes only. The monotonic relaxation of χ gives rise to an effective temporal ordering, while localized topological excitations correspond to particle-like configurations in the emergent geometric regime.

reference to external spacetime coordinates. The measure $d\mu(\sigma)$ denotes an invariant integration over configuration space, defined intrinsically from the correlation structure associated with χ.

Effective scalar descriptor.

In regimes where projected χ configurations admit a stable geometric interpretation, we introduce an *effective scalar descriptor* χ_{eff}. This quantity is a coarse-grained, projected representation of relational and spectral features of χ, defined only within the emergent spacetime description. It does not correspond to the fundamental substrate itself.

Operational time intervals are defined from the accumulated ordering of projected configurations along paths in configuration space:

$$\tau_{AB} \;\propto\; \int_{\gamma_{AB}} \mathcal{D}_\lambda \chi_{\text{eff}}\, d\lambda, \tag{1}$$

where $\mathcal{D}_\lambda \chi_{\text{eff}}$ is an effective relaxation functional and λ an ordering parameter.

Operational spatial separation is quantified by the decay of correlations between effective descriptors:

$$d(x,y) \;\propto\; -\log\!\left(\frac{\langle \chi_{\text{eff}}(x)\, \chi_{\text{eff}}(y)\rangle}{\langle \chi_{\text{eff}}^2\rangle}\right), \tag{2}$$

where $\langle \chi_{\text{eff}}(x)\, \chi_{\text{eff}}(y)\rangle$ denotes an effective correlation functional encoding relational proximity between projected configurations x and y.

Effective Metric as a Descriptive Tool

In regimes where projected configurations exhibit smooth and stable correlation patterns, the relational observables may be summarized by an operational tensor $g_{\mu\nu}[\chi_{\text{eff}}]$. This effective metric is a derived descriptor summarizing relational correlations, not a

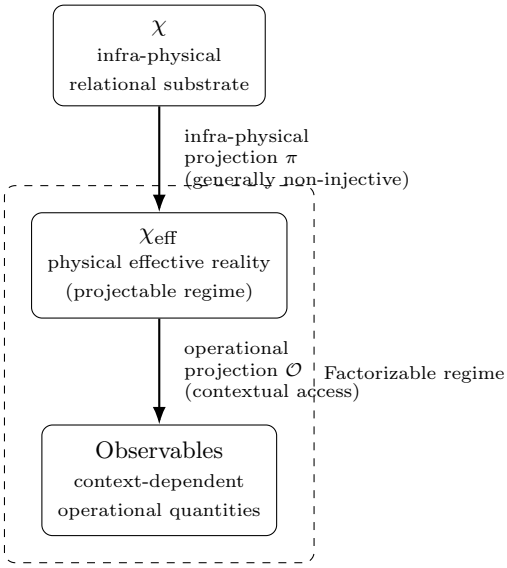

Fig. 2 Ontological pipeline in Cosmochrony. The infra-physical projection π maps the fundamental χ substrate to an effective physical reality χ_{eff} in projectable regimes, generally in a non-injective manner. Physical observables arise from an operational projection $\mathcal{O}$ that specifies how χ_{eff} is accessed under measurement contexts.

fundamental geometric structure. No background $\eta_{\mu\nu}$ is assumed; Minkowski space appears only as an effective approximation in weak-gradient regimes.

In projectable regimes admitting a low-dimensional embedding, one may write locally

$$d(i,j)^2 \;\approx\; g_{\mu\nu}(x)\,\Delta x^\mu \Delta x^\nu.$$

The continuum line element ds^2 is therefore a derived descriptive construct.

Consistency with General Relativity

The effective metric reproduces the phenomenology of general relativity in appropriate regimes: the weak-field limit yields Einstein-like dynamics; near localized χ excitations, the metric encodes time dilation and spatial curvature as emergent consequences of inhibited relaxation; homogeneous relaxation yields an effective Hubble-like expansion law. All predictive content resides in the underlying χ dynamics.

Operational origin of the effective metric.

The explicit construction of $g_{\mu\nu}$ from operational distances is given in Appendix E, where geometric quantities are shown to arise only in projectable regimes admitting a smooth continuum approximation.

2.3 Physical Interpretation

In regimes where the infra-physical projection from χ to an effective description χ_{eff} yields a factorisable structure, an approximate decomposition into subsystems and the

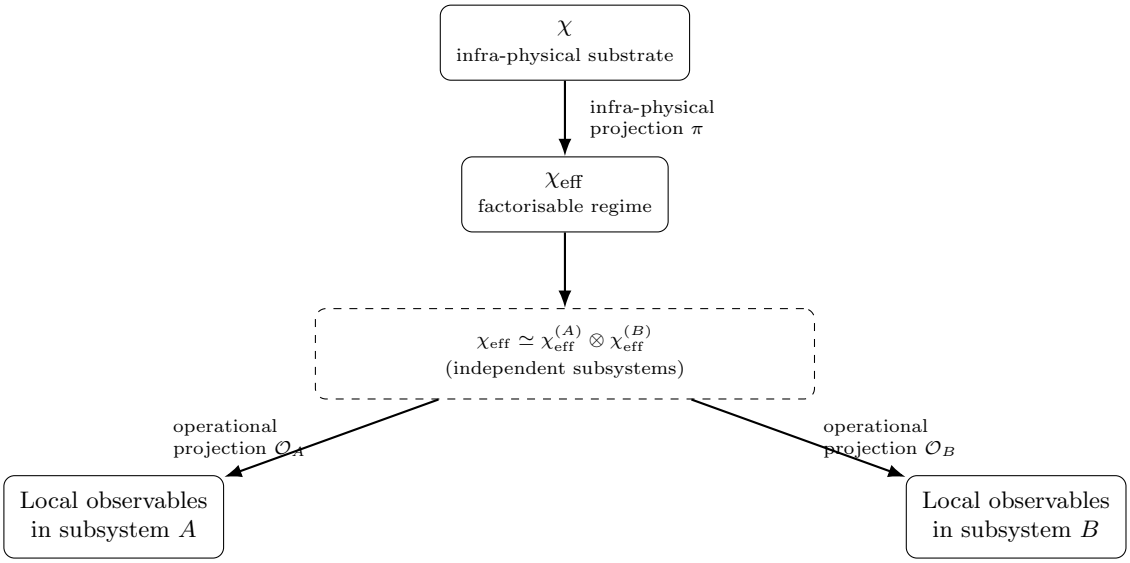

Fig. 3 Classical (factorisable) regime. After the infra-physical projection π, the effective description admits an approximate decomposition into independent subsystems. Operational projections then yield compatible local observables, recovering standard classical descriptions. This contrasts with the non-factorisable regimes discussed in Section 8.

definition of operational observables become possible. This factorisation underlies the emergence of classical locality, compatibility of measurements, and standard relativistic descriptions, as illustrated in Fig. 3.

Because the projection from χ to χ_{eff} is generically non-injective, distinct χ configurations may correspond to identical effective descriptions, while a single underlying configuration may admit multiple correlated operational realizations. This structural asymmetry is central to the emergence of both classical and quantum phenomenology. The physical content of the theory resides entirely in the dynamics of the fundamental substrate, while spacetime notions function as emergent, context-dependent descriptive tools.

2.4 Relational Projection and Spectral Admissibility

Admissible physical descriptions are defined by the spectral structure of the relational substrate χ, together with compatibility constraints imposed by the current effective state U.

Relational operator.

Let $\mathcal{H}_\chi$ denote the configuration space of admissible χ states. We introduce a relational operator

$$L_\chi : \mathcal{H}_\chi \to \mathcal{H}_\chi, \tag{3}$$

defined purely in terms of χ correlations. In discrete implementations (Appendix D), L_χ reduces to a graph Laplacian; in the continuum limit, it defines an effective self-adjoint operator encoding relational connectivity.

Spectral decomposition.

The operator L_χ admits a spectral decomposition

$$L_\chi \psi_n = \lambda_n \psi_n, \tag{4}$$

where $\{\lambda_n\}$ are non-negative eigenvalues and $\{\psi_n\}$ the associated eigenmodes.

Admissibility as constrained spectral filtering.

Projectable configurations are selected by a spectral filter acting on L_χ, subject to a compatibility condition with the effective state U. The infra-physical admissibility operator is defined as a selective projection

$$\Pi_{\lambda_*} : \mathcal{H}_\chi \rightrightarrows \mathcal{H}_{\text{eff}}, \qquad \Pi_{\lambda_*} \equiv f\left(\frac{L_\chi}{\lambda_*}\right), \tag{5}$$

where $f(x)$ is a fixed, smooth cutoff function satisfying $f(x) \to 0$ for $x \ll 1$ and $f(x) \to 1$ for $x \gg 1$. The scale λ_* sets the spectral threshold separating projectively admissible from non-admissible relational modes. The correspondence symbol emphasizes that Π_{λ_*} does not define a single-valued map, but selects admissible equivalence classes of effective descriptions.

Non-injectivity and equivalence classes.

The projection Π_{λ_*} is intrinsically non-injective. Distinct relational configurations sharing identical spectral content below the cutoff λ_* are identified into the same projected equivalence class, provided they remain compatible with the current effective state U. This structural non-injectivity—formalized here at the spectral level—constrains the class of admissible projected regimes and underpins the emergence of quantum correlations, internal degrees of freedom, and measurement processes developed in subsequent sections.

2.5 Structural Principles and Projective Regimes

All effective physical observables arise through a relational projection Π from the underlying configuration space Ω of the χ substrate. Effective descriptions are constrained by three structural principles that govern the admissibility of projected regimes.

Principle I: Substratic Locality and Bounded Relaxation.

The fundamental relaxation dynamics of χ is strictly local and subject to universal bounds. The transport of relational relaxation admits a maximal admissible flux, constraining the rate at which structural information can be redistributed. This bound arises from the intrinsic stability conditions of χ itself.

Principle II: Non-Injective Projective Realization.

The projection $\Pi : \Omega \to O$ from substratic configurations to effective observables is generically non-injective. Distinct configurations of χ may be structurally identified at the level of observable descriptions. This implies that effective descriptions need not admit a factorisable or locally complete representation, even when the underlying dynamics remains strictly local.

Principle III: Projective Compensation.

Whenever Π fails to resolve the full relational complexity of χ, effective descriptions compensate through the inflation of effective parameters—temperature, curvature, horizon structure—encoding unresolved relational structure within a reduced descriptive framework. These quantities function as Lagrange multipliers, not as additional fundamental degrees of freedom.

Together, these principles delineate distinct projective regimes. When the projection is approximately injective and relaxation is far from saturation, standard local and geometric descriptions apply. Near structural saturation or strong non-injectivity, effective parameters grow large, signaling the breakdown of spacetime-based descriptions.

2.6 Monotonicity and Arrow of Time

A central structural postulate is that the relational substrate χ admits an intrinsic, globally ordered relaxation structure. In effective descriptions, this ordering manifests as the monotonic behavior of the projected scalar descriptor along admissible ordering paths:

$$\mathcal{D}_\lambda \chi_{\text{eff}} \geq 0. \tag{6}$$

Here λ denotes an ordering parameter associated with relaxation, not a fundamental time coordinate. The inequality is a structural constraint on admissible projected representations.

Energy is interpreted as the remaining capacity of projected configurations to undergo further relaxation. Admissible ordering paths exclude any effective decrease of χ_{eff}, which would correspond to a restoration of relaxation capacity incompatible with the underlying ordering structure. The arrow of time is identified with this directional ordering: the progression from configurations with greater relaxation capacity toward configurations in which that capacity has been exhausted. This temporal orientation arises prior to any statistical or thermodynamic description [8, 14]. The relation to thermodynamic irreversibility is discussed further in Section 7.8.

Projectability and Kinematic Saturation.

A change of velocity corresponds to a modification of the relational coherence constraints maintained by the projection. As velocity increases, the informational demand on the projection grows, progressively saturating its capacity. The bound c_χ is a structural limit beyond which no stable and globally consistent projection can be maintained. Approaching saturation, part of the relational content of χ becomes inaccessible to the effective description, manifesting as time dilation, length contraction, and horizon

formation. Relativistic kinematics thus emerges as a consequence of finite projection capacity[2].

Planck Scale and Relativistic Bounds as Projection Limits.

The constants c and h are interpreted as complementary manifestations of a finite resolution of the projection from χ to effective observables. The bound c limits the maximal admissible rate at which relational ordering can be projected, while h sets a lower bound on the granularity with which the relational flux can be resolved. Relativistic and quantum constraints thus emerge as complementary facets of a single structural limitation: the finite capacity and resolution of the projection.

2.7 Local Relaxation Speed

The effective local ordering rate associated with projected χ configurations is bounded. In effective geometric descriptions, this constraint takes the form

$$|\mathcal{D}_{\mathrm{loc}}\chi_{\mathrm{eff}}| \leq c, \tag{7}$$

where $\mathcal{D}_{\mathrm{loc}}\chi_{\mathrm{eff}}$ denotes an effective local relaxation functional. This inequality limits the maximal rate at which effective causal connectivity can be established within admissible descriptions. The quantity c characterizes the causal structure of the projected regime.

Local particle propagation, signal transmission, and field interactions are all constrained by this bound in effective spacetime descriptions. Apparent superluminal recession velocities at cosmological scales arise from cumulative global effects of projected ordering and do not violate this local causal constraint.

2.8 Relation to Conventional Fields

Effective descriptions derived from projected χ configurations may formally resemble scalar or tensor fields used in cosmology and particle physics. This resemblance reflects the emergence of a spacetime-based descriptive language, not the presence of an additional fundamental field.

Energy and quantization are not fundamental attributes of χ but arise at the effective level as consequences of the non-injective projection. Matter, radiation, and interactions correspond to effective degrees of freedom arising from structural constraints, spectral organization, and long-lived relational patterns of projected configurations. Standard Model fields are recovered as accurate effective descriptions within the appropriate coarse-grained regimes.

Cosmochrony does not extend the Standard Model by introducing new fundamental fields. It provides an ontological explanation for the emergence, applicability, and structural properties of effective field descriptions themselves.

[2]This kinematic saturation concerns the ordering and coherence capacity of the projection itself and should not be conflated with thermodynamic entropy production.

2.9 Initial Conditions and Global Structure

The framework does not postulate initial conditions in the conventional temporal sense. It assumes that χ admits a minimal admissible ordering state, denoted χ_0, defining a structural boundary of admissible projected descriptions. This state does not correspond to a distinguished moment in time but to the earliest configurations for which an effective ordering interpretation becomes meaningful.

In effective geometric regimes, the characteristic scale near χ_0 coincides numerically with the Planck scale. This correspondence reflects the breakdown of projectability below this regime, not the presence of a fundamental cutoff or underlying discreteness.

Cosmic history is interpreted as the progressive and irreversible ordering of projected configurations away from this minimal admissible boundary. No spacetime singularity is required at the fundamental level. Apparent singular behavior arises only when classical notions are extrapolated beyond the regime in which projected configurations admit a stable geometric interpretation.

Ontological poverty and the growth of admissible structure.

The minimal state χ_0 corresponds to a regime of *ontological poverty*: only a severely restricted class of simple and highly coherent configurations can be projected. As relaxation proceeds, the space of admissible configurations expands, enabling the emergence of increasingly rich, localized, and hierarchical effective structures. The global structure of admissible descriptions is constrained by the ordering properties of the underlying substrate.

2.10 Ontological Interpretation

The χ Substrate as a Pre-Temporal Relational Reservoir

The substrate χ admits an ontological interpretation as a pre-temporal relational reservoir from which spacetime, matter, and effective physical laws emerge. It is not a dynamical history, nor a prescriptive blueprint of admissible universes, but a relational support supplying a continuous flux of configurational possibilities. Temporal succession is emergent, corresponding to an oriented ordering of projected configurations under irreversible relaxation.

The term "pre-temporal" emphasizes that χ does not encode time or causal succession as primitive notions. Rather, time arises as a property of stable projected descriptions that remain mutually compatible under successive updates. No teleology, determinism, or block-universe ontology is implied: multiple effective histories may correspond to the same relational substrate through non-injective projection.

Relational Ontology and Conceptual Lineage

The relational character of χ bears a conceptual affinity with relational approaches in physics, notably those of Rovelli [5, 15], which trace part of their lineage to Aristotelian relational ontology [16, 17]. Cosmochrony shares the rejection of intrinsic, observer-independent properties but extends relationalism to a deeper ontological level: χ

configurations are not relations *between* fundamental objects but relational structures that give rise to objects only upon projection.

Relativistic causality and spacetime locality emerge without postulating spacetime as fundamental [18]. Relationality is therefore not a property of spacetime itself, but of the pre-geometric substrate whose projected stabilization yields spacetime as an effective description.

Projection, Reality, and Ontological Asymmetry

The emergence of spacetime and physical law is a *projection* from χ, not a dual or bidirectional description. The projected universe is fully real at the level of physical experience, but ontologically derivative: spacetime entities and dynamical laws do not possess ontological primacy.

While all physical descriptions depend on the projection of χ, the admissibility of a given projection is constrained by the compatibility of the update with the current effective state U. This introduces an ontological asymmetry: χ supplies configurations, whereas U restricts which projected descriptions can remain stable under successive updates.

Apparent fine-tuning is thus reinterpreted as a projective selection effect: only those updates preserving the coherence of an effective state appear as physically realized universes. Cosmochrony does not postulate a multiverse; the universe is unique at the level of physical reality, even though its relational description in terms of χ is non-unique.

Formal developments related to projection, including its fiber-bundle formulation and the emergence of gauge interactions, are developed in Section 5.

Configurational State Structure

The substrate χ defines a configurational space of relational structures and an irreversible flux of candidate configurations. It does not prescribe a fixed set of admissible macroscopic states. Physical reality corresponds instead to projected realizations that remain stable under finite resolution and compatibility constraints imposed by the current effective state U.

What appears as temporal evolution corresponds, at the level of χ, to an ordering of projected configurations required to maintain descriptive coherence under continuous relaxation. Universal bounds such as c_χ and $\hbar_\chi$ reflect invariant limits of the projection and update process, rather than prescriptive constraints encoded in χ itself.

Intrinsic Structural Indeterminacy

A perfectly closed and fully symmetric relational substrate would admit a static, non-updating projected description. Cosmochrony therefore assumes an *intrinsic structural openness* of χ: relational configurations are not exhaustively specified by a finite, closed set of conditions.

This indeterminacy is ontological rather than dynamical. Observable variability and probabilistic behavior arise only at the level of projected descriptions, as a consequence of non-injective projection. Randomness is therefore *projective*: it reflects

the multiplicity of effective realizations compatible with a given relational substrate and a given effective state U.

Relation to Holographic Descriptions

Cosmochrony is not a holographic theory in the technical sense. It does not posit a lower-dimensional boundary description or a dual equivalence between bulk and boundary physics. The limitation of physically accessible information within a spacetime region reflects the degeneracy of underlying χ configurations corresponding to the same effective projection, as constrained by finite resolution and compatibility.

Scaling behaviors reminiscent of holography are interpreted as emergent signatures of projection. Similarly, Cosmochrony differs from thermodynamic approaches to gravity in that it does not posit entropy or information as primitive quantities. Thermodynamic descriptions arise only at the effective level, as secondary languages applicable when projected configurations admit coarse-grained statistical interpretations.

2.11 Energy, Mass, and Fundamental Constants

Energy as Capacity for Relaxation

Energy is the effective capacity of projected χ configurations to relax unresolved structural constraints. It is not a fundamental conserved substance but an emergent quantity characterizing the degree to which a given projected configuration retains the ability to undergo further relaxation. Conservation laws arise only at the effective level, as structural regularities of projected dynamics. Without intrinsic structural indeterminacy (Section 2.10), the notion of energy would be ill-defined: a fully determined substrate would admit no unresolved tension and therefore no capacity for relaxation. The quantitative formulation is developed in Section 4.3.

Mass as Frozen Information

Localized and long-lived configurations of χ correspond to regions in which further relaxation is strongly inhibited. Such configurations trap a fixed amount of unresolved structural information, preventing it from participating in the global relaxation process. Mass represents *frozen energy*: structural information whose capacity for further relaxation has been locally suppressed[3]. Particle annihilation, decay, or radiation emission correspond to the partial or complete release of frozen structural information. The operational definition $m = E/c^2$ and its derivation from resistance to relaxation ordering are developed in Section 4.3.

Quarks as Non-Projectable Internal Modes

Quarks are not independent localized excitations but internal structural modes of composite solitonic configurations. They are required to characterize the internal organization of hadronic excitations but do not admit an autonomous projection into spacetime. Confinement reflects a structural constraint: isolated quark-like modes do not

[3]This notion of frozen structural information should be distinguished from projection-induced entropy, which quantifies loss of distinguishability under non-injective projection.

correspond to admissible standalone projections of χ_{eff}. Only collective configurations in which such internal modes are topologically and relationally closed admit a stable spacetime manifestation. Quark confinement thus appears as a direct consequence of the non-injective character of the projection.

The Role of the Universal Bound c_χ

The universal invariant bound c_χ characterizes an absolute structural limit on the degree to which relational information can be locally confined within admissible configurations of χ. It is non-metric and non-temporal: it is not associated with distances, durations, or lightcones, since none of these are defined prior to projection. The constant c_χ expresses a maximal admissible rate of structural ordering.

The effective causal constraint c observed in spacetime is the projected manifestation of c_χ:

$$c \equiv \Pi(c_\chi),$$

acquiring operational meaning only once notions of locality and causal ordering become meaningful. In strong-gravity or near-deprojection regimes, c may lose its geometric interpretation while c_χ remains invariant.

The Role of $\hbar_\chi$ and Reprojection

The parameter $\hbar_\chi$ characterizes a fundamental structural scale of χ, determined by its intrinsic relational density and constraint structure. It specifies a minimal quantum of *reprojection*: intrinsic structural information encoded in χ can enter an effective spacetime description only in discrete units set by this scale. As spacetime structure stabilizes, reprojection events become increasingly localized, manifesting phenomenologically as vacuum fluctuations.

The Origin of Planck's Constant

Within Cosmochrony, $\hbar$ is a **spectral invariant** of the relaxation and projection process. At the substrate level, the quantum of reprojection is fixed by

$$\hbar_\chi = \frac{c^3}{K_0\,\chi_c}, \tag{8}$$

where K_0 denotes the coupling density of relational constraints and χ_c the characteristic correlation scale. This relation expresses the *spectral rigidity* of the substrate.

In effective spacetime descriptions, the same scale appears as $\hbar_{\text{eff}}$, functioning as the quantum of action in Hilbert-space formulations. The apparent universality of $\hbar$ reflects the fact that K_0 and χ_c are global invariants of the current relaxation epoch. The transition from $\hbar_\chi$ to $\hbar_{\text{eff}}$ involves a change in representation, not in value.

Spectral Invariance of Planck's Constant and the Fine-Structure Constant

The fine-structure constant α emerges as a dimensionless spectral ratio, determined by the geometry of the projection fiber Π and the spectral rigidity encoded by K_0:

$$\alpha \;=\; \mathcal{F}\!\left(\frac{\text{geometry and topology of } \Pi}{K_0}\right), \tag{9}$$

where $\mathcal{F}$ is a functional fixed by the structure of admissible projections. If the structural parameters K_0 or χ_c were to vary—for example in primordial high-constraint regimes—both $\hbar$ and α would scale accordingly, preserving the internal structural coherence of the framework.

Part II
Dynamics and Particles

This part develops the effective dynamics of the χ substrate and explains how localized, long-lived excitations emerge as particle-like structures. Starting from a parameter-independent relaxation principle, we derive the effective evolution equations governing χ and identify the conditions under which stable or metastable configurations arise.

Particles are interpreted not as fundamental objects but as structured excitations of the substrate, characterized by spectral, topological, and relaxation properties. Within this framework, inertial mass, energy–frequency relations, charge, spin, and antiparticles emerge as effective attributes of projected χ configurations.

The projection fiber and its transmittance properties are then introduced, providing a unified interpretation of gauge structures and internal symmetries. This part establishes the physical content of matter and interactions prior to any gravitational or quantum description.

3 Effective Dynamics of the χ Substrate

3.1 Parameter-Independent Relaxation

Physical evolution appears only at the effective level, as an ordered sequence of projected χ configurations $(\chi_{\mathrm{eff},\lambda})$, where λ is a strictly monotonic ordering parameter labeling admissible stages of relaxation. The ordering parameter λ does not represent time; it serves as an index ordering projected configurations once a macroscopic spacetime description becomes applicable.

Admissible projected descriptions are constrained by an effective relaxation condition:

$$\mathcal{D}_\lambda \chi_{\mathrm{eff}} = \mathcal{R}[\chi_{\mathrm{eff}}], \tag{10}$$

where $\mathcal{R}[\chi_{\mathrm{eff}}]$ denotes an effective relaxation functional characterizing the ordering of projected configurations. This relation is a consistency condition on admissible projections, not a fundamental dynamical law. The functional $\mathcal{R}$ is defined only in regimes admitting a stable geometric interpretation.

Quantities commonly interpreted as temporal derivatives arise exclusively within effective descriptions. Within this framework, relaxation does not occur *in* time; the ordering of projected configurations defines what is operationally identified as physical duration.

3.2 Hamiltonian Derivation of the Evolution Equation

Once projected χ configurations admit a smooth, stable coarse-grained description, admissible local relaxation patterns may be summarized by a constraint formally analogous to a Hamiltonian condition. The effective local relaxation ordering is bounded by the invariant causal constant c:

$$\left(\mathcal{D}_{\mathrm{loc}} \chi_{\mathrm{eff}}\right)^2 + \mathcal{V}_{\chi_{\mathrm{eff}}}^2 = c^2, \tag{11}$$

where $\mathcal{V}_{\chi_{\mathrm{eff}}}$ denotes an effective internal variation functional encoding the resistance of projected configurations to further relaxation (e.g., solitonic or bound configurations).

Restricting to the monotonic ordering branch yields

$$\mathcal{D}_{\mathrm{loc}} \chi_{\mathrm{eff}} = c \sqrt{1 - \frac{\mathcal{V}_{\chi_{\mathrm{eff}}}^2}{c^2}}, \tag{12}$$

expressing the universal slowdown of effective relaxation induced by localized structural constraints.

Emergent Gravitational Description

Projected configurations exhibiting strong resistance to relaxation locally reduce the admissible effective relaxation rate. In a spacetime interpretation, this reduction is conventionally described as gravitational time dilation. No independent gravitational field is postulated.

In weak-structure regimes, the spatial distribution of relaxation slowdown admits the simplified relation

$$\nabla \cdot \left(\frac{\nabla \chi_{\text{eff}}}{\sqrt{1 - |\nabla \chi_{\text{eff}}|^2 / c^2}} \right) \simeq \frac{4\pi G_{\text{eff}}}{c^2} \rho, \tag{13}$$

where ρ denotes the effective density of localized relaxation-resistant configurations and G_{eff} is an emergent coupling parameter. In the Newtonian limit, this yields an effective Poisson equation for a potential defined operationally by

$$\Phi \equiv c^2 \ln\left(\frac{\mathcal{D}_{\text{loc}} \chi_{\text{eff}}}{c} \right). \tag{14}$$

This potential is a compact summary of how localized variations in effective relaxation modulate physical clocks and rulers.

3.3 Microscopic Origin of the Coupling Tensor and the Poisson Equation

The effective coupling governing projected χ configurations depends on the internal structural state of the projected description. A convenient phenomenological parametrization is

$$K_{\text{eff}} = K_0 \exp\left(-\frac{(\Delta \chi_{\text{eff}})^2}{\chi_c^2} \right), \tag{15}$$

where $\Delta \chi_{\text{eff}}$ measures effective internal variation, K_0 is the maximal relaxation conductivity in a homogeneous background, and χ_c sets the scale beyond which inhomogeneities suppress relaxation efficiency.

Projected configurations exhibiting strong internal variation reduce the effective coupling and locally slow the admissible relaxation ordering, providing the microscopic origin of emergent gravitational phenomenology.

An effective gravitational potential Φ may then be introduced through

$$\frac{\mathcal{D}_{\text{loc}} \chi_{\text{eff}}}{\mathcal{D}_0} \simeq 1 + \frac{\Phi}{c^2}, \tag{16}$$

summarizing the relative slowdown of effective relaxation ordering. In the weak-structure regime, the spatial distribution of Φ admits a Poisson-type relation:

$$\nabla^2 \Phi \simeq 4\pi G_{\text{eff}} \rho, \tag{17}$$

where ρ is the effective density of relaxation-resistant configurations and G_{eff} an emergent coupling parameter. Gravitation appears as a descriptive manifestation of reduced relaxation conductivity induced by structured projected configurations.

A fully relational formulation is provided in Appendix F.

3.4 Variational Formulation and Born–Infeld Action

In regimes admitting a stable geometric interpretation, the effective relaxation constraints may be summarized in a compact variational form. Motivated by Born–Infeld-type non-linear actions [19, 20], we consider the effective Lagrangian density

$$\mathcal{L}_{\text{eff}} = -c^2\sqrt{1 - \frac{|\nabla\chi_{\text{eff}}|^2}{c^2}} + \mathcal{D}_{\text{loc}}\chi_{\text{eff}} - \frac{4\pi G_{\text{eff}}}{c^2}\,\rho\,\chi_{\text{eff}}, \tag{18}$$

where $\mathcal{D}_{\text{loc}}\chi_{\text{eff}}$ is the effective local relaxation ordering (Section 3.1) and ρ the effective density of localized relaxation-resistant configurations.

The linear dependence on $\mathcal{D}_{\text{loc}}\chi_{\text{eff}}$ enforces monotonicity without additional propagating degrees of freedom. The square-root structure acts as a non-linear regulator ensuring that effective spatial variations remain bounded by c. The Euler–Lagrange equation reproduces the non-linear elliptic relation

$$\nabla\cdot\left(\frac{\nabla\chi_{\text{eff}}}{\sqrt{1 - |\nabla\chi_{\text{eff}}|^2/c^2}}\right) = \frac{4\pi G_{\text{eff}}}{c^2}\,\rho, \tag{19}$$

coinciding with the effective relation obtained in Section 3.3.

This Born–Infeld-like action is an *auxiliary variational representation*. It does not define a fundamental action principle, nor equations of motion for the χ substrate. Its purpose is to regularize the effective description, enforce universal structural bounds, and facilitate comparison with standard gravitational phenomenology.

The physical interpretation is discussed in Appendix A.1, and the mathematical consistency with the relational dynamics is established in Appendix B.14.

Connection to Emergent Geometry.

In regimes where a geometric description is applicable, the Hessian of $\mathcal{L}_{\text{eff}}$ defines an emergent metric tensor $g_{\mu\nu}$, summarizing the effective geometric regularities of projected configurations.

Why This Is Not a Scalar–Tensor Theory.

The effective scalar descriptor χ_{eff} is not a fundamental dynamical field: it does not possess intrinsic values or conjugate momenta, and does not propagate independently. No modification of the gravitational sector is postulated, no scalar–tensor coupling of the form $f(\chi_{\text{eff}})R$ is introduced, and no additional propagating modes arise. Gravitation emerges from the local inhibition of relaxation ordering, not from the exchange of a scalar mediator.

Operational saturation scale and acceleration proxy

The invariant scale b_χ bounds the maximal rate of admissible relaxation transport in the substrate χ. The kinematic bound c appearing in the square-root structure is the effective projection of this invariant relaxation limit in weak-field geometric regimes.

In projectable regimes, the effective constitutive response therefore takes a Born–Infeld-like form. Projected gradients cannot grow without bound while remaining within a smooth quasi-injective update.

In the macroscopic limit, one may introduce an operational acceleration proxy $a_\star$ marking the onset of the saturated response. Dimensional consistency and bounded transport jointly imply that this threshold must scale inversely with the local descriptive resolution ℓ of the projected state U. We therefore parametrize

$$a_\star \sim \kappa \frac{b_\chi}{\ell}, \tag{20}$$

where κ is a dimensionless normalization factor encoding the convention adopted for the projective mapping Π. The role of ℓ and its scale dependence are discussed in Section 12.10.

3.5 Schwinger Effect as a Saturation Threshold of Relaxation Flux

In standard quantum field theory, the Schwinger effect is interpreted as a vacuum instability under an electric field exceeding a critical threshold. In Cosmochrony, the Born–Infeld-type effective dynamics provides a structurally different interpretation.

The Schwinger effect corresponds to a *threshold of flux saturation*. When the imposed electric field drives the effective relaxation flux beyond what can be transported smoothly through the projection fiber, the homogeneous relaxation regime becomes unstable. The system resolves this instability by activating additional admissible modes of the projection, corresponding to the nucleation of conjugate torsional excitations—naturally identified with electron–positron pairs. As discussed in Section 4.7, such pairs preserve global torsional neutrality, ensuring charge conjugation symmetry.

Pair production thus originates from a topological reconfiguration of the projection fiber under maximal relaxation stress, not from vacuum fluctuations. Matter creation acts as a dissipation channel that restores admissibility by redistributing excess relaxation flux into stable, projectable vortical modes. This enlarges the space of admissible configurations, in accordance with the principle of monotonic growth of admissible states.

Cosmochrony therefore predicts the existence of a Schwinger-like threshold *ab initio*, without invoking the Dirac sea or field quantization. The effect emerges as a universal transition between smooth relaxation and topologically mediated dissipation.

Dissipation by structure creation.

This mechanism illustrates a more general principle: when directional relaxation fluxes approach their maximal transport capacity, admissibility is restored by creating new stable structures that enlarge the space of admissible configurations. This suggests a unified interpretation of pair-loaded astrophysical jets, primordial matter production, and ultra-high-energy excitations in extreme curvature regimes (Section 11).

3.6 Causality and Locality

Within effective descriptions, the relaxation ordering encoded by χ_{eff} exhibits locality and causality. Effective locality follows from the fact that variations of χ_{eff} at a given effective event depend only on correlated neighboring projected configurations. Causality is enforced through the universal bound

$$|\mathcal{D}_{\text{loc}}\chi_{\text{eff}}| \leq c,$$

constraining the maximal rate at which correlations between effective configurations may be established. No superluminal propagation of signals or causal influence occurs within effective descriptions. Apparent superluminal recession velocities in cosmological contexts arise from cumulative integration of locally constrained relaxation ordering over extended regions and remain consistent with effective locality.

The effective causal bound c corresponds to the projected manifestation of the invariant structural bound c_χ defined at the level of the pre-temporal substrate (Section 2.11). Effective causality arises as a derived property of bounded projective realizations.

3.7 Homogeneous Cosmological Limit

In a homogeneous and isotropic regime, projected configurations exhibit no effective spatial variations and the admissible relaxation rate attains its maximal value:

$$\mathcal{D}_{\text{loc}}\chi_{\text{eff}} = c. \tag{21}$$

Expressed in terms of an effective cosmological time parameter t, this yields

$$\chi_{\text{eff}}(t) = \chi_{\text{eff},0} + c\,t, \tag{22}$$

where $\chi_{\text{eff},0}$ is a reference value. This linear regime underlies the emergent Hubble law derived in Section 7.5.

As shown in Appendix A.6, the monotonicity requirement in an expanding regime implies a minimal residual structural inhomogeneity in projected configurations, manifesting as a non-vanishing lower bound on gravitational acceleration. This bound provides a natural route to MOND-like phenomenology without postulating dark matter particles [21, 22].

3.8 Influence of Local Structure

In regions where projected configurations exhibit non-vanishing effective structural variations, the admissible local relaxation ordering is reduced. Localized relaxation-resistant configurations—describable as particle-like solitonic structures—act as constraints on the admissible ordering of projected configurations. By increasing the effective structural complexity, they locally inhibit relaxation without introducing any additional interaction or mediator.

When a geometric description is applicable, this inhibition manifests as gravitational time dilation and spatial curvature. Gravitation arises as a collective consequence of locally constrained effective relaxation ordering.

3.9 Unified Origin of Geometric and Field Effects

The relation between the χ substrate and the effective spacetime metric $g_{\mu\nu}$ is strictly hierarchical and may be summarized in three levels. First, at the fundamental level, physical reality is described solely in terms of χ and its intrinsic relational structure. Second, in regimes where projected configurations admit a stable and slowly varying description, the spacetime metric arises as an effective descriptor summarizing correlations and relaxation ordering. Third, localized relaxation-resistant projected configurations—describable as solitonic structures—are identified with matter degrees of freedom, and gravitational phenomena correspond to local modulations of effective relaxation ordering induced by such structures.

No independent gravitational interaction or fundamental field is postulated. Matter, geometry, and gravitation emerge as complementary aspects of the same constrained ordering of projected configurations.

3.10 Limitations and Scope

Equation (12) is intentionally minimal. It constrains admissible projected descriptions in regimes where a stable geometric interpretation is applicable, but does not provide a first-principles account of quantum fluctuations or correlations at the level of χ itself. Such phenomena arise from non-injective projection and coarse-graining. Higher-order structural effects and strongly non-projectable regimes lie outside the present scope.

Within these limitations, the constrained ordering relation provides a unified kinematic backbone from which gravitational, quantum, and cosmological phenomena can be consistently recovered at the effective level. More refined treatments of effective fluctuations and extended relational structures are left for future work.

4 Particles as Localized Excitations of the χ Field

4.1 Particles as Stable Wave Configurations

Particles are not fundamental point-like entities. They arise at the level of effective descriptions as stable, localized configurations within projected χ descriptions [23]. Such configurations correspond to persistent patterns that locally constrain the admissible relaxation ordering. In effective geometric regimes, they may be described using soliton-like language. Their stability reflects localized regions in which further relaxation is strongly inhibited. Apparent particle propagation corresponds to a continuous reorganization of admissible projected descriptions, not to the motion of an object through a fundamental spacetime.

4.2 Topological Stability

The stability of particle-like excitations does not rely on fundamental conserved charges postulated *a priori*. Certain projected configurations exhibit non-trivial internal organization that prevents them from being continuously deformed into homogeneous effective descriptions without violating admissibility conditions.

This stability is topological in character: it reflects the existence of inequivalent classes of admissible projected configurations that cannot be smoothly connected through continuous reconfiguration while preserving monotonic relaxation ordering. The long-lived character of solitonic structures follows from this topological incompatibility, not from a dynamical balance of forces.

Detailed geometric constructions of topological solitons, including vortex, skyrmion, and knotted configurations, are provided in Appendix C.2. The fully relational formulation is developed in Appendix F.8.

Stability through self-consistency.

The projection Π does not operate independently of the effective description already in place, but is constrained by the current state U through a compatibility condition. Among the relational configurations supplied by the χ substrate, only those transitions $\chi_n \to \chi_{n+1}$ whose projection remains compatible with U admit a stable effective realization. In this sense, physical laws are not imposed by the substrate χ, but emerge as the only update rules supporting projective continuity across successive descriptions [24].

4.3 Mass as Resistance to χ Relaxation

Building on the ontological interpretation of mass as frozen structural information (Section 2.11), we develop the quantitative formulation. Mass emerges at the effective level as a measure of how strongly a localized projected configuration resists admissible relaxation ordering.

The effective structural energy associated with a projected solitonic configuration $\chi_{\text{eff},s}$ is

$$E[\chi_{\text{eff},s}] \equiv \int_\Sigma \left(\frac{1}{\sqrt{1 - |\nabla \chi_{\text{eff},s}|^2/c^2}} - 1 \right) d\Sigma, \tag{23}$$

where Σ denotes a hypersurface of constant effective ordering parameter and $|\nabla \chi_{\text{eff},s}|$ quantifies effective structural deformation. The inertial mass is then defined operationally as

$$m \equiv \frac{E[\chi_{\text{eff},s}]}{c^2}. \tag{24}$$

For example, the electron mass m_e reflects its topological stability as a 4π-periodic soliton (Section C.4), while the proton mass arises from a composite 3-soliton configuration.

The relation $E = mc^2$ is interpreted as a kinematic identity: mass quantifies relaxation resistance, while energy expresses the same quantity in relaxation units. The question of how distinct particle masses arise from different classes of projected configurations is addressed in Appendix C.2.

4.4 Metastability, Projection, and Particle Decay

A stable particle corresponds to a deep basin of admissible projected configurations; an unstable particle occupies a shallow or fragile basin. Particle decay is interpreted as the structural reorganization of a metastable configuration: when the concentration of constraints exceeds what can be sustained by a single projected entity, admissibility is recovered through factorization into less constrained localized configurations, possibly accompanied by weakly structured excitations.

Entanglement and decay represent two regimes of the same projection structure. Entanglement corresponds to non-factorizability without fragmentation, while decay corresponds to non-factorizability that forces fragmentation. The distinction lies in the stability properties of the projected description under admissible fluctuations.

The finite lifetime of unstable particles reflects the probability of crossing a structural reorganization threshold under admissible variations, yielding the observed exponential decay law as a statistical signature of metastability.

A more technical characterization of metastability, admissible factorization channels, and decay widths is provided in Appendix C.14.

4.5 Energy–Frequency Relation

The energy associated with a particle-like excitation is linked to a characteristic internal spectral scale of the corresponding projected configuration. Configurations associated with higher characteristic frequencies correspond to more tightly constrained structures and encode greater effective resistance to relaxation. This yields

$$E \propto \nu, \tag{25}$$

where ν characterizes the spectral scale of internal organization. Planck's constant appears as an effective proportionality factor whose universality reflects the robustness

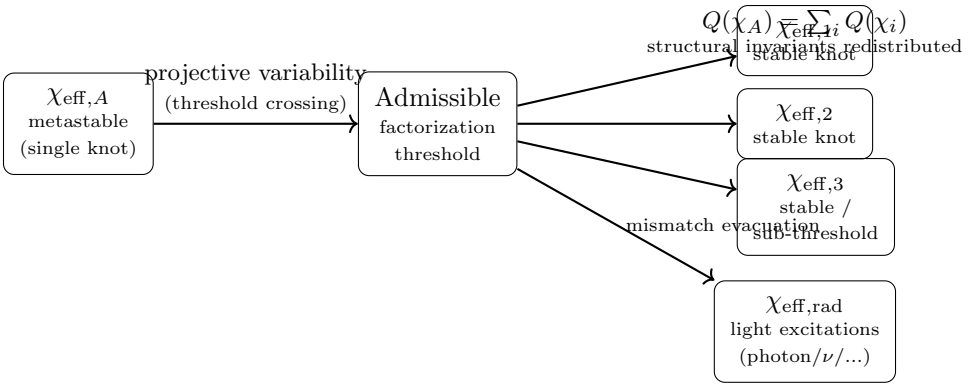

Fig. 4 Structural interpretation of particle decay. A metastable localized projected configuration transitions, via an admissible factorization threshold, into several more stable configurations plus weak excitations that evacuate the residual structural mismatch.

of spectral scales in the current relaxation epoch. A more explicit realization in the context of radiation is presented in Section 9.3.

4.6 Fermions, Bosons, and Spin

Particle statistics emerge from the topological structure of admissible projected configurations. Configurations requiring a 4π rotation to return to an equivalent projected description give rise to fermion-like behavior, while 2π-periodic configurations correspond to bosons. This distinction reflects a topological obstruction rather than a symmetry principle imposed at the fundamental level.

Spin as a Topological Property

Spin is not an intrinsic kinematic degree of freedom but a purely topological property of admissible projected configurations. Fermionic configurations require a 4π transformation in configuration space to return to an equivalent effective description, implying that the relevant configuration space admits a double covering with fundamental group

$$\pi_1(\mathcal{C}_{\mathrm{eff}}) = \mathbb{Z}_2. \tag{26}$$

When an effective quantum description is applicable, a 2π transformation induces a sign change of the associated wavefunction,

$$\psi \longrightarrow -\psi, \tag{27}$$

while a 4π transformation restores the original state. This 4π-periodicity directly implies fermionic antisymmetry and the Pauli exclusion principle, as detailed in Section F.9.

Exchanging two identical fermionic excitations corresponds topologically to a 2π loop in the combined configuration space and induces a sign change, dynamically excluding symmetric configurations [25]. The spin–statistics connection thus admits a unified topological origin within the effective descriptive framework.

4.7 Charge as a Topological and Relaxational Property of χ

Unified Relaxation Budget for Mass and Charge

Both inertial mass and electric charge draw on the same finite relaxation capacity of χ. A localized excitation mobilizes capacity in two structurally distinct channels: a scalar inhibition channel associated with inertial response (mass), and an oriented or chiral channel associated with a net topological flux (charge). Admissible projected configurations satisfy a single combined bound

$$\mathcal{B}_m[\chi] + \mathcal{B}_e[\chi] \leq \mathcal{B}_{\max}, \tag{28}$$

where $\mathcal{B}_{\max}$ is fixed by the universal relaxation capacity constraint (Section 3.4). Effective mass and charge are therefore competing manifestations of a common substrate resource, and the observed discreteness of particle masses may be approached as a classification of admissible stable configurations under a single saturation constraint.

Charge as a Directed and Conjugate Relaxation Mode

Charges arise only after projection, as stable invariants characterizing admissible projected configurations. Charge conjugation is reinterpreted as a transformation between *relationally conjugate* projected configurations: paired topological classes related by an internal reversal of relational organization, reflecting the internal duality of the projection fiber.

At the discrete level, the χ dynamics induces a bounded relaxation flux $\vec{J}_\chi \sim \nabla\chi$. Charge corresponds to the non-integrability of this flux around localized excitations: the resulting winding number defines an integer-valued topological invariant whose sign encodes chirality. Electric attraction and repulsion arise from the geometric compatibility or frustration between torsional flux patterns of neighboring excitations. The bounded nature of $\vec{J}_\chi$ implies a maximal admissible charge density and naturally removes short-distance singularities.

The robustness of this chiral–torsional invariant is tested in Appendix C.17.

CP Symmetry as Projective Chirality.

CP symmetry corresponds to a combined transformation acting on the orientation of the projection itself. When the projection is achiral, conjugate configurations are mapped symmetrically and CP is preserved. When the projection is chiral, CP is violated as a direct consequence of projective asymmetry, without introducing explicit CP-violating terms at the level of χ.

4.8 Antiparticles, Creation/Destruction, and CPT

Antiparticles as Relationally Conjugate Configurations

A particle and its antiparticle correspond to projected configurations belonging to distinct but conjugate topological classes within the space of admissible projected descriptions, related by an internal reversal of relational organization. Annihilation occurs when a particle-like configuration and its conjugate combine into a composite

description that no longer supports localized structural constraints, redistributing relational structure into delocalized radiation-like excitations. This constitutes a process of *structural unknotting*: mass itself measures the degree of topological obstruction to relaxation.

Why Antimatter Does Not Require Time Reversal.

The monotonic ordering of χ defines an absolute arrow of admissible projection that cannot be inverted. Antiparticles correspond to topologically conjugate classes, not to reversed temporal trajectories. The apparent association between antimatter and time reversal in standard formalisms is a feature of the effective representation.

Matter–Antimatter Asymmetry without Fundamental CP Violation.

If the projection from χ to effective spacetime is chiral, conjugate classes need not be realized with equal stability or projectability. Matter–antimatter asymmetry emerges as a selection effect imposed by differential projectability, without requiring dynamical CP-breaking interactions.

Particle Creation and Destruction

Particle creation corresponds to a projected configuration acquiring sufficient structural organization to support a stable topological class. Particle destruction occurs when a configuration loses its topological admissibility and admits continuous deformation toward a delocalized effective description.

CPT as a Global Projective Property

C, P, and T are individually effective and representation-dependent. Their combined action corresponds to a full relational conjugation of projected descriptions, mapping any admissible effective configuration to another admissible configuration representing the same underlying χ structure. CPT invariance is therefore not a microscopic symmetry but a global projective consistency condition ensuring that the space of admissible descriptions is closed under full relational conjugation. Violations of CPT would signal a breakdown of projectability itself.

CPT as an Admissibility Consistency Condition

Certain projected configurations carry orientation-sensitive structural invariants (chirality, phase winding, relational orientation). Under admissible factorization, these signed invariants must be redistributed, possibly requiring paired localized excitations carrying opposite orientations—interpreted as particle–antiparticle pairs. CPT symmetry reflects the invariance of admissibility under a combined reversal of signed structural invariants, effective spatial orientation, and the effective ordering parameter. A technical formulation is provided in Appendix C.16.

Why CPT Survives Quantum Gravity.

CPT survives because it expresses the minimal requirement for a coherent physical projection. Quantum gravity may challenge locality, geometry, and the notion of time,

but cannot violate CPT without undermining the possibility of a consistent emergent universe.

4.9 Neutrinos as Partially Projectable Modes

Neutrinos correspond to *partially projectable modes* of χ: configurations whose relational structure admits a stable projection in some degrees of freedom while remaining weakly or non-projectable in others. This partial projectability explains their extremely small effective masses, weak interaction strength, and sensitivity to global rather than local structural properties of the projection.

Dirac vs. Majorana Character.

A Dirac neutrino admits distinct conjugate projected realizations; a Majorana neutrino corresponds to a configuration whose partial projectability collapses the distinction between conjugate classes. The Dirac or Majorana character is not a fundamental choice but a manifestation of how fully the projection resolves relational conjugation. Lepton number conservation emerges only in regimes where conjugate configurations are distinguishable; when partial projectability erases this distinction, effective lepton number violation becomes admissible.

Neutrino Oscillations without Fundamental Mass Eigenstates.

Different flavors correspond to closely related partially projectable configurations whose internal relational structures overlap but are not identical. As projected descriptions evolve along the monotonic ordering of χ, the relative projectability of these configurations varies, leading to coherent transitions between flavor labels without invoking mass eigenstates as fundamental objects.

Stability of the Projection Boundary.

Neutrinos occupy an intermediate regime between fully localized particles and delocalized radiation. They act as carriers of marginal structural information, redistributing relational organization without inducing strong backreaction, thereby preventing abrupt transitions between projectable and non-projectable regimes. In strong-gravity or near-deprojection regimes, neutrinos remain among the last modes to retain partial projectability.

Why Neutrinos Are the Lightest Fermions.

Neutrino configurations reside closest to the boundary of projectability. Their absence of electromagnetic coupling and partial self-conjugacy prevent the formation of tightly bound projected structures. The smallness of neutrino masses is a structural necessity imposed by their role as marginally projectable modes.

Neutrinos as Probes of Pre-Geometric Structure.

Because neutrinos operate near the projection boundary, they provide a unique observational window into the pre-geometric structure of χ. Their weak localization allows them to sample relational structures inaccessible to fully projectable modes, and deviations in their phenomenology may encode signatures of pre-geometric ordering.

Failure of Absolute Localization.

Neutrinos cannot be fully confined within a bounded spacetime region without loss of admissibility, explaining their absence of sharply defined position operators and extremely small interaction cross-sections.

Limits of Effective Quantum Field Theory.

Neutrinos systematically probe the limits of local QFT assumptions. Their weak localization, extended coherence, and oscillatory behavior signal a breakdown of the strict particle ontology. Standard QFT constructs (mass eigenstates, flavor mixing matrices) are understood as effective bookkeeping devices for marginally projectable configurations.

Experimental Signatures.

Potential signatures include small departures from standard oscillation patterns at ultra-long baselines, coherence and decoherence effects sensitive to global spacetime properties, constraints from neutrinoless double beta decay on the projective resolution of conjugate configurations, and cosmological neutrino backgrounds encoding information about the approach to the projection boundary.

Synthesis.

Neutrinos mark the transition between physics described by local quantum fields on spacetime and the pre-geometric relational dynamics of χ. They constitute the structural frontier of emergent spacetime, where effective geometry, quantum description, and pre-geometric ontology converge.

4.10 Spectral Stability and the Lamb Shift

The stability of charged particle-like excitations is governed not only by topological admissibility but also by the fine spectral structure induced by the coupling between localized modes and the global relaxation flow. While the linear effective description predicts degenerate energy levels for certain atomic configurations, this degeneracy is lifted once non-linear saturation effects and projectability constraints are taken into account.

In standard QED, the Lamb shift arises from radiative corrections requiring renormalization. In Cosmochrony, no vacuum degrees of freedom are introduced. Atomic bound states correspond to admissible localized relaxation modes. S-states ($\ell = 0$) probe finer scales of the projection fiber where Born–Infeld saturation and spectral frustration are maximal, whereas P-states ($\ell = 1$) remain less sensitive to these inner-core constraints.

The effective Born–Infeld dynamics induces a finite upward shift of the S-state energy:

$$\Delta E_{\mathrm{Lamb}} \sim \kappa\, \alpha^5 m_e c^2, \tag{29}$$

where α is the dimensionless ratio between the local relaxation flux and the maximal saturation flux c_χ, and κ is a numerical factor of order unity. Numerically, $\alpha^5 m_e c^2 \simeq 10^{-5}\,\mathrm{eV}$, corresponding to a frequency shift of order $1\,\mathrm{GHz}$, in agreement with the

observed $2S_{1/2}$–$2P_{1/2}$ splitting. This correction is intrinsically finite thanks to the maximal relaxation speed c_χ.

Hyperfine Structure.

The same spectral-probe logic extends to hyperfine structure. When the electron occupies an S-state, its non-vanishing density at the nucleus brings electronic and nuclear torsional cores into spectral proximity. Hyperfine splitting reflects the relative alignment of torsional fluxes: parallel alignments accumulate frustration and oppose relaxation, while antiparallel alignments partially compensate torsion. Together with the Lamb shift, hyperfine structure emerges as a finite spectral correction governed by Born–Infeld saturation at different relational scales.

4.11 Summary

Particles arise as stable, localized projected configurations that resist admissible relaxation ordering. Mass is identified with the degree of effective resistance to χ relaxation, naturally yielding $E = mc^2$ as a kinematic identity. Spin and statistical behavior originate from topological obstructions: fermionic configurations exhibit 4π periodicity, providing a unified origin for spin-$\frac{1}{2}$ behavior, fermionic antisymmetry, and the Pauli exclusion principle [25, 26]. Electric charge is interpreted as a chiral–torsional invariant of the relaxation flux. Residual spectral splittings—such as the Lamb shift and hyperfine structure—arise as finite corrections induced by non-linear saturation and projectability constraints.

Localized excitations of the χ field may also admit collective coherent regimes in the $U(1)$ fiber sector, to be analyzed in Section 5.7.

5 The Projection Fiber and Gauge Emergence

The projection fiber Π is a central structural element linking the pre-geometric substrate χ to effective spacetime descriptions. It encodes the admissible equivalence classes and internal degrees of freedom through which relational configurations of χ can be consistently projected into geometric and field-like representations.

Gauge interactions do not arise from fundamental interaction fields. They emerge as symmetry structures of the projection process itself, under local re-identification of equivalent representatives along the fiber. This section develops the geometry of the projection fiber and clarifies how distinct classes of gauge phenomena naturally emerge from its structure.

5.1 The Geometry of the Π Subspace

The relational substrate χ is not accessed in its full structural complexity but through admissible local projections onto a reduced projection fiber $\Pi \cong S^3$. Here Π denotes the projection *fiber*, i.e. the space of admissible internal representatives associated with a projected configuration, not the projection map itself.

The identification $\Pi \cong S^3$ is not imposed *a priori* but follows from the minimal compact geometry (in dimension and connectivity) required to support non-injective yet stable projections. Its associated Hopf fibration naturally induces an effective $SU(2) \times U(1)$ symmetry structure, which emerges as an invariance of the projection process.

The metric on Π is dynamically induced by the local density of relational connections encoded in the underlying relational graph G, used as a numerical and representational support, not as a physical discretization. The mapping from the global graph Laplacian Δ_G to the effective projected Laplacian Δ_Π is

$$\Delta_\Pi = P^\dagger \Delta_G P, \tag{30}$$

where P denotes the projection operator onto the admissible spectral subspace. The smooth three-sphere geometry corresponds to a large-N spectral coarse-graining limit of the discrete relational structure.

Throughput constraints and channel counting.

The projection Π does not merely discard information. It enforces an admissibility constraint: local updates must remain operationally compatible with the surrounding global projected state U. This constrains the total admissible throughput by the number of independent relational channels (fibers) that can be synchronized across the update interface within one refresh step. Accordingly, capacity scalings commonly expressed as "area-law" behavior should be understood as consequences of projective throughput constraints rather than geometric postulates. This point becomes central when discussing resolvability bounds across scales in Section 12.10.

5.2 Gauges as Relaxation Transmittance

Gauge interactions are reinterpreted as degrees of freedom of the relaxation flow within the projection fiber Π, encoding how locally admissible projections are coherently related despite non-injectivity.

- **Electromagnetism ($U(1)$):** Corresponds to the phase degree of freedom of the relaxation flow along the fibers of the Hopf fibration of $\Pi \cong S^3$. This emergent geometric parameter reflects the freedom to locally re-identify projected descriptions without altering global relational consistency. The fine-structure constant α characterizes the *transmittance* of the relaxation flow through the fiber: the stability of admissible projective re-identifications along the fiber.
- **Weak Interaction ($SU(2)$):** Emerges from the rotational degrees of freedom of the S^3 projection fiber itself. These encode non-abelian modes of relaxation transmittance, corresponding to shear-like distortions of admissible projections. The massive character of the $W^{\pm}$ and Z^0 bosons follows from a non-zero spectral gap associated with these modes, interpretable as spectral drag or torsion intrinsic to the fiber geometry.
- **Strong Interaction ($SU(3)$):** Associated with topological constraints arising from non-trivial winding structures of projected configurations. The effective $SU(3)$-like symmetry reflects the threefold (triality) structure of the minimal self-intersecting stable soliton, identified with the trefoil knot ($w = 3$). Color symmetry emerges as a geometric consequence of topological stability classes within the projection fiber.

5.3 Topological Constraints and Invariants

The stability of localized physical descriptions within Π is governed by the conservation of topological invariants. When an excitation of χ admits a closed, non-contractible configuration within Π, it forms a persistent topological obstruction to complete relaxation. Such configurations cannot be eliminated by smooth deformation without violating admissibility constraints.

These obstructions are described in terms of knot-like (non-contractible loop and self-linking) topological structures within the projection fiber. Once formed, they impose global constraints on the relaxation process and give rise to long-lived, localized projected configurations. Particles correspond to stable topological defects of the projection.

The winding number w constitutes the primary invariant characterizing these obstructions. It labels distinct equivalence classes of admissible projected configurations and plays a central role in the organization of the mass spectrum (Section 10). The energetic cost required to maintain a non-trivial winding against the global pressure of relaxation is perceived, at the effective level, as rest energy (mc^2). Mass emerges as a spectral and topological consequence of persistent non-contractible structures within the projection fiber.

5.4 The Vacuum State as a Minimal Surface

In the absence of localized excitations, the projection fiber Π relaxes toward a configuration of minimal spectral tension: the smoothest admissible projected configuration compatible with global relaxation constraints. Geometrically, the vacuum corresponds to a minimal surface in a purely spectral sense (not a spatial embedding): curvature, torsion, and winding modes are simultaneously minimized within Π. In this state, the relaxation flow encounters no topological obstruction and propagates uniformly across the fiber. Any deviation—localized curvature, torsional distortion, or non-trivial winding—manifests as the presence of effective fields or particles.

The usual notion of field quantization is replaced by the quantization of admissible topological modes within a finite-volume projection fiber. Only a discrete set of deviations from the minimal surface is compatible with stability and projectability constraints, leading naturally to a discrete spectrum of excitations.

Vacuum energy is neither divergent nor arbitrary. It is intrinsically bounded by the spectral cutoff imposed by the relational graph underlying Π. The finiteness of vacuum energy reflects the finiteness of admissible spectral deformations of the minimal configuration, rather than the summation of zero-point energies of independent field modes.

5.5 The Inaccessibility of Absolute Zero as a Projective Necessity

Within the present framework, the Third Law of Thermodynamics is reinterpreted as a structural requirement for temporal projectability. Temperature T is not introduced as a primitive measure of kinetic agitation, but as an effective indicator of the rate at which distinct projected descriptions remain differentiable under successive updates.

A strict absolute zero ($T \to 0$) would correspond to a regime of projective stasis in which successive effective descriptions become indistinguishable. Formally, this would imply

$$U_{n+1} = U_n, \tag{31}$$

so that no non-trivial ordering of projected states could be defined. Since time is introduced operationally as the ordering of distinguishable effective states, such a regime would eliminate the very notion of temporal succession.

Absolute zero is therefore not merely energetically inaccessible, but structurally excluded: a perfectly stationary projection would terminate the temporal description itself. The persistence of time requires that projected states remain minimally non-degenerate under admissible updates.

In this context, the so-called zero-point fluctuations ($\frac{1}{2}\hbar\omega$) are reinterpreted as the minimal projective variance required to maintain the distinguishability of successive effective states. They represent the irreducible resolution limit of the projection process Π, marking the regime where descriptive continuity encounters the quantized structure of the underlying relational substrate [24].

5.6 Necessity of Non-Injective Projection for Emergent Gravity and Mass

This section addresses a structural necessity question distinct from sufficiency. We do not show that the χ-substrate implies gravity. That derivation is developed in Sections 6 and A.8. We show here that, under minimal operational assumptions matching what is empirically observed, a non-injective projection Π is required. A bounded relaxation flux is additionally required to select a unique infrared gravitational dynamics. The structural necessity argument is complemented by two technical appendices: the classification of admissible injective projections and their trivial holonomy (Appendix B), and the infrared derivation and selection mechanism (Appendix B.8).

Operational definitions and standing assumptions

We work with a microscopic configuration space $\mathcal{C}_\chi$ endowed with an autonomous relaxation rule F (the χ-dynamics of Section 2). The space of effective observables is $\mathcal{M}$. A projection (coarse-graining) map $\Pi : \mathcal{C}_\chi \to \mathcal{M}$ defines the effective state $y = \Pi(x)$ for each substrate configuration $x \in \mathcal{C}_\chi$.

Emergence.

An effective quantity Q_{eff} is called *emergent* if and only if

$$Q_{\text{eff}} = Q(\Pi, F, x), \tag{32}$$

determined solely by the relaxation rule F and the projection Π. No independent free parameter carrying Q is introduced at the effective level.

Ontological uniqueness.

The complete substrate is $(\mathcal{C}_\chi, F)$. All effective structures, metric, connection, mass, and charge, are derived from the pair (F, Π) only. No fundamental geometric field is postulated independently of this pair.

Observed gravity.

We assume the effective description admits a Lorentzian geometric formulation satisfying:

(D1) Effective locality. Field equations are local on $\mathcal{M}$.
(D2) Covariance. Diffeomorphism invariance as an invariance of description, not of the substrate.
(D3) Infrared dominance of a low-derivative action.
(D4) Universal coupling to energy-momentum.

Hypothesis H (descriptive redundancy).

The effective geometry is a structure on $\mathcal{M}$, not on $\mathcal{C}_\chi$. Formally,

$$g_{\text{eff}} = g(y), \quad y = \Pi(x), \quad \text{not } g(x). \tag{33}$$

This expresses that gravity is attributed to the stability of the projection, not to an intrinsic geometry defined on the substrate itself.

Remark. Hypothesis H is not an additional postulate of Cosmochrony. It is the formal translation of the claim that the effective geometric description belongs to the level of observables $\mathcal{M}$. This is operationally required by the definition of emergent gravity. A geometry that depends on x rather than on $y = \Pi(x)$ would be a substrate-level geometric structure. Any attempt to define $g(x)$ therefore violates Hypothesis H by construction.

Lemma 1: Injectivity is incompatible with emergent gravity under H

Lemma 5.1 (Injectivity forbids universal geometric emergence under H)**.** *Assume ontological uniqueness and Hypothesis H, Eq. 33. If $\Pi : \mathcal{C}_\chi \to \mathcal{M}$ is injective, then there is no intrinsic mechanism producing simultaneously*

(i) a spatially variable inertial rigidity, and
(ii) a non-trivial effective curvature,

without adding an independent geometric postulate at the effective level.

Proof Suppose Π is injective. Then $\mathcal{M}$ is isomorphic to $\mathcal{C}_\chi$ via Π, and any geometric structure $g(y)$ on $\mathcal{M}$ is equivalent to a structure on $\mathcal{C}_\chi$. Under ontological uniqueness, such a structure must be derived from (F, Π) alone.

However, an injective Π generates no descriptive redundancy. There is no quotient, no non-trivial fiber $\Pi^{-1}(y)$, and no re-identification symmetry between distinct substrate configurations. Without descriptive redundancy, no gauge-like or diffeomorphism-like invariance can arise as an invariance of description. Such an invariance can only be postulated independently. Without an invariance of description, universal geometric emergence cannot arise as a constraint shared by all effective couplings. In particular, this is incompatible with the operational meaning of universal coupling in condition (D4).

Therefore, either g_{eff} and/or inertial parameters are introduced as independent postulates (violating ontological uniqueness and emergence), or no emergent gravity in the sense of Hypothesis H is obtained.

The core of the argument is not the arithmetic identity $|\Pi^{-1}(y)| = 1$. It is the structural implication:

injective $\Rightarrow$ no redundancy $\Rightarrow$ no re-identification symmetry $\Rightarrow$ no universal geometric emergence by constraint.

The vanishing of the multiplicative gradient $\partial \log |\Pi^{-1}(y)|$ is a corollary of this chain, not its premise. □

Lemma 2: Non-injectivity is the general form of descriptive redundancy

Lemma 5.2 (Descriptive invariance implies an effective quotient)**.** *In any framework where gravity is an invariance of description, there exists an effectively non-injective morphism. Equivalently, there exists an equivalence relation $x \sim x'$ on $\mathcal{C}_\chi$ such that observables and geometry coincide for distinct micro-configurations.*

Structural exhaustion We consider representative classes of frameworks realizing gravitational invariance of description.

General relativity. Physical configurations are defined modulo $\mathrm{Diff}(\mathcal{M})$. The physical state space is a quotient by a continuous group action. A quotient is a non-injective projection, since multiple representatives correspond to one physical state.

Discretized approaches (spin networks, causal sets, CDT). Macroscopic geometry is an invariant of sets of micro-configurations and is therefore many-to-one by construction. The non-injectivity is present even when it is not explicitly labeled as a projection.

Stochastic approaches (stochastic mechanics, GRW-type). The measure or filtration identifies micro-histories that are indistinguishable at the level of observables. This defines an effective quotient structure, hence a non-injectivity.

In each case, non-injectivity is not imported from Cosmochrony. It is the generic mathematical form of descriptive redundancy compatible with universal coupling. Cosmochrony renders this structure explicit by identifying it with Π, rather than concealing it in a gauge orbit, a sum over histories, or a stochastic measure. □

Lemma 3: Saturation selects a unique infrared dynamics

Lemma 5.3 (Non-injectivity alone does not select a unique IR completion)**.** *Non-injectivity of Π is sufficient for geometrization and descriptive invariance, but insufficient to select a unique infrared gravitational dynamics. A finite-capacity constraint, the saturation bound $|\partial_t \chi| \leq c_\chi$ on the relaxation flux, acts as a selection principle. It picks a class of bounded effective actions whose infrared expansion reproduces the Einstein–Hilbert term and whose nonlinear regime is Born–Infeld-like. More precisely, the selection yields a unique dominant IR term plus a controlled expansion in powers of c_χ^{-2}, organized by a single capacity parameter.*

Selection argument Conditions (D1)–(D4) constrain the effective gravitational sector but do not uniquely determine it. They allow the Einstein–Hilbert action plus an unbounded set of higher-derivative corrections not fixed by symmetry and covariance alone.

The saturation bound $|\partial_t \chi| \leq c_\chi$ plays three distinct roles.

1. *Nonlinear completion.* The bound enforces bounded response, yielding a Born–Infeld-like structure for the full effective action (Section 3, Appendix A.12). This eliminates the freedom in ultraviolet completions that conditions (D1)–(D4) alone leave open.
2. *Exclusion of projective pathologies.* Unbounded relaxation gradients correspond to configurations where the fiber $\Pi^{-1}(y)$ collapses, meaning the projection becomes locally injective and the geometric description breaks down. The bound excludes these configurations, ensuring the projective description remains globally admissible.
3. *Quantitative prediction.* The bound relates the effective gravitational coupling G to microscopic capacity parameters:
$$G = G(c_\chi, \hbar_\chi, \ldots), \tag{34}$$
turning the underdetermined effective family into an organized expansion with a single capacity scale. This yields a falsifiable prediction independent of the geometric effective description.

Without the saturation bound, no intrinsic principle selects among the family of actions compatible with (D1)–(D4). In particular, no principle fixes the coefficient of the Einstein–Hilbert term or the structure of higher-derivative corrections. □

Theorem: Necessity of non-injective projection and bounded relaxation flux

Theorem 5.1 (Necessity of non-injective projection and bounded relaxation)**.** *Assume:*

(i) mass and gravity are emergent in the operational sense of Section 5.6,
(ii) ontological uniqueness, with no independent fundamental geometric fields,
(iii) observed gravity satisfying (D1)–(D4),
(iv) Hypothesis H, Eq. 33.

Then:

(a) Π *must be non-injective. Equivalently, there must exist an effective equivalence relation on* $\mathcal{C}_\chi$ *compatible with universal coupling.*
(b) The substrate relaxation flux must be bounded, providing the selection principle required for a unique infrared dynamics with controlled higher-order corrections.

Proof Part (a). By Lemma 5.1, if Π were injective under Hypothesis H and ontological uniqueness, universal geometric emergence would require an independent geometric postulate at the effective level. This violates the operational notion of emergence. Lemma 5.2 further shows that any alternative framework implementing descriptive invariance introduces an effective quotient, hence a non-injectivity in disguise, regardless of terminology.

Part (b). By Lemma 5.3, non-injectivity alone does not select a unique infrared dynamics compatible with (D1)–(D4). The bounded relaxation flux $|\partial_t \chi| \leq c_\chi$ supplies the selection mechanism by fixing the nonlinear completion and organizing higher-order corrections by a single capacity scale. □

Remaining technical steps toward a quantitative derivation

Two technical steps remain to convert Theorem 5.1 from a structural necessity result into a fully quantitative derivation.

Step A: Classification of admissible injective projections.

One must formalize the class of admissible injective maps $\Pi : \mathcal{C}_\chi \to \mathcal{M}$. One must then show that within this class, no re-identification symmetry can arise without adding extra structure. This program is carried out in Appendix B, where injective admissible projections are shown to have trivial holonomy. It is not a claim that curvature cannot be defined mathematically on $\mathcal{M}$. It is the claim that emergent gravity as descriptive invariance cannot arise from (F, Π) under injectivity and Hypothesis H.

Step B: Derivation of Einstein–Hilbert from the coherence functional.

One must construct the coherence functional

$$S_{\mathrm{coh}}[g, \psi] = \int_{\mathcal{M}} \mathcal{L}_{\mathrm{defect}}(\Pi, F, y)\, \mathrm{d}^4 y, \tag{35}$$

defined as the integrated cost of projective defect, the mismatch between successive projected descriptions under the relaxation rule F. The infrared expansion and the selection mechanism induced by the saturation bound are developed in Appendix B.8.

One must then show that:

1. the infrared expansion of S_{coh} yields $\int \sqrt{-g}\, R$ as the dominant term compatible with (D1)–(D4),
2. the saturation bound enforces a Born–Infeld-like completion whose expansion begins with R,
3. the coefficient of R in the expansion determines G via Eq. 34, yielding a falsifiable quantitative prediction relating the effective coupling to c_χ and $\hbar_\chi$.

This would establish the Einstein–Hilbert term not as a postulate, but as the unique dominant term permitted by projective coherence, with Cosmochrony fixing the nonlinear completion and the coupling constant.

Non-injectivity also implies the possibility of composite winding classes and coherent collective phases, discussed below.

5.7 Collective Coherent Phases of the $U(1)$ Fiber

In the previous sections, electric charge and gauge structure were derived from the non-injective projection of the χ substrate onto an effective $U(1)$ fiber. We now consider the possibility that this fiber sector admits collective coherent phases.

The analysis below does not introduce new fundamental fields. It studies a specific collective regime of already established degrees of freedom. Superconductivity is interpreted as a macroscopic coherent phase of the $U(1)$ fiber, arising from the stabilization and phase locking of composite topological excitations.

5.7.1 Stability of $w = 2$ Composite Classes

Section 4 established that charged excitations correspond to topological configurations of the χ field projected onto the $U(1)$ fiber. A single excitation carries winding number $w = 1$ and effective charge e.

We now consider composite configurations of winding number $w = 2$. Such configurations are not trivial superpositions of two independent $w = 1$ modes. They define a distinct topological class characterized by a continuous fiber raccordement.

Let L_Π denote the effective relaxation operator restricted to the fiber sector. We define the projective stability gap

$$\Delta_\Pi \equiv \lambda_{\min}\left(L_\Pi\big|_{w=2}\right), \tag{36}$$

as the lowest positive eigenvalue around the $w = 2$ configuration.

A finite Δ_Π implies that the composite class is metastable against separation into two $w = 1$ excitations or local phase defects. The existence of this gap is a structural consequence of bounded projective transport capacity established in Section 5.6.

5.7.2 Phase Coherence and the London Structure

If a macroscopic density of $w = 2$ composites occupies a common fiber phase sector, we may introduce the order parameter

$$\Psi = |\Psi| e^{i\theta}, \tag{37}$$

where $|\Psi|^2$ measures the density of coherent composites.

Gauge covariance fixes the unique admissible covariant gradient

$$D\theta = \nabla\theta - \frac{2e}{\hbar} A. \tag{38}$$

The leading contribution to the free energy must then take the form

$$F_{\text{grad}} = \frac{\hbar^2 \rho_s}{2m^*} \left(\nabla\theta - \frac{2e}{\hbar} A \right)^2, \tag{39}$$

where ρ_s is the phase stiffness and m^* an effective inertia.

This term is not postulated as a symmetry-breaking potential. It represents the energetic cost of breaking global fiber coherence. The London equation and flux quantization follow directly from this structure.

5.7.3 Frustration-Induced Stabilization in Strongly Correlated Regimes

In conventional low-T_c materials, mediator-assisted interactions lower Δ_Π and stabilize the $w = 2$ class.

In strongly correlated systems, stabilization may arise instead from real-space frustration in admissibility constraints of the fiber. Let F denote a frustration density proxy, operationally linked to staggered magnetic correlations.

In this regime, isolated $w = 1$ excitations increase local mismatch, whereas a $w = 2$ composite redistributes phase incompatibility over an extended region. Pair formation thus minimizes a geometric cost functional rather than resulting from a specific momentum-space interaction kernel.

The amplitude scale for composite formation is set by the dominant frustration energy scale J,

$$\Delta_\Pi^{\text{ampl}} \sim J. \tag{40}$$

5.7.4 Phase Stiffness and BKT-Type Transition

Global superconductivity requires phase locking across the system. The relevant control parameter is the phase stiffness ρ_s, which measures the relaxation capacity of the projected substrate.

In doped quasi-two-dimensional systems, the density of active composites scales with carrier concentration δ. To leading order,

$$\rho_s(0) \propto \delta J. \tag{41}$$

In strongly anisotropic layered systems, the transition temperature is governed by vortex unbinding and satisfies approximately

$$k_B T_c \simeq \frac{\pi}{2} \rho_s(T_c^-). \tag{42}$$

This naturally allows separation between amplitude formation ($T^* \sim \Delta_\Pi^{\mathrm{ampl}}/k_B$) and global phase coherence (T_c).

5.7.5 Superconductivity as Collective Saturation

The emergence of superconductivity can thus be interpreted as a collective saturation phase of the $U(1)$ fiber.

At the microscopic level, bounded projective transport constrains admissible field gradients. At the macroscopic level, coherent occupation of a single fiber phase sector minimizes relaxation cost and expels magnetic flux from the bulk.

In this perspective, superconductivity is structurally analogous to other saturation phenomena derived in this work. Mass corresponds to isotropic inhibition of χ relaxation. Schwinger pair production corresponds to saturation of directed flux. Gravitational curvature corresponds to collective slowdown of relaxation ordering.

Superconductivity represents the coherent phase of the same bounded projective dynamics in the electromagnetic sector.

No modification of Standard Model interactions is required. The phenomenon emerges as a specific collective regime of the already established $U(1)$ fiber structure.

Part III
Gravitation and Cosmology

This part addresses gravitation and cosmology as collective, large-scale manifestations of substrate relaxation rather than as fundamental interactions. Gravitation is shown to arise from the local inhibition of relaxation ordering induced by particle excitations, leading to an emergent curvature description consistent with general relativity in appropriate regimes.

Cosmological expansion is interpreted as a global consequence of sustained relaxation, without invoking inflation, dark matter particles, or a fundamental dark energy component. Observable phenomena such as galactic rotation curves, gravitational lensing, cosmic voids, and the Hubble tension are reinterpreted as effective responses to structural saturation and projective compensation.

This part connects the microscopic dynamics of χ to astrophysical and cosmological observables, providing the bridge between foundational principles and large-scale data.

6 Gravity as a Collective Effect of Particle Excitations

6.1 Local Slowdown of Relaxation Ordering

Gravitation emerges from the collective influence of localized projected configurations on admissible relaxation ordering. When particle-like configurations are present in significant number, their combined effect leads to a macroscopic reduction of the admissible ordering rate. In an effective spacetime parametrization, this may be expressed as

$$\mathcal{D}_{\text{eff}}\chi_{\text{eff}} \;\simeq\; c\,(1-\alpha\,\rho)\,, \tag{43}$$

where ρ denotes the effective density of localized projected configurations and α encodes their average contribution to relaxation resistance. This first-order approximation is valid when localized constraints are dilute and weakly overlapping.

The coupling parameter α is emergent and scales as $\alpha \propto G/c^2$ in terms of effective inertial mass densities. The collective slowdown manifests as gravitational time dilation and curvature effects, without introducing any independent gravitational force or mediator.

6.2 Collective Gravitational Coupling and Operational Geometry

The collective reduction of admissible relaxation ordering modulates how efficiently structural variations can be correlated between different effective locations. In regions where projected descriptions are nearly homogeneous, the effective coupling approaches a uniform value; localized configurations weaken it by introducing structural constraints.

From an operational perspective, this modulation can be interpreted as a *self-consistency overhead*: maintaining mutual compatibility of projected descriptions across separated regions requires an increasing consistency cost as local constraints accumulate. Inertial and gravitational responses arise precisely as manifestations of this overhead in collective updates of the effective state.

Spatial separation is defined operationally: two effective regions are close if structural variations can be efficiently correlated between them. In the continuum and weak-constraint regime, this operational notion admits a compact description in terms of an effective spatial metric summarizing the collective response to relative variations. Spacetime curvature emerges as a descriptive manifestation of how localized configurations modulate collective ordering, correlation efficiency, and the associated self-consistency overhead.

A more explicit relational construction of the coupling mechanism is presented in Appendix E.1.

6.3 Emergent Curvature

Spatial variations in admissible relaxation ordering lead to non-uniform correlation patterns within projected descriptions. When a smooth geometric parametrization is applicable, these non-uniformities are summarized by gradients of an emergent metric structure, reproducing the phenomenology traditionally attributed to curved spacetime: gravitational time dilation, geodesic deviation, and lensing effects.

Einstein's Equations as a Structural Equilibrium Principle.

When projected configurations admit a smooth, locally injective geometric description, their collective structural constraints can be summarized by an effective metric $g_{\mu\nu}$. Einstein's equations emerge *necessarily* as the unique consistency condition relating curvature to the effective distribution of relaxation-resistant configurations. The Einstein tensor encodes a geometric identity constraining admissible macroscopic descriptions; the stress–energy tensor summarizes how localized configurations resist relaxation ordering. Einstein's equations therefore express a balance condition between geometry and physical structure.

This interpretation explains the extraordinary universality of general relativity: as long as a smooth spacetime description exists and relaxation ordering is monotonic, bounded, and weakly inhomogeneous, the same geometric relations must hold, independently of the microscopic nature of the underlying substrate. General relativity thus plays a role analogous to thermodynamics—exact within its domain, silent outside it.

When projection ceases to be locally injective, Einstein's equations do not break down; they simply no longer apply, because the concept of spacetime has not yet emerged.

6.4 Recovery of the Schwarzschild Metric

For a static, approximately spherically symmetric distribution of localized projected configurations, the collective reduction of admissible relaxation ordering admits a simple effective description.

Operational potential from χ-relaxation slowdown.

The dimensionless lapse-like factor is

$$N(r) \;\equiv\; \frac{D^{\chi}_{\mathrm{loc}}(r)}{D^{\chi}_{0}}, \qquad 0 < N(r) \leq 1, \tag{44}$$

with the weak-field identification

$$\frac{D^{\chi}_{\mathrm{loc}}}{D^{\chi}_{0}} \;\simeq\; 1 + \frac{\Phi}{c^2}, \qquad \left|\frac{\Phi}{c^2}\right| \ll 1. \tag{45}$$

Poisson-like equation and exterior solution.

In the weak-structure regime:

$$\nabla^2 \Phi \;\simeq\; 4\pi G_{\mathrm{eff}}\, \rho, \tag{46}$$

yielding, for an isolated spherical source of mass M:

$$\Phi(r) \;\simeq\; -\frac{G_{\mathrm{eff}} M}{r}. \tag{47}$$

Metric components from Φ.

The static spherically symmetric ansatz reads

$$ds^2 = -N(r)^2 c^2 dt^2 + N(r)^{-2} dr^2 + r^2 d\Omega^2. \tag{48}$$

In the weak-field limit:

$$g_{tt} \simeq -\left(1 + 2\frac{\Phi}{c^2}\right), \tag{49}$$

$$g_{rr} \simeq \left(1 + 2\frac{\Phi}{c^2}\right)^{-1} \simeq 1 - 2\frac{\Phi}{c^2}, \tag{50}$$

coinciding with the standard Schwarzschild weak-field expansion:

$$g_{tt} \simeq -\left(1 - \frac{2G_{\text{eff}}M}{c^2 r}\right), \quad g_{rr} \simeq \left(1 - \frac{2G_{\text{eff}}M}{c^2 r}\right)^{-1}. \tag{51}$$

Comparison to classic observational tests.

Gravitational redshift follows directly from g_{tt}:

$$\frac{\nu_{\text{obs}}}{\nu_{\text{emit}}} \simeq 1 + \frac{\Phi(r_{\text{emit}}) - \Phi(r_{\text{obs}})}{c^2}. \tag{52}$$

Light deflection yields the standard angle

$$\alpha \simeq \frac{4G_{\text{eff}}M}{bc^2}, \tag{53}$$

with b the impact parameter.

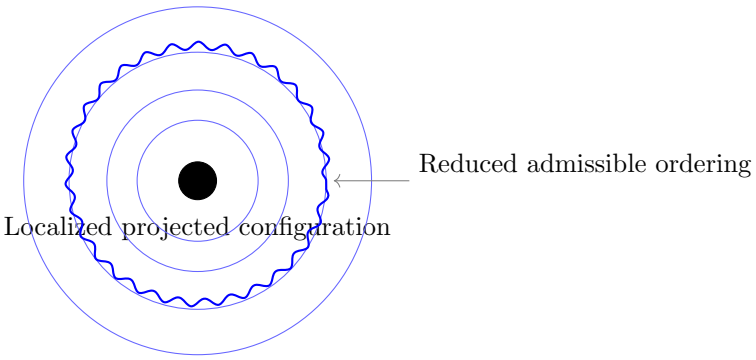

Fig. 5 Emergence of Schwarzschild-like behavior. A localized projected configuration induces a spatially varying reduction of admissible relaxation ordering, manifesting as differential proper-time accumulation and emergent metric curvature.

6.5 Equivalence Principle

All admissible localized projected configurations constrain relaxation ordering in the same universal manner. Their internal composition plays no role in how they affect or respond to the admissible ordering environment. Inertial resistance and gravitational response are two effective manifestations of the same underlying constraint, and the equivalence principle arises as an emergent symmetry of admissible projected descriptions.

6.6 Gravitational Waves

Time-dependent variations in the distribution of localized projected configurations induce collective and transient modulations of admissible relaxation ordering. These modulations propagate at the maximal admissible ordering speed c and are described, in an effective spacetime language, as gravitational waves. Unlike electromagnetic radiation, they represent collective variations of the admissible ordering and correlation structure itself.

The standard properties—propagation at speed c, transverse polarization, and energy transport—are recovered as effective features of collective ordering dynamics. Gravitational-wave descriptions remain valid only within regimes where projection onto an effective spacetime remains well defined; in strong-gravity environments approaching the deprojection threshold (Section 6.7), such modulations may become attenuated or lose a clear spacetime interpretation.

6.7 Strong Gravity and Black Holes

Projectable	$\rightarrow$	**Horizon**	$\rightarrow$	**Non-projectable**
Gravitational Waves		Boundary of Projection		Deprojected Regime
Effective Modulations		Π non-injective		No spacetime Representation

Fig. 6 Conceptual regimes of projection in Cosmochrony. Black holes mark the boundary beyond which spacetime representations cease to be injective.

In regions of sufficiently high density of localized projected configurations, admissible relaxation ordering becomes strongly constrained, defining an effective horizon. Black holes correspond to domains where physical processes become asymptotically inaccessible due to the loss of injectivity of spacetime projection. This naturally accounts for extreme time dilation without requiring divergent curvature invariants.

Because admissible ordering is bounded, configurations corresponding to infinite curvature or density cannot be physically realized. Apparent singularities signal the breakdown of spacetime representability, not genuine divergences of the underlying relational structure.

Black Holes, Deprojection, and Vacuum Reprojection

In strong-gravity regimes, the projection $\Pi : \mathcal{C}_{\text{rel}} \longrightarrow \mathcal{M}$ loses injectivity: multiple inequivalent relational configurations correspond to the same effective spacetime event. This *deprojection* does not destroy information. Relational information ceases to be expressible in spatiotemporal form but remains encoded structurally and is in principle reprojectable once projectability is restored. Reprojection manifests as radiation-like excitations or particle–antiparticle pairs.

Black Hole Entropy as Relaxation Saturation

Black hole entropy measures the saturation of relaxation capacity at the horizon. Near the boundary where the effective temporal ordering ceases to be resolvable, a large multiplicity of distinct χ micro-configurations become indistinguishable at the level of the effective metric:

$$S_{\text{BH}} \;\sim\; \log \left|\Pi^{-1}(g_H)\right|, \tag{54}$$

where g_H denotes the saturated horizon geometry. The area law follows from the fact that saturation occurs at the boundary between projectable and non-projectable regimes. Hawking thermality arises from the coarse-grained statistics of discrete reprojection events at the saturation interface.

The numerical factor $1/4$ in $S = A/4$ arises from the fourfold degeneracy in the stability spectrum of χ excitations, linked to the intrinsic 4π periodicity discussed in Section 4.2.

Saturation as a projectability boundary.

In Cosmochrony, strong-gravity regimes correspond to configurations in which the demanded update rate approaches the admissible projective throughput set by b_χ. An effective horizon can be interpreted as a boundary beyond which the projected description cannot remain smooth and approximately injective under admissible updates. This does not require a loss of substrate information, but reflects a loss of projectability in the effective state U.

6.8 Black Hole Evaporation and the Information Problem

Black hole evaporation is an effective process arising from the gradual restoration of projectability near the boundary separating projectable and non-projectable domains. The apparent information loss identified by Hawking [27] arises from applying a spacetime-based description beyond its domain of validity. In Cosmochrony, information is encoded in the global relational configuration independently of its spacetime projection.

Horizon Reprojection Equation

The energy flux emerging from the horizon is a sum over discrete reprojection events:

$$\Phi_\chi \equiv \frac{dE}{dt} = \sum_k \delta(t - t_k)\, \hbar_\chi\, \nu_k(L_{\text{sol}}).$$

Here $\hbar_\chi$ is the fundamental quantum of reprojection, the $\nu_k(L_{\rm sol})$ are resonance frequencies of the stability operator at the horizon, and t_k label the instants at which local configurations reach the projection threshold.

Emergent Temperature and Relaxation Gradient

The apparent Hawking temperature is determined by the gradient of effective χ relaxation normal to the horizon:

$$k_B T_\chi = \frac{\hbar_\chi c}{2\pi} \, |\nabla_\perp \chi_{\rm eff}|_H \, .$$

For more massive black holes, the relaxation gradient is distributed over a larger area, reducing the frequency of reprojection events and explaining the inverse mass–temperature relation without invoking vacuum particle creation.

Information Conservation and Spectral Encoding

During deprojection, information is stored in the nonlinear degrees of freedom of χ within the projection fiber. During reprojection, each emitted quantum carries the spectral imprint of the eigenmodes governing the χ configuration, ensuring global information conservation.

Entropy as a Projection Saturation Limit

The Bekenstein–Hawking area law

$$S = \frac{A}{4} \tag{55}$$

is reinterpreted as the informational capacity of the projection map at the horizon boundary. Entropy quantifies hidden relational structure—the structural multiplicity of χ configurations no longer distinguishable at the metric level—rather than thermal ignorance.

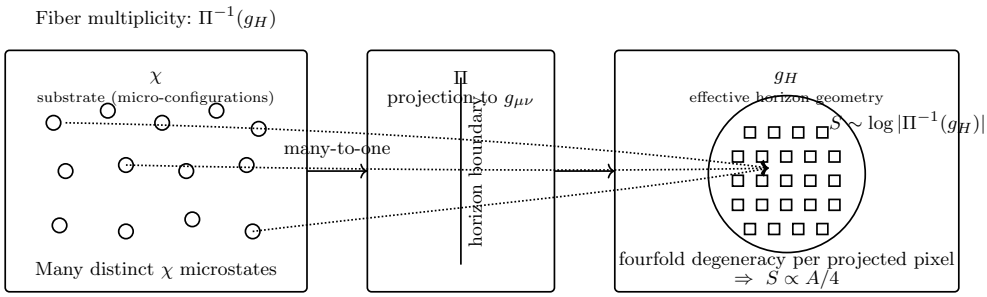

Fig. 7 Saturation of the projection map at the horizon. Multiple micro-configurations of χ collapse onto the same effective horizon geometry g_H. Entropy measures the structural multiplicity of the fiber $\Pi^{-1}(g_H)$.

Prediction: Spectral Granularity

If Hawking radiation is fundamentally discrete, it cannot be a perfect black-body continuum. The spectral line width of a reprojected quantum is

$$\Delta\nu_k \approx \frac{1}{\tau_\chi}\sqrt{\alpha}\,\ln(Q), \tag{56}$$

where τ_χ is the characteristic relaxation time near the horizon, $\alpha \simeq 3 \times 10^{-7}$ is the spectral packing fraction, and Q is the topological charge of the emitted configuration. The ratio between line width and line spacing is universally governed by α:

$$\frac{\Delta\nu}{\delta\nu} \propto \alpha. \tag{57}$$

Observational Prospects

In the late stages of evaporation, the spectral spacing may enter the sensitivity bands of next-generation interferometers (LISA, Einstein Telescope). The universal relation $\Delta\nu/\delta\nu \simeq \alpha$ should also apply to analogue gravity systems, where current experiments in Bose–Einstein condensates approach the required spectral resolution ($\delta f/f \sim 10^{-5}$), making near-term tests feasible.

6.9 Unified Origin of Gravitational and Electromagnetic Effects

Gravitational and electromagnetic phenomena arise as complementary effective manifestations of the same relational substrate. Gravitational effects correspond to sustained, quasi-static constraints on admissible relaxation ordering induced by persistent localized configurations. Electromagnetic phenomena arise from time-dependent, phase-structured patterns within admissible projected descriptions, admitting an effective formulation in terms of propagating oscillatory modes. The familiar distinction between the two interactions emerges at the level of effective descriptions rather than from fundamentally separate fields.

An explicit derivation of Maxwell-like equations within the Cosmochrony framework is provided in Appendix B.13.

6.10 Effective Gravitational Lensing

In the weak-field and thin-lens regimes, the lens equation is

$$\boldsymbol{\beta} = \boldsymbol{\theta} - \frac{D_{ls}}{D_s}\,\nabla_{\boldsymbol{\theta}}\psi(\boldsymbol{\theta}), \tag{58}$$

with the lensing potential

$$\psi(\boldsymbol{\theta}) = \frac{2D_{ls}}{c^2 D_l D_s}\int \Phi_{\rm eff}(D_l\boldsymbol{\theta}, z)\; dz. \tag{59}$$

The effective potential Φ_{eff} is a geometric descriptor encoding collective constraints of the projected χ-substrate. All observable lensing quantities (convergence, shear, magnification, caustics) follow in the usual way. No additional dark matter component is required: lensing directly probes the emergent geometry.

6.11 Summary

Gravity emerges as a macroscopic consequence of localized projected configurations collectively constraining admissible relaxation ordering. Classical gravitational phenomena—time dilation, curvature, gravitational waves, and black holes—are recovered as distinct descriptive regimes of this collective constraint. In extreme regimes, the spectral structure of horizon-associated phenomena encodes direct information about the relaxation dynamics and projection topology of the underlying substrate.

7 Cosmological Implications

7.1 The Big Bang as a Maximal Constraint Regime of the χ Substrate

The Big Bang is interpreted as the boundary of applicability of effective spacetime descriptions. In this regime, the density of structural and topological constraints within χ exceeds the threshold required for stable geometric projection: effective notions of spatial distance, temporal duration, and causal ordering cease to be well-defined. The apparent singular behavior of standard cosmological models reflects the extrapolation of geometric descriptions beyond their domain of validity.

Cosmological evolution is therefore described as the progressive relaxation of this maximal constraint regime. The Big Bang marks not the origin of spacetime, but the transition beyond which spacetime becomes an appropriate effective framework. The arrow of time arises from the intrinsic monotonic ordering of χ configurations (Section 2.6).

7.2 Cosmological Cycles of Constraint and Reprojection

The maximally constrained regime is not confined to the early universe. It may be locally reapproached whenever structural constraints saturate, most notably in black holes. Deprojection does not destroy information but renders it inaccessible to spacetime descriptions. Reprojection is the restoration of descriptive projectability once relational consistency conditions are satisfied.

Phenomena commonly associated with the quantum vacuum reflect the persistent presence of reprojectable relational structures within χ. The vacuum represents a regime of minimal yet non-vanishing projectability. Cosmological evolution involves a continuous interplay between global relaxation, local reconfinement, deprojection, and reprojection across scales.

7.3 Cosmic Expansion Without Inflation

In standard cosmology, an inflationary phase resolves the horizon problem [28, 29]. In Cosmochrony, large-scale homogeneity and isotropy reflect the global relational coherence of the χ substrate in the maximally constrained regime, rather than the outcome of a rapid expansion of spacetime. Prior to the emergence of a stable geometric projection, notions such as distance, light cones, and causal disconnection are undefined. The horizon problem therefore does not arise.

7.4 Cosmic Expansion as χ Relaxation

Cosmic expansion reflects the progressive relaxation of the relational substrate [30]. As the ordering parameter increases monotonically, projected descriptions admit an ever broader range of mutually distinguishable relational configurations. Expansion is not driven by an external energy component but is an intrinsic consequence of the relaxation ordering. Localized matter configurations act as persistent structural

constraints, leading to spatially inhomogeneous unfolding that later manifests as large-scale structure.

7.5 Emergent Hubble Law

In homogeneous regimes, the relaxation ordering is uniform and admits the linear representation

$$\chi(t) = \chi_0 + c\,t. \tag{60}$$

Identifying effective spatial scales with accumulated relational differentiation yields a Hubble-like law [31, 32] with

$$H(t) \equiv \frac{1}{\chi}\,\frac{d\chi}{dt}, \tag{61}$$

where H_0 quantifies the current state of global relaxation.

Observational discriminant: Cosmochrony predicts a $\sim 5\%$ higher $H(z)$ at $z \sim 1$ compared to ΛCDM, testable with DESI/Euclid (Section 11.1).

Cosmic Acceleration Without Dark Energy.

The observed late-time acceleration does not require a cosmological constant. As structure formation proceeds, localized configurations increasingly constrain local relaxation, introducing growing spatial inhomogeneities. When interpreted within homogeneous and isotropic models, these inhomogeneities manifest as apparent acceleration. Cosmic acceleration is an emergent interpretative effect arising from progressively uneven relaxation across cosmic scales.

7.6 Cosmic Microwave Background

The CMB reflects the imprint of early relaxation and reprojection processes as the substrate transitioned toward a regime admitting stable geometric descriptions. Large-scale correlations arise from the global relational coherence of χ prior to geometric differentiation, rather than from superluminal expansion. Acoustic features are interpreted as resonance patterns arising once the standard photon–baryon plasma description becomes applicable [33–35].

Effective closure: primordial spectrum.

The standard Boltzmann transfer functions remain unchanged. Cosmochrony modifies the CMB spectra only through the primordial curvature spectrum:

$$C_\ell^{XY} = 4\pi \int_0^\infty \frac{dk}{k}\, P_\zeta(k)\, \Delta_\ell^X(k)\, \Delta_\ell^Y(k), \tag{62}$$

with a projectability-induced infrared filter and emergent tilt:

$$P_\zeta(k) = A_s \left(\frac{k}{k_*}\right)^{n_\chi - 1} C^2\!\left(\frac{k}{k_p}\right), \qquad C(x) \xrightarrow{x\ll 1} 0, \quad C(x) \xrightarrow{x\gg 1} 1. \tag{63}$$

Relational spectral scales and angular multipoles.

The admissibility cutoff can be expressed in terms of the low-lying spectrum of the relational operator L_χ (Section 2.4):

$$k_n \;\propto\; \sqrt{\lambda_n(\lambda_*)}, \qquad \ell_n \;\approx\; k_n\, D_A(z_*), \tag{64}$$

yielding the robust ratio constraint

$$\frac{\ell_n}{\ell_1} \;\approx\; \sqrt{\frac{\lambda_n}{\lambda_1}}. \tag{65}$$

Numerical relaxation experiments (Appendix D.7) indicate $\lambda_2/\lambda_1 \simeq 8/3$, implying $\ell_2/\ell_1 \approx 1.63$, searchable as a scale-independent modulation signature in the low-ℓ sector. These ℓ_n characterize relational angular modulations associated with admissibility, not the acoustic peak indices of the photon–baryon plasma.

7.7 Dark Matter as Residual Relaxation Effects

Dark matter phenomena correspond to configurations of χ that resist relaxation while failing the projectability conditions required for Standard Model interactions. These **non-projected spectral modes** possess inertial mass and contribute to gravitational curvature while remaining invisible to electromagnetic or electroweak probes.

Galactic Rotation and Effective Spectral Stiffness.

The flattening of rotation curves is interpreted as a spatial variation of G_{eff} induced by the local relaxation state. At large radii, a transition in the effective spectral stiffness leads to a logarithmic gravitational potential, reproducing MOND-like behavior without invoking a modification of gravity or a universal acceleration scale. Unlike the universal constant a_0 in MOND, the transition threshold $\mathcal{K}_c$ is local and environment-dependent, naturally explaining the observed variation of the apparent dark matter fraction among galaxies.

Gravitational Lensing and Substrate Memory.

Lensing phenomena (e.g. the Bullet Cluster) are manifestations of **relaxation lag**: the projective geometry associated with mass-solitons persists after baryonic gas has lost coherence. Light deflection is treated as effective refraction within the spectral gradient of the projected χ geometry.

Predictive Distinction from Particulate Dark Matter.

Cosmochrony predicts non-local correlations between gravitational mass discrepancies and the global spectral age of a system, the absence of sharp central cusps, a minimum smoothing scale imposed by the spectral response, and **spectral echoes**—faint gravitational signatures in regions where matter was previously present.

7.8 Entropy and the Arrow of Time

The arrow of time is a fundamental structural feature arising from the intrinsic monotonic relaxation ordering of χ, not a derived statistical phenomenon. Entropy increase emerges only at the level of effective spacetime descriptions, providing a statistical summary of how macroscopic degrees of freedom evolve under the irreversible relaxation of χ. Entropy growth does not explain the arrow of time; it reflects the underlying temporal asymmetry already present in the substrate.

This reverses the standard explanatory hierarchy: time asymmetry is imposed intrinsically by the relaxation structure, not attributed to special initial conditions. Processes involving deprojection do not correspond to entropy decrease or temporal reversal but represent a transition to a level of description where thermodynamic notions no longer apply.

7.9 Cosmic Voids as Maximal Relaxation Probes

Cosmic voids are regions where the relaxation of χ is least frustrated by localized excitations. Within the effective description (Section 3.4), near-maximal substrate relaxation produces enhanced geodesic defocusing, leading to a negative gravitational lensing signal and non-linear peculiar velocity outflows at void boundaries—effects absent or suppressed in ΛCDM.

Connection to local H_0 determinations.

Enhanced outward peculiar velocities at void boundaries can bias low-redshift distance–redshift inferences toward higher locally inferred expansion rates. A decisive test is the cross-correlation between void lensing profiles and locally inferred H_0 maps.

Phenomenological void parametrization.

Observable void signals are modeled as a ΛCDM baseline plus a saturating correction controlled by a single dimensionless amplitude $\beta_{\rm void}$:

$$\kappa_{\rm obs}(R) = \kappa_{\Lambda\rm CDM}(R)\left[1 + \beta_{\rm void}\,\mathcal{S}\big(\mathcal{A}(R)\big)\right], \tag{66}$$

$$v_{\rm obs}(r) = v_{\Lambda\rm CDM}(r)\left[1 + \beta_{\rm void}\,\mathcal{S}\big(\mathcal{B}(r)\big)\right], \tag{67}$$

with $\mathcal{S}(x) = x/\sqrt{1+x^2}$ interpolating between linear and saturated regimes.

7.10 The Hubble Tension

The discrepancy between early- and late-universe determinations of H_0 is well established [35–38]. In Cosmochrony, different observational probes access different regimes of effective projectability. Early-universe measurements probe a regime close to the transition from maximal constraint to geometric projectability; late-time measurements probe a more weakly constrained regime where effective spacetime descriptions are more fully developed. The tension arises from using a single spacetime-based parametrization to describe observations sampling distinct stages of relational relaxation.

The Hubble Tension as a Diagnostic of Topological Decoherence

The effective Hubble parameter may be expressed as

$$H_{\text{eff}}(\mathbf{x}, t) \sim \frac{1}{\tau_\chi(\mathbf{x}, t)}, \tag{68}$$

where τ_χ is an effective relaxation timescale. Regions of high structural complexity (clusters, filaments) correspond to topologically frustrated configurations in which the relaxation timescale acquires a spatial dependence:

$$\tau_\chi(\mathbf{x}) = \tau_\chi^{(0)} \left[1 + \epsilon\, \mathcal{T}(\mathbf{x})\right], \tag{69}$$

where $\mathcal{T}(\mathbf{x})$ encodes local topological density. The tension reflects a non-commutativity between cosmological averaging and local projection.

Cosmochrony predicts that locally inferred values of H_0 should exhibit weak but systematic correlations with the surrounding topological environment. Quantitative estimates are provided in Section 11.1 and Appendix D.3.

7.11 Large-Angle Temperature Anomalies

Large-angle CMB anomalies—low-multipole power suppression and unexpected large-scale alignments—remain only partially explained within ΛCDM [39]. In Cosmochrony, these features are residual relational correlations inherited from the pre-geometric regime of χ.

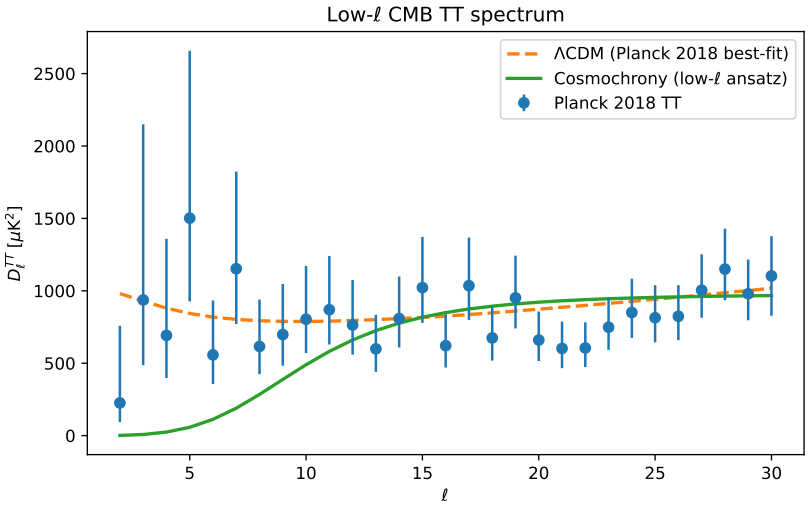

Fig. 8 Low-ℓ CMB TT power spectrum comparison. The Cosmochrony ansatz (green) shows natural suppression of power at large angular scales ($\ell < 10$) compared to ΛCDM (dashed orange).

A complementary unsmoothed representation, directly confronting the raw Planck low-ℓ data with the same attenuation mechanism, is provided in Appendix D.1 (Fig. 20).

Structural Admissibility and Low-ℓ Suppression

The primordial spectrum is modulated by an admissibility filter:

$$P_{\rm obs}(k,t) = \mathcal{A}^2(k,t)\, P_0(k), \tag{70}$$

with a natural phenomenological form

$$\mathcal{A}(k,t) = \exp\left[-\left(\frac{k_c(t)}{k}\right)^p\right], \tag{71}$$

where $k_c(t)$ is the coherence scale associated with the maximal size of projectively admissible configurations. For $k \ll k_c(t)$, power suppression arises from the structural impossibility of supporting such global modes within the available relational complexity. The scale $k_c(t)$ admits a graph-theoretic interpretation through the spectral gap $\lambda_2(t)$ of the effective connectivity graph.

Testable Predictions

A. Correlated Suppression Across TT, TE, and EE Spectra.

The coherence scale k_c should be consistent across temperature and polarization spectra. Future high-precision measurements (e.g. *LiteBIRD*) provide a decisive test.

B. Absence of Primordial Non-Gaussianities.

The framework predicts an exceptionally small $f_{\rm NL}$. A significant detection would falsify this scenario.

C. Scale-Dependent Spectral Tilt Near the Cutoff.

A mild running of n_s localized near k_c is expected. A detailed treatment is provided in Appendix D.1.

7.12 Effective Potential for Galactic Dynamics from χ-Relaxation Saturation

Operational status.

The effective potential is defined only through observable kinematics:

$$g_{\rm eff}(r) \equiv -\frac{d\Phi_{\rm eff}}{dr}, \qquad v^2(r) = r\,\frac{d\Phi_{\rm eff}}{dr}. \tag{72}$$

Emergent acceleration scale.

The nonlinear χ-relaxation constraint induces an effective background kinematic scale

$$a_0(t) \sim c\,H(t), \tag{73}$$

Aspect	**ΛCDM**	**MOND**	**Cosmochrony**
Ontology	Non-baryonic halo	Modified dynamics	Relaxation properties of χ
Flat rotation curves	Invisible mass	$g \simeq \sqrt{g_N a_0}$	Saturation: $g \simeq \sqrt{g_N a_0(t)}$
Key scale	Halo profile parameters	Universal a_0	Emergent $a_0(t) \sim cH(t)$
Tully–Fisher	Formation models	$v^4 \propto GM_b a_0$	$v^4 \propto GM_b a_0(t)$
Discriminating signature	Cusps vs. cores	Strict universality	Slow evolution of $a_0(t)$

Table 1 Conceptual comparison of flat-rotation-curve explanations.

weakly time-dependent, with a projection efficiency factor $\eta = O(0.1)$ for galactic dynamics.

Asymptotic regimes and flat rotation curves.

Let $g_N(r) = GM_b(r)/r^2$. In the high-acceleration regime ($g_N \gg a_0$), $g_{\rm eff} \simeq g_N$. In the low-acceleration regime ($g_N \ll a_0$), saturation yields

$$g_{\rm eff}(r) \simeq \sqrt{g_N(r)\, a_0(t)}, \tag{74}$$

implying

$$\Phi_{\rm eff}(r) \simeq \sqrt{GM_b\, a_0(t)}\, \ln\left(\frac{r}{r_s}\right) + \text{const.}, \tag{75}$$

a logarithmic potential producing asymptotically flat rotation curves. The transition radius is $r_s(t) = \sqrt{GM_b/a_0(t)}$.

Minimal smooth interpolation.

A parsimonious operational fit function is

$$g_{\rm eff}(r) = \sqrt{g_N(r)^2 + a_0(t)\, g_N(r)}. \tag{76}$$

Baryonic Tully–Fisher scaling.

In the deep-saturation regime:

$$v_\infty^4 \simeq G\, M_b\, a_0(t), \tag{77}$$

with a mild redshift dependence through $a_0(t) \sim cH(t)$.

Observed rotation curves: multi-galaxy test

The Cosmochrony prediction is confronted with observed rotation curves of NGC 3198 (flat), NGC 2403 (rising), and NGC 5055 (mildly declining). No dark matter halo is introduced. Baryonic contributions are taken from the literature; the only fitted parameter is the stellar mass-to-light ratio $\Upsilon_\star$. The acceleration scale is fixed by $a_0(t_0) \sim cH(t_0)$.

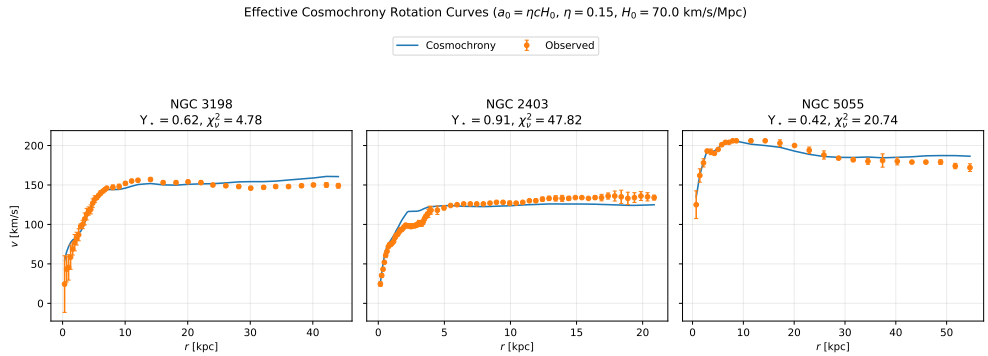

Fig. 9 Observed rotation curves compared with the Cosmochrony saturation prediction. Left: NGC 3198. Center: NGC 2403. Right: NGC 5055. See Appendix E.8 for data sources.

7.13 Summary

Cosmological phenomena emerge from the global relaxation ordering of χ. Cosmic expansion, large-scale homogeneity, late-time acceleration, and the arrow of time arise naturally from the relaxation process, without invoking an inflationary phase, dark energy, or an initial spacetime singularity. The Big Bang is a limiting regime of maximal constraint; black holes represent localized reapproaches to the same descriptive boundary. At the effective level, the framework reproduces the Hubble law, CMB structure, and large-scale gravitational behavior as emergent consequences of a single relational relaxation process.

Part IV
Quantum Mechanics

This part presents a unified treatment of quantum phenomena as consequences of non-injective projection rather than as fundamental departures from classical logic. Quantum correlations, indeterminacy, and entanglement are derived from the structural non-factorizability of projected χ descriptions.

Violations of Bell inequalities are interpreted as signatures of ontological projection failure, not as evidence of superluminal influences. Measurement, decoherence, and apparent wave-function collapse are described as context-dependent stabilization processes within projected regimes.

The relation to the standard quantum formalism is clarified, including the emergence of Hilbert space structure, effective Schrödinger dynamics, and the Born rule. Quantum mechanics is thus situated as a consistent and predictive effective framework arising from deeper relational constraints.

8 Quantum Phenomena and Entanglement

Building on the non-injectivity of the projection Π (Section 2.4), this section shows how entanglement, nonlocal correlations, measurement statistics, and the formal apparatus of quantum mechanics emerge without introducing additional ontological degrees of freedom. The framework adopts **ontological monism**: there is a single ontological substrate χ, while apparent multiplicity and spatial separation are properties of the projected description.

8.1 Non-Factorizable Projected Descriptions and Quantum Correlations

A single admissible configuration of χ may correspond to multiple distinct effective degrees of freedom. What appear as separate particles or subsystems are multiple projective manifestations of a single underlying ontological configuration. Effective degrees of freedom cannot be assigned independent states; any admissible description must be globally consistent with the underlying χ configuration, leading to persistent correlations that do not rely on signal exchange or spacetime proximity.

Ontological Monism and the Shared Projection Hypothesis

A single connected excitation in χ can be represented as several spatially separated effective excitations. The observed separation is a property of the projected metric representation, not a fundamental separation of the underlying entity.

Shared Fiber Phase and Spin Correlations.

Spin correlations can be read as correlations of a *shared* internal degree of freedom of the projection fiber. A measurement at one location selects a locally stable reprojection of that shared fiber degree of freedom; the correlated statistics at the distant location reflect the restricted set of reprojections still compatible with the same underlying configuration.

8.2 Nonlocality and the Holistic Character of Projected Descriptions

Quantum nonlocality does not arise from superluminal interactions but reflects the intrinsically non-factorizable character of certain admissible projected descriptions [40]. Entangled systems correspond to single projected configurations that cannot be decomposed into independent subsystems without loss of admissibility.

8.3 Nonlocal Correlations Without Superluminality

Correlated outcomes arise because spacelike separated measurements correspond to different local reprojections of a single non-factorizable description. The factorization assumptions underlying Bell-type inequalities are violated, while dynamical locality and relativistic causality remain intact (see Appendix F.2). The correlations are *ontological*—fixed by the non-injective global relational structure—rather than *dynamical*.

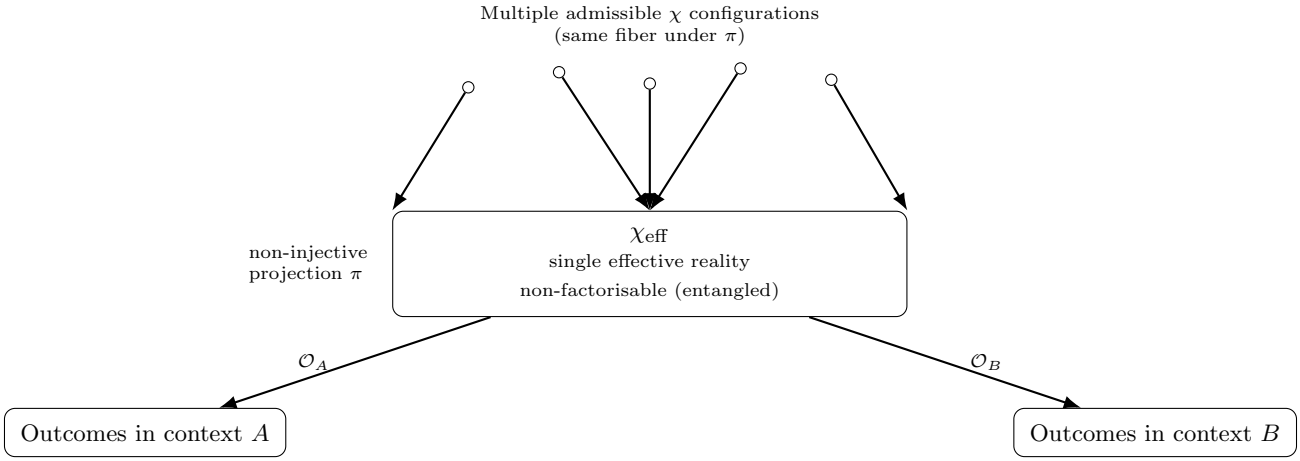

Fig. 10 Entangled (non-factorisable) regime. Multiple underlying χ configurations map to the same χ_{eff}. Different measurement contexts define distinct operational projections producing correlated outcomes without introducing multiple effective realities.

Attosecond-resolved measurements have demonstrated that quantum correlations become experimentally accessible on timescales far shorter than any interaction-based mechanism [41]. Within Cosmochrony, the observed timescale corresponds to the resolution time of the effective projection Π, not to a physical propagation time: it probes projective accessibility rather than dynamical formation of correlations.

8.4 Temporal Ordering and Relativistic Consistency

Temporal ordering arises only at the effective level. Different observers may assign different orderings to spacelike separated events; such differences reflect observer-dependence of spacetime slicing and have no impact on the relational consistency of admissible descriptions. Relativistic covariance is preserved by the invariance of the underlying non-injective relational configuration across all admissible projected descriptions.

8.5 Relation to Bell Inequalities

Bell's theorem [40] rules out any ontological completion of quantum mechanics based on factorizable hidden-variable models. Cosmochrony fully accepts Bell's theorem and identifies the ontological assumption that fails: the factorization hypothesis $P(a, b|x, y, \lambda) = P(a|x, \lambda)\, P(b|y, \lambda)$.

Because the projection Π is generically non-injective, admissible projected states are not associated with independent ontic pre-images for their subsystems. The factorization hypothesis is not merely violated but *ill-defined* within the space of admissible projected descriptions.

Bell-type violations arise in an intermediate regime of projective compression: the effective description is sufficiently coarse-grained to permit subsystem separation, yet

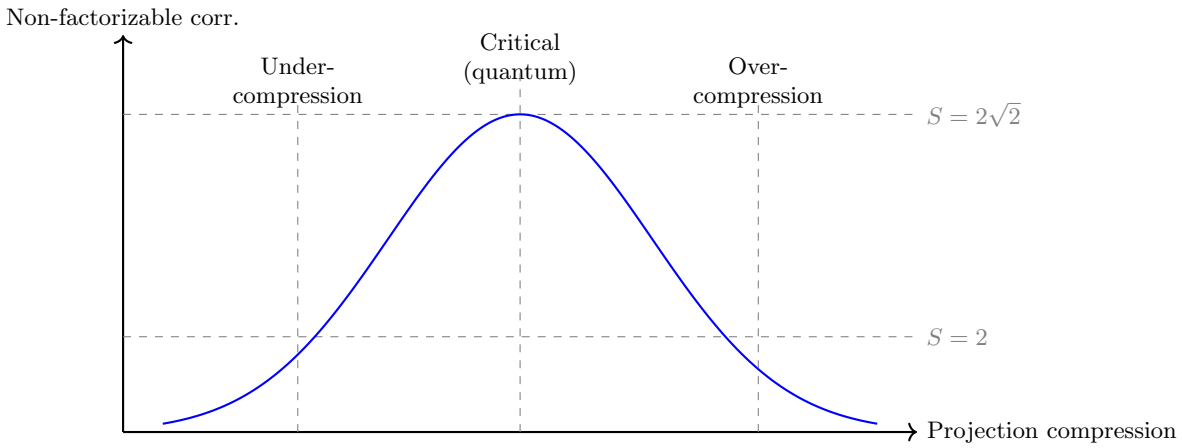

Fig. 11 Bell inequality violations as a function of the compression induced by Π. Non-factorizable correlations emerge in an intermediate regime.

retains enough global relational structure to prevent factorization. In the limit of extreme coarse-graining, projected descriptions become effectively classical.

No hidden variables and no superluminal influence are introduced. Quantum nonlocality is ontological rather than dynamical: the failure of Bell-type factorizability arises from the structure of admissible projected descriptions, not from nonlocal interaction.

8.6 Measurement, Decoherence, and Apparent Collapse

Quantum measurement does not involve fundamental wavefunction collapse. Measurement corresponds to the transition from a non-factorizable admissible projected description to a set of effectively factorized local projections. Decoherence suppresses interference between incompatible descriptive branches by rendering their relative phase information inaccessible within spacetime representations [42]. The underlying relational structure remains globally well defined. The apparent collapse is the effective manifestation of a non-injective relational structure becoming only partially projectable into spacetime.

8.7 Limits of Entanglement and Environmental Effects

Entanglement arises only within restricted regimes in which a non-factorizable global description remains jointly projectable. Environmental coupling progressively restricts the set of admissible projected descriptions to locally stable, approximately factorizable regimes. Entanglement is most robust for effectively isolated systems and becomes increasingly fragile in macroscopic environments. Classical behavior emerges when only factorized projected descriptions remain admissible, without requiring any modification of the underlying relational structure.

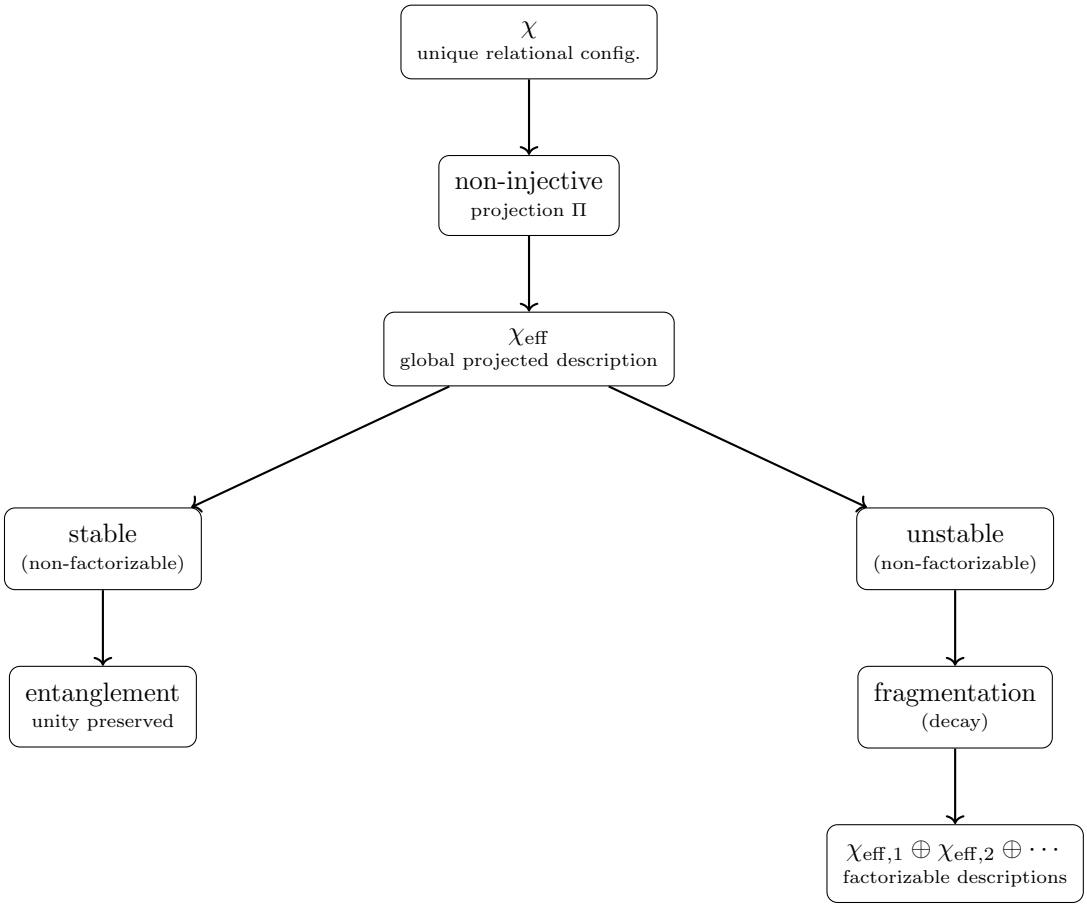

Fig. 12 Conceptual branching induced by non-injective projection. Stable non-factorizable descriptions manifest as entanglement; unstable ones fragment into localized factorizable descriptions (particle decay).

8.8 Structural Stability of Projected Descriptions

Entanglement, measurement, and decay correspond to distinct stability regimes of projected descriptions. Entanglement corresponds to the regime in which a non-factorizable projected description remains structurally stable. Measurement and decoherence correspond to selective stabilization: interaction with an environment amplifies certain relational features while rendering alternative descriptions inadmissible. Particle decay represents the regime in which the non-factorizable description becomes unstable, and stability is recovered through factorization into several localized configurations.

A technical analysis is provided in Appendix C.14.

8.9 Entanglement as a Critical Regime of Projective Compression

Quantum entanglement arises as a structural consequence of the non-injective projection $\Pi : \chi \to \chi_{\text{eff}}$. The projection reduces a high-dimensional relational configuration to a lower-dimensional effective description; the resulting fiber $\Pi^{-1}(\chi_{\text{eff}})$ constitutes an information-theoretic channel whose bandwidth depends on unresolved modes of χ.

Non-factorizable correlations emerge only in an intermediate *critical* regime of projective compression: the effective description is sufficiently coarse-grained to permit subsystem identification, yet retains enough global relational structure to prevent full factorization. Increased compression (environmental coupling, decoherence) suppresses correlations, yielding classical behavior; decreased compression breaks subsystem separation. The critical regime may be intermittent, with correlations appearing during specific spectral reconfiguration events (Appendix E).

8.10 Implications for Quantum Computation

Effective resources exploited in quantum computation may be reinterpreted as manifestations of structural non-injectivity and global consistency constraints. Multiple underlying relational configurations may correspond to the same effective observable state, providing a natural origin for effective parallelism without explicit information exchange. Part of the computational advantage may reflect general properties of non-factorizable descriptive mappings rather than exclusively quantum dynamical effects.

8.11 Integration with the Standard Model: A Spectral Interpretation

Weak Boson Masses from Spectral Geometry

The masses of $W^{\pm}$ and Z^0 emerge from the spectral properties of the Hodge Laplacian Δ_1 acting on 1-forms of the fiber bundle Π. The space of 1-forms decomposes into gauge-invariant subspaces $\Omega^1_{SU(2)}$ and $\Omega^1_{U(1)}$. Effective masses are

$$m_W \propto \sqrt{\lambda_{1,SU(2)}}, \qquad m_Z \propto \sqrt{\lambda_{1,U(1)}},$$

with the mass ratio governed by the metric anisotropy and curvature structure of the χ-induced geometry on Π.

Emergent Gauge Couplings

Gauge couplings are defined through normalized heat-kernel traces:

$$g^2 = 4\pi \left[\widehat{\mathrm{Tr}}_{SU(2)}\big(e^{-t_0 \Delta_{SU(2)}}\big) - \widehat{\mathrm{Tr}}_{U(1)}\big(e^{-t_0 \Delta_{U(1)}}\big) \right],$$

$$g'^2 = 4\pi\, \widehat{\mathrm{Tr}}_{U(1)}\big(e^{-t_0 \Delta_{U(1)}}\big),$$

with $t_0 = L^2_{\text{fiber}}$. The Weinberg angle follows from spectral asymmetry:

$$\tan^2 \theta_W = \frac{\widehat{\text{Tr}}_{U(1)}(e^{-t_0 \Delta_{U(1)}})}{\widehat{\text{Tr}}_{SU(2)}(e^{-t_0 \Delta_{SU(2)}})}.$$

Geometric Phase Transition and Mass Generation

Mass generation is a geometric phase transition of the χ substrate. Below a critical spectral density χ_{crit}, only massless modes are supported. Above it, spectral weight condenses into specific invariant subspaces, generating discrete non-zero eigenvalues $m_n \propto \sqrt{\lambda_n}$.

Strong Sector: Topological Confinement and Color

Color charge maps to the three fundamental degrees of freedom of the proton's trefoil topology ($Q = 3$). Topological confinement: separating components of a $Q = 3$ soliton requires linear energy increase exceeding the pair-creation threshold. Asymptotic freedom: at short distances the global topological constraint is not yet engaged, rendering the interaction effectively weaker.

The Origin of Mass: Spectral Overlap

Fermion masses are emergent quantities determined by the resonance between internal stability spectra and the global relaxation flux:

$$m_{\text{eff}} \propto \int_{\text{Fiber}} \mathcal{S}(\phi_n) \cdot \mathcal{R}(\chi)\, d\Pi. \tag{78}$$

Multiple fermion generations correspond to distinct stable topological classes of solitonic χ-configurations. The mass hierarchy $m_e \ll m_\mu \ll m_\tau$ arises from the ordered spectrum of L_{sol}:

$$m_n \sim \text{Spec}(L_{\text{sol}})_n. \tag{79}$$

Mixing matrices (CKM, PMNS) encode the misalignment between the mass basis (eigenvectors of L_{sol}) and the interaction basis (principal axes of Π). CP violation originates from non-trivial topological torsion of the projection fiber.

8.12 Relation to Quantum Formalism

The formal apparatus of quantum mechanics arises as an effective framework organizing admissible projected descriptions in regimes where localization, linearity, and approximate factorization hold. Quantum mechanics is not replaced but reinterpreted as an effective theory whose validity is restricted to regimes admitting a stable, approximately linear, spacetime-based description.

Status of the Wavefunction.

The wavefunction ψ is not a fundamental physical entity but a statistical encoding of admissible local reprojections compatible with a given non-factorizable projected

configuration. Its complex phase encodes relational constraints between alternative local descriptions; its modulus determines the statistical weight of accessible reprojections.

Emergence of Hilbert Space Structure.

In regimes where relational constraints are weak and approximately factorizable, distinct admissible descriptions can be combined, giving rise to approximate linear structure. Superposition reflects the formal coexistence of compatible descriptive alternatives. The inner product encodes mutual compatibility; orthogonality corresponds to mutually exclusive descriptive regimes. Unitary evolution is a consistency-preserving transformation valid as long as projectability and factorizability remain intact.

Emergence of the Schrödinger Equation.

In the non-relativistic regime, separating a rapidly varying rest-energy phase from a slowly varying envelope yields

$$i\hbar\,\partial_t\psi = -\frac{\hbar^2}{2m}\nabla^2\psi + V(x)\psi. \tag{80}$$

Operators and Non-Commutativity.

The canonical commutation relation $[\hat{x}, \hat{p}] = i\hbar_{\text{eff}}$ expresses the non-commutativity of geometric measurements induced by projection from the pre-geometric substrate. The uncertainty principle emerges as a geometric consistency condition on admissible effective descriptions.

This canonical non-commutativity operates at the level of effective spacetime observables. It should be distinguished from the spectral and sectorial non-commutativities discussed in Sections 10.2 and 10.4, which arise within the projection fiber itself and manifest respectively as inertial mass and CP-violating geometric phases.

Origin of Quantization.

Only a restricted class of localized projected configurations admits long-lived, internally consistent descriptions. Admissible configurations form discrete equivalence classes, yielding effective energy quantization. Planck's constant emerges as a universal conversion factor characterizing the minimal structural scale at which projected descriptions remain stable.

Measurement and the Born Rule.

Measurement outcomes correspond to effective reprojections onto mutually exclusive descriptive regimes. The Born rule emerges as the unique stable measure on the space of admissible projected descriptions that remains invariant under loss of phase coherence, coarse-graining, and environmental coupling.

Entanglement and Nonlocal Correlations.

Entangled systems arise when a unified relational configuration admits an effective projection onto spatially separated degrees of freedom. Correlations are fully compatible with relativistic causality (Appendix F.2).

Spin and Statistics.

Spin emerges as a topological property of admissible projected configurations. 4π-periodic configurations correspond to fermionic behavior; 2π-periodic ones to bosonic behavior. The spin–statistics connection follows from the same topological constraints (Appendix C.4).

Orbital Geometry as Probabilistic Visibility.

Atomic orbitals correspond to effective probabilistic visibility patterns of admissible projected descriptions. Regions of high probability correspond to domains where consistent reprojection is most robust; nodal regions correspond to incompatible descriptive regimes.

Scope and Limitations.

All standard quantum-mechanical formalisms remain valid and unchanged within their domains. Cosmochrony provides an interpretative and unificatory account of the structural origin of quantum phenomena without introducing new degrees of freedom or hidden variables. A complete formal correspondence between the relational substrate and the operator-based structures of quantum theory is left for future work.

8.13 Summary

Gauge interactions emerge as admissible modes of the projection process. The photon corresponds to scalar transmission modes; $W^{\pm}$ and Z^0 bosons arise as shear-like spectral modes whose masses reflect the spectral rigidity of the projection fiber. Strong interactions and confinement are reinterpreted through topological stability of knotted solitonic configurations. Mass emerges from spectral overlap between localized configurations and the global relaxation flux. Entanglement and nonlocal correlations reflect the persistence of non-factorizable admissible projected descriptions. Quantum mechanics appears as an effective statistical framework describing the limits of local projectability imposed by a globally non-injective relational structure. Classical behavior emerges as the limiting case in which only locally stable, factorizable projected descriptions remain admissible.

Part V
Predictions, Discussion, and Conclusion

This final part collects the phenomenological consequences of the Cosmochrony framework and confronts them with observation. Radiation processes, mass spectra, and quantization effects are revisited from a unified structural perspective, leading to concrete and falsifiable predictions.

Testable signatures are identified across cosmology, gravitation, particle physics, and high-energy regimes, with particular attention to discriminating Cosmochrony from ΛCDM-based models and standard quantum-gravitational extensions.

The concluding discussion situates Cosmochrony with respect to existing theoretical frameworks, clarifies its domain of validity, and highlights open challenges. Rather than proposing a final theory, this part frames Cosmochrony as a coherent pre-geometric research program constrained by internal consistency and empirical accessibility.

9 Radiation and Quantization

9.1 Radiation as χ–Matter Interaction

Radiation arises when a localized, relaxation-resistant configuration undergoes a transition toward a less constrained state. The excess relational content ceases to admit a particle-like projected description and becomes expressible only through delocalized projected modes. In effective spacetime descriptions, this redistribution appears as radiative emission—a transfer of descriptive weight from particle-like configurations to propagating field-like descriptions, without invoking discrete objects or stochastic processes.

9.2 Emergence of Photons

Photons are not fundamental entities. Prior to emission or detection, no photon exists as an independent object. A reconfiguration of relational structure within χ ceases to admit a localized projection and becomes expressible only through extended, delocalized effective modes—represented in spacetime as electromagnetic waves.

Photon-like events emerge only at interaction: when a delocalized projective mode becomes locally constrained by interaction with a localized excitation, the projection resolves into a discrete transfer of relaxation capacity. Quantization is a property of interaction and local reprojection, not of propagation. Wave–particle duality reflects a duality of description rather than of underlying ontology. Interference phenomena arise from the coherence of delocalized projective modes; individual detection events correspond to localized reprojections.

In contrast to the coherent composite regime discussed in Section 5.7, photon modes correspond to linear excitations around the unsaturated fiber sector

9.3 Geometric Origin of $E = h\nu$

Building on Section 4.5, the Planck relation

$$E = h\nu \tag{81}$$

acquires a geometric interpretation in the context of radiative processes. The energy E measures the relaxation potential redistributed during a reprojection event; the frequency ν characterizes the minimal temporal resolution required for a coherent effective description of this redistribution. The constant h is the effective projection of the fundamental substrate invariant $\hbar_\chi \equiv c^3/(K_{0,\mathrm{bare}}\,\chi_{c,\mathrm{bare}})$ (Section E.6), acting as a universal conversion factor between structural relaxation capacity and temporal projective resolution.

In the photoelectric effect, the threshold frequency ν_0 corresponds to the minimal projective resolution required to destabilize a bound electronic soliton. Quantization of radiative energy arises not from discretized propagation but from the discrete nature of local reprojection events, which impose a minimal unit of effective relaxation transfer determined by the spectral graininess $\hbar_\chi$.

9.4 Vacuum Fluctuations and the Casimir Effect

Vacuum fluctuations reflect the intrinsic structural indeterminacy of χ in regimes where no stable localized excitations are present. The relaxation admits a wide range of locally compatible projective descriptions; these fluctuations represent variability of effective descriptions rather than physical energy stored in the vacuum.

When material boundaries impose structural constraints on local projectability, certain effective descriptions become incompatible with the boundary conditions, reducing the set of admissible projective configurations between the boundaries. The Casimir effect arises from this asymmetry: a difference in the density of admissible effective reprojections, manifesting as a pressure on the confining surfaces. No fundamental vacuum energy density or propagating vacuum modes are required.

9.5 Weakly Interacting Radiation

Weakly interacting radiation corresponds to delocalized projective regimes whose structural contrast is insufficient to efficiently induce localized reprojection upon encountering matter. Low-frequency or weakly coupled modes are characterized by smooth, slowly varying relational structure, strongly suppressing the probability of stable localized energy transfer. Small interaction cross sections reflect the low likelihood that a given projective configuration satisfies the geometric and topological conditions required for localized reprojection.

9.6 Summary

Radiation and quantization arise from interactions between localized matter excitations and the χ substrate. Photon-like events emerge only during interaction-induced reprojection. Quantization reflects geometric and topological constraints of the relaxation dynamics at the level of projection: discrete energy transfer occurs when continuous projective descriptions satisfy the conditions required for localized reprojection.

10 Spectral Mass Spectrum and Hierarchy

10.1 Spectral Stability and the Unit of Mass

Rest mass is a spectral invariant associated with the stability of admissible projected configurations. It is identified with the fundamental eigenmode of the scalar Laplacian $\Delta_G^{(0)}$ acting on the projection fiber Π, subject to topological constraints $\mathcal{T}$:

$$m^2c^2 \;=\; \lambda_{\mathcal{T}} \;\equiv\; \mathrm{Eig}\Big(\Delta_G^{(0)}\Big)\,\Big|_{\mathcal{T}}. \tag{82}$$

Here $\lambda_{\mathcal{T}}$ encodes the minimal energetic cost required to maintain the configuration against the global relaxation of χ. Mass therefore quantifies resistance to relaxation.

The electron mass m_e corresponds to the lowest non-trivial admissible eigenmode λ_1, representing the fundamental resonance of χ within the finite-volume geometry $\Pi \cong S^3$. The conversion to physical mass units is

$$m \;=\; m_e\sqrt{\frac{\lambda_{\mathcal{T}}}{\lambda_1}}. \tag{83}$$

10.2 Non-Commutativity as a Source of Mass

Torsion acts as a dynamical constraint that competes with relaxation transport through the projection fiber.

Inhibition of Relaxation

Let Ω_w be the effective torsion operator associated with winding number w. For the fundamental lepton configuration ($w = 1$), relaxation and torsion are spectrally compatible:

$$[\Delta_G^{(0)}, \Omega_1] = 0. \tag{84}$$

For higher-winding configurations ($w \geq 2$), torsional constraints become spectrally frustrated:

$$[\Delta_G^{(0)}, \Omega_w] \neq 0 \qquad (w \geq 2). \tag{85}$$

This non-commutativity inhibits uniform relaxation across the fiber and induces irreducible spectral compression, manifesting as amplified inertial mass. The torsional action is a purely spectral invariant:

$$\mathcal{A}(w) \;\equiv\; \frac{1}{2}\ln\left(\frac{\det\Big(\Delta_G^{(0)} + \Omega_w\Big)}{\det\Big(\Delta_G^{(0)}\Big)}\right), \tag{86}$$

where the determinant is understood in the zeta-regularized sense.

The Pisano Ratio as a Stability Fixed Point

For $w = 2$, the projection fiber ceases to be spectrally isotropic and splits into competing sectors $\Pi = \Pi_{\parallel} \oplus \Pi_{\perp}$. Dynamical stability selects the most irrational admissible ratio

between their spectral frequencies, in analogy with KAM-type criteria:

$$\frac{\lambda_{\parallel}}{\lambda_{\perp}} = \varphi \qquad \Longrightarrow \qquad \beta \equiv \frac{1}{\varphi}, \tag{87}$$

where $\varphi = (1+\sqrt{5})/2$ is the golden ratio.

Leptonic Spectrum Synthesis

For the muon, non-commutative torsion yields the parameter-free prediction

$$\boxed{\frac{m_\mu}{m_e} = \sqrt{\frac{\lambda_2}{\lambda_1}} \cdot \frac{3}{2\alpha} \cdot \frac{1}{\varphi}} \qquad \text{with} \qquad \frac{\lambda_2}{\lambda_1} = \frac{8}{3}. \tag{88}$$

The robustness of the ratio $\lambda_2/\lambda_1 = 8/3$ is demonstrated independently in Appendix E.7.

10.3 Gravitational Shadows and the Spectral Wake

The torsional constraint Ω_w induces an extended spectral deformation of the surrounding substrate—a persistent modification of the local spectral density of relaxation modes, referred to as a *spectral wake* or gravitational shadow. This shadow does not correspond to additional matter or propagating degrees of freedom, but to a long-lived redistribution of relaxation capacity induced by the topological obstruction. It provides an ontological basis for phenomena usually attributed to dark matter without introducing new particles.

Two characteristic features emerge. *Elastic remanence*: the deformation persists under displacement of the baryonic configuration, accounting for the observed offsets in systems such as the Bullet Cluster. *Non-local susceptibility*: when the local gradient falls below $a_0 \sim cH_0$, the substrate response transitions from linear to non-linear, recovering MOND-like phenomenology as an emergent phase of spectral response. Dark matter effects are thus reinterpreted as manifestations of persistent spectral memory in the relational substrate.

10.4 Flavor Structure and CP Violation

The spectral interpretation of mass developed in the preceding sections naturally extends to the structure of flavor. In the present framework, distinct fermionic generations correspond to spectrally separated relaxation modes of the same projection fiber Π, whose geometry was introduced in Section 5.1. The associated eigenvalues determine the relaxation energy of the projected configurations and are therefore directly related to the inertial masses defined in Eq. (24).

Spectral non-degeneracy and the $n = 3$ threshold.

Let $\{\lambda_i\}$ denote the spectral eigenvalues governing three distinct relaxation modes. If two eigenvalues become degenerate,

$$\lambda_i = \lambda_j,$$

the corresponding subspace admits a rotational freedom, allowing any accumulated phase to be reabsorbed by a redefinition of the projected basis. No irreducible CP-odd invariant remains.

The existence of a non-trivial CP-violating sector therefore requires at least three spectrally distinct modes. The threshold $n \geq 3$ signals that the projective holonomy of the flavor sector can no longer be embedded in a two-dimensional manifold. An irreducible geometric phase becomes unavoidable once the spectral complexity of the fiber exceeds this minimal bound.

Dual spectral hierarchies.

In the Standard Model, CP violation depends on the incompatibility between the up-type and down-type quark sectors. Within Cosmochrony, this structure is interpreted as the non-alignment of two sectorial spectral restrictions of the same projection fiber.

Let Π_u and Π_d denote the effective operators selecting the up-type and down-type relaxation modes from the admissible spectral subspace of $\Pi \cong S^3$. These operators do not define independent geometries; they act within the same projection fiber but correspond to distinct spectral extractions.

Because the projected state U has finite descriptive capacity, characterized by the bandwidth constraint b_χ, the two extraction channels cannot in general be simultaneously diagonalized. They compete for the same relational degrees of freedom. This induces a structural non-commutativity,

$$[\Pi_u, \Pi_d] \neq 0,$$

reflecting the operational mismatch between the two flavor sectors.

Cubic commutator invariant.

The physically relevant CP-odd quantity is identified with the imaginary part of the trace of the cubic commutator,

$$\mathcal{J} \propto \mathrm{Im}\,\mathrm{Tr}\big([\Pi_u, \Pi_d]^3\big). \tag{89}$$

The cubic order is minimal for which the invariant vanishes identically in a two-generation system and becomes non-trivial only when three independent generations are present. If the sectorial operators commute, $[\Pi_u, \Pi_d] = 0$, then $\mathcal{J} = 0$ and CP symmetry is effectively restored, even in the presence of mass hierarchies.

When combined with the spectral separations $\lambda_{u,i}$ and $\lambda_{d,i}$, the CP-odd invariant scales structurally as

$$\mathcal{J} \propto \mathrm{Im}\,\mathrm{Tr}([\Pi_u, \Pi_d]^3) \prod_{i<j} (\lambda_{u,i}^2 - \lambda_{u,j}^2) \prod_{k<l} (\lambda_{d,k}^2 - \lambda_{d,l}^2).$$

Degeneracy in either sector suppresses the invariant, recovering the structural constraint known from the Jarlskog formulation of the Standard Model.

On the magnitude of the invariant.

The experimentally observed smallness of the Jarlskog invariant, $\mathcal{J} \sim 3 \times 10^{-5}$, suggests that the flavor sector operates near a *quasi-commutative fixed point* of the projection algebra. Within Cosmochrony, this is interpreted as a structural constraint: global operational closure favors approximate alignment of sectorial spectral restrictions, thereby minimizing projective non-commutativity.

Let the misalignment between the up-type and down-type operators be characterized by a dimensionless parameter $\epsilon \ll 1$ such that

$$[\Pi_u, \Pi_d] \sim \epsilon\, K,$$

where K denotes a normalized operator in the flavor algebra. Since the physically relevant CP-odd quantity is cubic in the commutator, one obtains

$$\mathcal{J} \propto \mathrm{Im}\,\mathrm{Tr}([\Pi_u, \Pi_d]^3) \sim \mathcal{O}(\epsilon^3). \tag{90}$$

The cubic dependency provides a natural geometric mechanism for suppressing CP violation. Even a moderate primary misalignment (e.g. $\epsilon \sim 10^{-2}$) is sufficient to generate an invariant of order $\mathcal{J} \sim 10^{-6}$, consistent with the observed hierarchy.

Fixed-point stability and alignment residue.

We postulate that the flavor sector is attracted toward a regime of minimal non-commutativity compatible with spectral separation. The residual parameter ϵ can be interpreted as the minimal misalignment compatible with maintaining spectral non-degeneracy among the three generations. In this view, the Jarlskog invariant is not a fine-tuned constant but a *topological compression*: the projection of a three-generation spectral fiber onto a smooth manifold U necessarily generates a small but non-vanishing geometric twist, whose cubic magnitude explains the precision-scale character of CP violation in particle physics.

A first-principles derivation of ϵ from the dynamics of χ remains an open problem.

Structural interpretation.

Within Cosmochrony, CP violation is not introduced as an independent complex phase. It emerges as a geometric residue of incompatible spectral extractions from a single relational substrate. The non-commutativity of the sectorial operators reflects the finite

projective capacity of the fiber and the impossibility of simultaneously synchronizing distinct relaxation hierarchies within one global ordering.

This construction provides a structural reconstruction of the CP-violating sector. A full derivation of the numerical value of the invariant would require an explicit characterization of the operator space of the projection fiber and of the constraints imposed by the bandwidth parameter b_χ. Nevertheless, the emergence of a non-trivial cubic invariant at the three-generation threshold offers a geometric rationale for the observed structure of flavor mixing.

The non-commutativity considered here differs from the torsion–relaxation mismatch discussed in Section 10.2. There, the commutator operates within a single topological excitation and manifests as inertial mass. Here, it arises between distinct sectorial spectral restrictions of the same projection fiber and manifests as a CP-odd geometric phase. Both effects reflect different levels of the same finite projective capacity constraint.

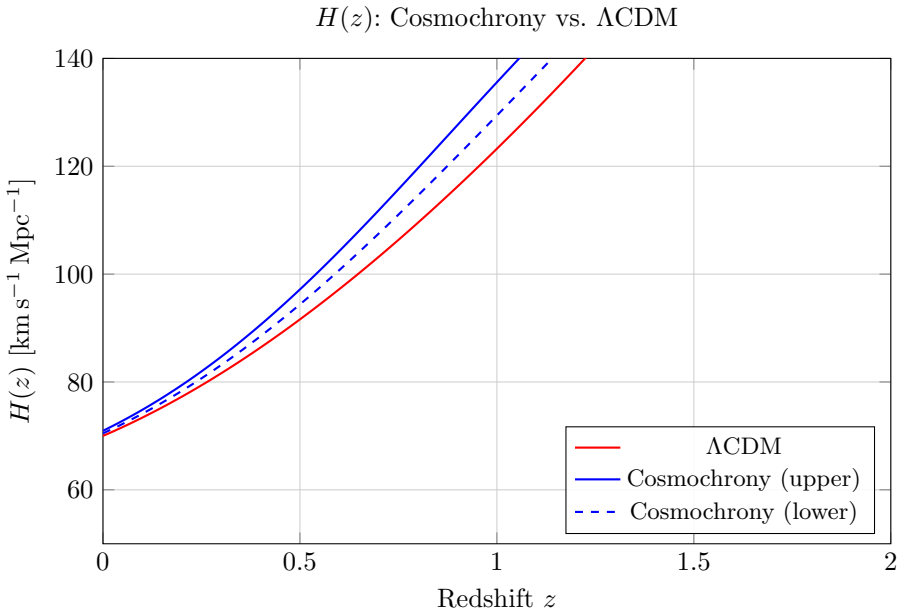

Fig. 13 Schematic comparison of $H(z)$. Cosmochrony predicts a mild enhancement at intermediate redshifts due to relaxation inhomogeneities.

11 Testable Predictions and Observational Signatures

Numerical estimates presented below are order-of-magnitude consistency estimates derived from the geometric coupling between the χ substrate and the effective relaxation fraction Ω_χ. Their role is to demonstrate that the framework operates within a phenomenologically relevant regime.

11.1 Hubble Constant from χ Dynamics

The Hubble parameter arises as an effective quantity:

$$H(t) = \frac{\dot{\chi}}{\chi}. \tag{91}$$

Assuming $\dot{\chi}_{\text{eff}} \simeq c$, the present-day value is $H_0 \simeq c/\chi(t_0)$. Early- and late-universe probes sample χ at different relaxation stages, naturally leading to systematically different inferred values of H_0 without invoking additional cosmological components.

Resolution of the Hubble tension.

The effective $H(z)$ acquires a mild redshift dependence departing from ΛCDM at intermediate redshifts ($0.1 \lesssim z \lesssim 10$), testable through upcoming BAO and supernova surveys.

11.2 Redshift Drift

Monotonic relaxation dynamics implies a slowly evolving cosmological redshift. The effective drift rate is

$$\dot{z}_{\text{eff}} \;\sim\; H_0(1+z) - \frac{c}{\chi(t)}, \tag{92}$$

corresponding to a secular variation of order $\Delta z \sim 10^{-10}\,\text{yr}^{-1}$ at $z \sim 1$, differing from ΛCDM at the $\sim 10\%$ level. Future extremely large telescopes equipped with ultra-stable spectrographs may probe this effect.

11.3 Gravitational Wave Propagation

In regions of high excitation density near compact objects, local suppression of χ relaxation modifies the persistence and coherence of gravitational-wave projective descriptions. This effect induces frequency-dependent phase shifts or amplitude suppression, rather than purely dissipative losses.

We predict a relative amplitude deviation from general relativistic templates scaling as

$$\frac{\Delta A}{A} \sim \left(\frac{r_s}{r}\right)^2,$$

where $r_s = 2GM/c^2$ is the Schwarzschild radius and r the effective propagation radius of the dominant ringdown mode.

For propagation at $r \approx 10\,r_s$, this yields

$$\frac{\Delta A}{A} \sim 10^{-2},$$

corresponding to a percent-level suppression of coherent gravitational-wave amplitudes relative to general relativity.

This deviation should manifest most clearly during the late-time ringdown phase of binary black hole mergers as a systematic, frequency-dependent mismatch with general relativistic ringdown templates. The effect preserves luminal propagation speed but alters coherence structure.

Falsifiability condition. If future high signal-to-noise detections (SNR $\gtrsim 100$) by space-based observatories such as LISA constrain $\Delta A/A < 10^{-3}$ at $r \sim 10\,r_s$, the present scaling law would be excluded at the predicted amplitude level.

11.4 Galaxy Rotation Curves from Structural Relaxation

Persistent relaxation gradients in the χ-substrate modify the effective inertial response of orbiting matter, producing approximately flat rotation curves without introducing dark matter components (Section 7.12). Observable consequences include a correlation between rotation curve flattening and indicators of structural relaxation activity, deviations from baryonic scaling relations in dynamically young galaxies, and a reduced need for fine-tuned dark matter profiles in low-surface-brightness systems.

11.5 Spin and Topological Signatures

If spin originates from topologically nontrivial configurations of χ (Section 4.6), ultra-high-precision interference experiments sensitive to 4π rotational symmetry may probe deviations associated with the internal topology of localized projectable configurations. Such deviations would appear as extremely small phase shifts under closed 2π versus 4π rotational cycles. These signatures are expected to be strongly suppressed and lie beyond current experimental resolution.

11.6 Absence of Dark Energy Signatures

Because cosmic acceleration emerges as a geometric consequence of global relaxation, no independent dark energy component is introduced. The framework predicts the absence of signatures associated with dynamical dark energy: no evolving equation of state, no clustering, no additional propagating degrees of freedom. The combined absence of these features, together with suppressed low-ℓ CMB power, specific angular correlations, and the absence of an inflationary tensor imprint at large angular scales, provides a potential observational discriminator.

11.7 CMB Polarization Signatures (Outlook)

Residual large-scale projective correlations inherited from the pre-geometric relaxation of χ are expected to imprint scale-dependent signatures on the CMB (Section 7.6). The observed $\sim 10\%$ suppression of the CMB quadrupole power relative to ΛCDM arises naturally from these relaxation dynamics [43]. Appendix D.1 provides quantitative estimates.

The* $8/3$ *Scaling in CMB Polarization.

The fundamental ratio $\lambda_2/\lambda_1 = 8/3$ is expected to leave a structural signature in the polarization sector. The bare geometric tensor-to-scalar ratio is

$$r_0 = \frac{\Delta_t^2}{\Delta_s^2} = \frac{\lambda_{\text{base}}}{\lambda_{\text{fiber}}} = \frac{3}{8} \simeq 0.375. \tag{93}$$

The observed ratio undergoes topological decoherence:

$$r_{\text{obs}}(t) = r_0 \cdot \exp\left(-\zeta \frac{\tau_\chi}{t}\right), \tag{94}$$

providing a structural explanation for the low observed $r < 0.036$ without invoking slow-roll dynamics.

11.8 Neutrino-Mediated Relaxation and Decay Signatures

Particle decay and neutrino emission are manifestations of structural reorganization (Sections 4.4, 4.9). Neutrino-like excitations act as non-local relaxation channels, contributing to irreversible smoothing of admissible configurations.

11.9 Environmental Modulation of Particle Lifetimes

Particle stability may exhibit a weak environmental dependence. At leading order:

$$\frac{\delta\Gamma}{\Gamma} \simeq \beta \frac{\Delta U}{c^2}, \tag{95}$$

where $\beta \lesssim 10^{-6}$ (from local position invariance constraints) and $\Delta U/c^2 \sim 10^{-7}$–$10^{-6}$ for typical galactic environments, yielding

$$\frac{\delta\tau}{\tau} \sim 10^{-13}\text{–}10^{-12}, \tag{96}$$

well below current sensitivities but conceptually distinct from standard effects. The cleanest experimental target is leptonic weak decay; the most amplified interferometric target is neutral-meson mixing. Near compact objects ($\Delta U/c^2 \sim 10^{-4}$), the effect rises to $\delta\tau/\tau \sim 10^{-10}$, manifesting as environment-correlated spectral biases in hadronic cascades.

11.10 Strong Gravitational Lensing

The effective lensing potential decomposes as $\Phi_{\rm eff} = \Phi_{\rm bar} + \Phi_\chi$, with convergence

$$\kappa(\boldsymbol{\theta}) = \frac{D_l D_{ls}}{c^2 D_s} \int \nabla_\perp^2 \Phi_{\rm eff}(D_l\boldsymbol{\theta}, z)\, dz, \tag{97}$$

yielding $\kappa = \kappa_{\rm bar} + \kappa_\chi$. The emergent contribution is parametrized as

$$\Phi_\chi(\mathbf{x}) = \frac{c^2}{2} \ln\!\left(\frac{K(\bar{\chi}(\mathbf{x}))}{K_\infty}\right). \tag{98}$$

Testable signatures include partial decorrelation between baryonic mass and lensing strength, enhanced sensitivity to cluster morphology, strong lensing without dark matter substructure, and redshift dependence tracing relaxation rather than mass accretion history.

Early Massive Structures in the JWST Era

Massive galaxies and strong lensing at $z \gtrsim 8$ are naturally accommodated: effective mass reflects localized resistance to relaxation associated with spectrally robust projected configurations, rather than requiring rapid hierarchical assembly.

"Impossibly Early" Galaxies

Their large effective masses encode strong resistance to relaxation rather than cumulative accretion. Cosmochrony predicts that such galaxies should exhibit relatively stable

effective masses over extended redshift intervals, contrasting with the rapid growth required in hierarchical scenarios.

Qualitative Predictions

Massive galaxies at $z \gtrsim 8$ should persist with only moderate mass evolution. Early strong-lensing configurations should display weak redshift evolution of their effective convergence, with an early onset followed by moderate evolution.

Strong Gravitational Lensing in Abell-1689

The emergent convergence is isolated as

$$\kappa_\chi(\boldsymbol{\theta}) = \kappa_{\rm eff}(\boldsymbol{\theta}) - \kappa_{\rm bar}(\boldsymbol{\theta}), \tag{99}$$

with the emergent lensing potential obtained from $\nabla^2_{\boldsymbol{\theta}}\psi_\chi = 2\kappa_\chi$. In Cosmochrony, κ_χ is emergent geometric focusing from collective χ-substrate constraints, not additional dark matter.

Quantitative Scaling and Falsifiability

Beyond qualitative decorrelation effects, the emergent contribution κ_χ admits an order-of-magnitude scaling in saturated cluster cores.

We parameterize the relative excess convergence as

$$\frac{\kappa_\chi}{\kappa_{\rm bar}} \sim \gamma \left(\frac{\Sigma_{\rm bar}}{\Sigma_*} \right), \tag{100}$$

where $\Sigma_{\rm bar}$ is the baryonic surface density, Σ_* denotes a characteristic structural relaxation scale of the χ substrate, and γ is a dimensionless response coefficient encoding substrate efficiency.

For massive clusters with $\Sigma_{\rm bar} \sim \Sigma_*$, this yields

$$\frac{\kappa_\chi}{\kappa_{\rm bar}} \sim \gamma, \tag{101}$$

with a natural expectation $\gamma \sim 10^{-2}$–10^{-1}, corresponding to percent-to-ten-percent level decorrelation between baryonic mass distribution and total lensing convergence.

This deviation should manifest as a systematic mismatch between high-resolution baryonic mass reconstructions and gravitational lensing maps, particularly in morphologically complex cluster cores such as Abell-1689.

Falsifiability condition. If future lensing reconstructions constrain $\kappa_\chi/\kappa_{\rm bar} < 10^{-2}$ in saturated cluster environments, the present scaling law would be excluded at the predicted amplitude level.

11.11 Superconducting Gap Symmetry from Fiber Geometry

The collective coherent regime of the $U(1)$ fiber discussed in Section 5.7 leads to concrete and falsifiable predictions for the symmetry of the superconducting gap. In

the present framework, gap symmetry is not determined by a specific momentum-space interaction kernel, but by a real-space minimization problem in the fiber raccordement cost under lattice constraints.

Geometric Selection Principle

Let $\mathcal{C}_{\mathrm{tot}}[\theta]$ denote the effective cost functional associated with fiber phase mismatch in the presence of lattice symmetry group $\mathcal{G}$ and dominant frustration wavevector $\mathbf{Q}$. Admissible composite configurations must satisfy simultaneously:

1. minimization of overlap with the dominant frustrated sector,
2. global continuity of the fiber phase without introducing additional defects.

Among the irreducible representations of $\mathcal{G}$ available to a $w = 2$ composite class, the physically realized superconducting gap corresponds to the representation that minimizes $\mathcal{C}_{\mathrm{tot}}$.

This selection principle is independent of microscopic pairing details. It depends only on lattice symmetry and the dominant frustration structure.

Prediction for Cuprate Superconductors

In cuprate materials, the relevant lattice symmetry is D_{4h} and the dominant frustration vector is approximately (π, π), as measured through the magnetic structure factor $S(\pi, \pi)$.

Under these constraints, the minimization of the fiber raccordement cost selects the B_{1g} irreducible representation. The resulting gap symmetry is therefore

$$\Delta(\mathbf{k}) \propto \cos k_x - \cos k_y, \tag{102}$$

corresponding to $d_{x^2-y^2}$ symmetry.

This prediction does not rely on a specific spin-fluctuation mechanism. It follows from geometric frustration in the projected fiber sector. The nodal lines arise from the required sign alternation that reduces overlap with the (π, π) frustration sector while preserving global fiber continuity.

Prediction for Nickelate Superconductors

In infinite-layer nickelates, the antiferromagnetic frustration sector is reduced and partially isotropized relative to cuprates. Let r_F denote a dimensionless proxy for the relative frustration amplitude, operationally linked to the normalized structure factor.

For sufficiently reduced staggered frustration ($r_F < r_F^{\mathrm{crit}}$), the minimization of $\mathcal{C}_{\mathrm{tot}}$ favors an extended A_{1g} representation with sign-changing structure across Fermi surface sheets,

$$\Delta(\mathbf{k}) \sim s^{\pm}. \tag{103}$$

The framework therefore predicts a symmetry transition between $d_{x^2-y^2}$ and extended $s^{\pm}$ depending on the frustration ratio r_F. This constitutes a direct and falsifiable structural prediction.

Disorder Sensitivity

Because sign-changing order parameters are sensitive to non-magnetic disorder, the predicted $s^{\pm}$ regime in nickelates should display intermediate sensitivity to impurity scattering, weaker than pure d-wave cuprates but stronger than conventional isotropic s-wave superconductors.

Systematic impurity studies therefore provide a discriminating test of the fiber-geometry selection mechanism.

Scaling of the Critical Temperature

To leading order, the phase stiffness scales as

$$\rho_s(0) \propto \delta J f(r_F), \tag{104}$$

where δ is the carrier concentration, J the dominant frustration scale, and $f(r_F)$ a dimensionless function encoding the geometric reduction of frustration.

In quasi-two-dimensional systems,

$$k_B T_c \simeq \frac{\pi}{2} \rho_s(T_c^-), \tag{105}$$

yielding

$$T_c \sim \frac{\pi}{2k_B} \delta J f(r_F). \tag{106}$$

All quantities entering this relation are independently measurable through spectroscopy, transport, and neutron scattering. No free fitting parameter specific to superconductivity is introduced.

Falsifiability

The present mechanism would be falsified if:

- cuprates exhibited a robust fully isotropic s-wave gap at optimal doping despite strong (π, π) frustration,
- nickelates with reduced staggered frustration showed stable $d_{x^2-y^2}$ symmetry across all doping levels,
- the critical temperature displayed no correlation with independently measured exchange or frustration scales.

The symmetry channel is therefore not an adjustable ingredient. It is fixed by lattice group and frustration geometry, providing a sharp structural test of the framework.

11.12 Experimental Outlook and Discriminating Signatures

Particle creation is reinterpreted as a universal dissipation channel activated whenever directional relaxation approaches its maximal transport capacity. This unifies several high-energy phenomena:

Astrophysical Jets.

Relativistic jets are dynamically selected channels through which excess substrate tension is discharged by continuous structure creation. A predicted *saturation clamping* near the horizon—a non-linear relation between near-horizon stress and plasma density—is testable with Event Horizon Telescope observations.

Primordial Cosmology.

Matter production emerges as a byproduct of relaxation-driven expansion. Cosmochrony predicts that primordial fluctuations may carry imprints of discrete nucleation events, suggesting specific non-Gaussianity and phase correlations at large angular scales.

Ultra-High-Energy Cosmic Rays.

UHECRs exceeding the GZK threshold may be locally produced during transient saturation spikes near compact objects. A predicted strong anisotropy correlated with nearby compact objects and multimessenger correlations would provide a decisive signature.

Multi-Scale Falsification Program.

The framework suggests a hierarchy of tests: precision atomic physics (Section 4.10), Schwinger threshold in ultra-intense lasers, saturation clamping in relativistic jets, and large-scale CMB anomalies as relics of discrete primordial nucleation.

11.13 Summary

Cosmochrony yields observationally testable signatures spanning cosmology, gravitation, galactic dynamics, and particle phenomena. All arise from non-injective projection and structural relaxation. Predicted deviations from ΛCDM at the percent level include suppression of low-ℓ CMB power, a mild redshift-dependent modulation of $H(z)$, and coherence-modifying effects in gravitational-wave propagation near compact objects. These signatures define a coherent phenomenological pattern from a single underlying mechanism—the irreversible relaxation and partial projectability of the χ substrate.

12 Discussion and Comparison with Existing Frameworks

12.1 Relation to General Relativity

Spacetime curvature in Cosmochrony is an emergent descriptive construct (Section 6.3). No *a priori* metric dynamics is postulated; instead, an effective geometry emerges from variations in local relaxation dynamics. Matter configurations locally constrain the relaxation of χ, leading to differential rates of effective proper-time evolution that are reinterpreted as effective metric deformations. In the weak-field regime, Newtonian gravity is reproduced; in the strong-field limit, Schwarzschild-like solutions emerge. General Relativity is recovered as the appropriate effective theory within its empirically validated domain.

12.2 Relation to Quantum Formalism

Cosmochrony does not treat quantization or wave dynamics as fundamental [44]. Particles correspond to localized, topologically stable configurations; discrete observables arise from boundary conditions, topological constraints, and interaction-induced reprojection. The Planck relation $E = h\nu$ is a geometric correspondence between redistributed relaxation potential and minimal projective resolution. Entanglement reflects a shared, non-factorizable χ configuration persisting only within a finite critical regime of projection, while decoherence reflects irreversible loss of relational accessibility.

12.3 Analogy with Collective Phenomena in QCD

A useful structural analogy may be drawn with low-energy QCD [45], where fundamental degrees of freedom (quarks, gluons) do not appear as isolated entities in the infrared. The observable spectrum consists instead of collective bound states, whose properties are not transparently reducible to perturbative constituents.

Similarly, Cosmochrony formulates fundamental dynamics solely in terms of χ and its relaxation ordering. Observable quantities arise only after projection into regimes admitting stable effective descriptions. What appear as elementary constituents at a given effective level may represent stable, regime-dependent invariants of the underlying dynamics, in direct analogy with QCD confinement.

The analogy extends beyond particle confinement. In QCD, the vacuum itself admits multiple collective phases, including chiral symmetry breaking and color superconductivity, which emerge from non-perturbative organization of the same underlying degrees of freedom. In Cosmochrony, different physical phenomena likewise correspond to distinct collective regimes of a single substrate.

Gravitational curvature arises as a collective slowdown of relaxation ordering. Schwinger pair production corresponds to saturation of directed relaxation flux. Superconductivity, as discussed in Section 5.7, represents a coherent collective phase of the $U(1)$ fiber sector, in which composite winding classes stabilize and lock globally.

In all these cases, the effective phenomena are not introduced as additional dynamical postulates. They correspond to regime-dependent reorganizations of the same projective structure. The underlying ontology remains unchanged, while the effective

description undergoes phase-like transitions analogous to those observed in strongly coupled gauge theories.

This analogy is structural rather than dynamical. Cosmochrony does not import the specific field content of QCD. The comparison serves to clarify how radically different effective laws may arise from a single underlying relational dynamics, without multiplying fundamental entities.

12.4 Comparison with ΛCDM Cosmology

ΛCDM introduces cold dark matter, dark energy, and inflation as effective postulates [9, 46]. In Cosmochrony, cosmic expansion follows from monotonic relaxation of the substrate, with $H(t) = \dot{\chi}/\chi$ and $H_0 \sim c/\chi(t_0)$. Dark energy is reinterpreted as the large-scale relaxation dynamics; cosmic acceleration reflects cumulative relaxation over cosmological timescales. The coincidence problem and the Hubble tension may admit interpretations in terms of epoch-dependent relaxation dynamics rather than new fundamental constituents. Low-ℓ CMB suppression is explored as a structural consequence of relaxation constraints rather than a statistical fluctuation.

Table 7 summarizes the conceptual differences between Cosmochrony, ΛCDM, and Loop Quantum Gravity.

12.5 Historical Admissibility of Projected Degrees of Freedom

The set of effective degrees of freedom depends on the admissibility conditions imposed by the relaxation state. In the early Universe, only highly coherent, low-complexity global configurations were admissible. As relaxation proceeds, the admissible space progressively enlarges, enabling increasingly localized invariants described as particles, fields, and interactions. The particle spectrum is therefore a historically conditioned outcome of relaxation dynamics, not a timeless feature. This perspective reconciles the emergence of complexity with monotonic entropy increase: the early Universe is characterized by both low entropy and low admissible complexity. Low-ℓ CMB anomalies may be interpreted as relics of this early regime of restricted admissibility.

12.6 Inflation, Horizon Problems, and Initial Conditions

Because χ describes a global relaxation process rather than metric expansion, causal connectivity is not defined in terms of spacetime lightcones at the fundamental level. Large-scale coherence arises from initial relational smoothness and subsequent monotonic relaxation, without requiring an inflationary phase. The horizon problem is rendered inoperative by the absence of an initially fragmented causal structure at the pre-geometric level. A detailed quantitative treatment of primordial perturbations and their CMB imprint remains an open direction for future work.

12.7 Ontological Parsimony and the Metric

Cosmochrony achieves genuine ontological simplification rather than relabeling. In GR, the metric $g_{\mu\nu}$ is a fundamental tensor field with ten independent components; matter and energy are conceptually distinct from geometry. In Cosmochrony, only χ is

fundamental; the metric carries no independent ontological status; matter, energy, and geometry correspond to distinct regimes of the same relational structure.

The frameworks are operationally distinct: GR propagates two tensorial gravitational-wave polarizations from the metric; Cosmochrony has no independent geometric degrees of freedom. Singularities signal breakdown of effective geometric descriptions while χ remains well-defined. Quantization applies only to effective excitations within projectable regimes, not to χ itself [47].

$$\text{Standard:} \quad g_{\mu\nu} \text{ (geometry)} + \psi \text{ (matter)} + \Lambda \text{ (dark energy)}, \tag{107}$$

$$\text{Cosmochrony:} \quad \chi \text{ (single substrate)} \longrightarrow \{\text{spacetime, matter, expansion}\}. \tag{108}$$

12.8 Relation to the Higgs Mechanism: Emergence from χ Dynamics

The Higgs field and its VEV are reinterpreted as effective low-energy descriptors of a specific projective regime of χ. In this framework, mass generation does not originate from an independent scalar sector, but from the stabilization of relaxation-resistant configurations of the underlying substrate.

Structural Transition

Below a critical scale χ_c (homogeneous regime), only massless globally coherent configurations are admissible. Above χ_c (structured regime), localized relaxation-resistant configurations stabilize as massive excitations. The electroweak scale is related through

$$\langle \phi_H \rangle \;\propto\; \frac{\hbar_{\text{eff}}\, c}{\chi_c}, \tag{109}$$

naturally recovering the observed scale for $\chi_c \sim 10^{-18}\,\text{m}$.

Mass Generation as Solitonic Stabilization

Fermion masses scale as $m_f \propto y_f\, \hbar_{\text{eff}}/\chi_c$; gauge boson masses as $m_W \propto g\, \hbar_{\text{eff}}/\chi_c$. These relations reproduce standard Higgs-generated mass terms at the effective level.

Within the spectral interpretation developed in Section 10.4, the Yukawa parameters encode the effective projection of underlying relaxation eigenvalues. The observed flavor hierarchies and associated CP structure therefore reflect the same spectral organization, rather than introducing independent mass-generating dynamics.

Distinction from Superconducting Mass Generation

A potential source of confusion concerns the appearance of an effective mass term for gauge fields in superconductivity, discussed in Section 5.7. In that regime, global phase locking of $w = 2$ composites produces a London term proportional to A^2, leading to Meissner screening and an effective photon mass inside the medium.

This phenomenon is not interpreted here as fundamental symmetry breaking. It corresponds to emergent projective coherence in a condensed phase of the $U(1)$ fiber

sector. The underlying gauge symmetry of the χ substrate remains intact. The apparent mass arises from collective reorganization of degrees of freedom within a bounded projective regime.

By contrast, electroweak mass generation operates in the vacuum structure of the effective theory and is associated with a distinct projective transition at the scale χ_c. Although both mechanisms yield quadratic gauge-field terms at the effective level, their ontological status differs. The superconducting London mass is medium-dependent and disappears above the coherence temperature, whereas electroweak gauge boson masses persist in the vacuum.

The formal similarity between the two mechanisms reflects a deeper structural principle: mass terms emerge whenever a collective projective configuration restricts admissible gauge variations. However, no additional fundamental Higgs-like degree of freedom is introduced in the superconducting case. The effective mass acquisition of the gauge field in superconductivity is therefore a manifestation of emergent projective coherence, not a reinvention of the Higgs mechanism.

Phenomenological Status

No deviation from established collider results is implied at accessible energies. Departures may arise only in extreme regimes where the mapping between solitonic stabilization scales and effective parameters becomes nonlinear. Open challenges include deriving the detailed correspondence between χ soliton spectra and the full Standard Model mass hierarchy.

12.9 Structural Interpretation: Projective Thermodynamics

Physical observables arise through a generically non-injective projection $\Pi : \Omega \to O$. In saturation regimes, the resulting loss of distinguishability induces a structural entropy:

$$S_\Pi = -\sum_{o \in O} \mu(\Pi^{-1}(o)) \log \mu(\Pi^{-1}(o)), \tag{110}$$

which is an objective property of the projection.

Effective parameters such as temperature or metric curvature emerge as Lagrange multipliers absorbing unresolved relational complexity. High effective temperatures or anomalous geometric features reflect the compression of a bounded relational flux into a reduced observable description, not excess local energy density. The bounded character of substratic relaxation ensures that projection-induced quantities remain finite, rendering the framework predictive despite the non-injective nature of the projection.

12.10 Bounds on Projective Resolvability Across Scales

Saturation phenomena across scales—bounded gravitational response in low-density environments and the operational accessibility of quantum correlations—reflect a common limitation on projective resolvability. In Cosmochrony, the projected description U does not expose the full relational content of the substrate χ. It exposes only what

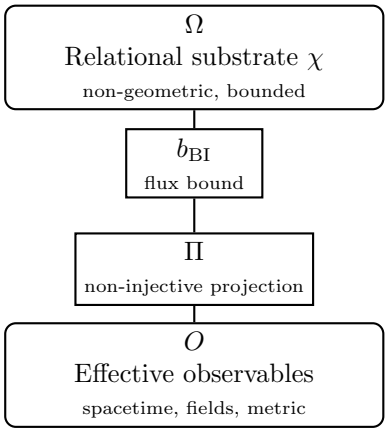

Fig. 14 Projective regimes in Cosmochrony. The substrate Ω undergoes bounded relaxation (b_{BI}). Observables arise through non-injective projection Π.

can be rendered operationally accessible through the non-injective mapping Π under admissible update transport. The relevant limitation is therefore not a postulated geometric cutoff, but a throughput bound on the rate at which relational structure can be updated while maintaining operational closure of the projected state.

Attosecond chronoscopy experiments illustrate this principle. Measured delays can be interpreted as the minimal temporal resolution required for a non-factorizable projected description to become operationally resolvable, rather than as a dynamical buildup of correlations [41].

We summarize this limitation by an effective inequality on projected update rates,

$$\left| \frac{\partial \mathcal{O}_{\mathrm{eff}}}{\partial \tau} \right| \leq b_\chi \, \mathcal{S}_\Pi, \tag{111}$$

where b_χ is the invariant bound on admissible relaxation transport in the substrate and $\mathcal{S}_\Pi$ parametrizes the effective structural complexity of the projection for the class of observables under consideration. The factor $\mathcal{S}_\Pi$ is not a new dynamical field. It encodes how many independent relational channels can be synchronized within one operational update step.

Distinct phenomenological manifestations correspond to distinct choices of $\mathcal{O}_{\mathrm{eff}}$ and the associated resolution scale. In macroscopic weak-field regimes, the same bound induces an operational saturation threshold that can be expressed as an effective acceleration proxy,

$$a_\star \sim \kappa \frac{b_\chi}{\ell}, \tag{112}$$

where ℓ is the local descriptive resolution of the projected state and $\kappa = \mathcal{O}(1)$ encodes the normalization convention of Π. In measurement-limited quantum protocols, the bound similarly appears as a bandwidth constraint,

$$B_\Pi(\mathcal{M}) = \eta_{\mathcal{M}} \, b_\chi \, \mathcal{S}_\Pi, \tag{113}$$

for a measurement procedure $\mathcal{M}$, with $\eta_{\mathcal{M}}$ absorbing protocol-dependent conventions. These expressions represent different dimensional projections of the same underlying transport bound. A modification of the effective resolvability of the $\chi \to \Pi$ mapping would therefore induce correlated shifts in both galactic saturation scales and quantum chronoscopy thresholds.

A further generic consequence is the divergence of projective stress under sufficiently deep refinement. Let D denote an operational update demand, defined as a characteristic rate at which projected relations must be recomputed to preserve admissibility. Let C denote the admissible projective throughput under the bound b_χ for the same class of updates. The dimensionless stress ratio

$$\Xi \equiv \frac{D}{C} \tag{114}$$

provides a regime indicator. Whenever a process increases D faster than C can be redistributed by the available synchronized channels, Ξ grows and a saturated reconfiguration becomes unavoidable. This statement is independent of any particular emergent geometry and follows solely from bounded transport and finite projective resolvability.

12.11 Projective Non-Termination and the Condition of Temporal Ordering

Time is identified with the ordering of distinguishable projected states: $\Delta\tau \sim \mathrm{dist}(U_n, U_{n+1})$. A hypothetical terminal state U_0 satisfying $\Pi(\chi + \delta\chi) = U_0$ for all admissible $\delta\chi$ would imply $\Delta\tau \to 0$ for all internal observers.

The inaccessibility of absolute zero emerges as a projective necessity: zero-point fluctuations are reinterpreted as the minimal projective bandwidth required to prevent collapse of the observable description into a stationary state. Time ceases only when the projection becomes stationary—a regime structurally forbidden by the existence of a finite bound on projective resolvability.

12.12 Conceptual Implications and Open Challenges

Temporal ordering arises from the monotonic relaxation of χ; energy quantifies residual capacity to resist this relaxation; irreversibility reflects its progressive exhaustion. Time, energy, and irreversibility are not independent axioms but complementary effective descriptions of the same relational dynamics.

Open challenges include the quantitative reconstruction of CMB anisotropies from early-time χ dynamics, the detailed treatment of non-equilibrium decoherence and reprojection, the emergence of gauge symmetries from topological features, the explicit derivation of the full flavor hierarchy and the quantitative determination of the CP-violating invariant from first-principles χ dynamics, and the long-term stability of solitonic configurations under extreme conditions. Progress will require large-scale simulations of χ dynamics, discretized lattice realizations, and targeted experimental tests.

Possible Cosmological Implications of Flavor Misalignment.

Within the present framework, the Jarlskog invariant $\mathcal{J}$ is interpreted as a structural residue of quasi-commutative sectorial restrictions of the projection fiber Π (Appendix C.17). In the effective low-energy regime, this invariant is treated as a stable characteristic of the stabilized flavor manifold.

Because the operators Π_u and Π_d are defined as restrictions of the global non-injective mapping, their algebraic structure is ultimately rooted in the global state of the relational substrate χ. In extreme regimes approaching global saturation—such as the early Universe—the admissible spectral subspace of the fiber could differ from its present quasi-stationary configuration.

Whether such regimes might modify the effective structure of flavor misalignment remains an open question. No quantitative model is presently derived. Establishing a predictive relation between $\mathcal{J}$ and cosmological relaxation conditions constitutes a significant theoretical challenge for future work.

13 Conclusion and Outlook

Cosmochrony reduces the fundamental assumptions of physics to a single dynamical origin: the irreversible relaxation of a pre-geometric relational substrate χ. From this substrate, time, spacetime geometry, and a wide spectrum of physical phenomena emerge as effective descriptions.

A central result is the *ab initio* derivation of the effective dynamical laws: the Born–Infeld-like Lagrangian is the unique functional compatible with causal saturation of relaxation fluxes at c_χ. The speed limit c_χ and Planck's constant h appear as complementary bounds on projectability, respectively limiting the maximal propagation rate and the minimal resolvable granularity. General Relativity is recovered as a thermodynamic limit of the underlying relational dynamics.

The framework provides a unified geometric origin for the Standard Model: gauge interactions emerge as projection dynamics; matter and mass arise from topological obstructions and spectral frustration; the dark sector is reinterpreted as non-projected spectral density (dark matter) and global relaxation flux (dark energy). Quantum entanglement arises when a single relational configuration admits multiple admissible effective realizations under non-injective projection, persisting only within a finite critical regime.

At cosmological scales, expansion and the arrow of time follow from the diminishing tempo of relaxation. At galactic scales, saturation of the relaxation constraint produces flat rotation curves without dark matter halos. In strong-gravity regimes, black hole evaporation is reinterpreted as discrete reprojection ensuring information preservation.

The space of admissible projected configurations evolves as relaxation proceeds: the particle content of the Universe is a historically conditioned outcome, not a timeless input.

Conceptual Shift and Outlook

Cosmochrony represents a shift from a "matter-on-spacetime" paradigm to a "relaxation-of-substrate" ontology. Immediate falsifiable research directions include: cosmological signatures (low-ℓ CMB anomalies from finite relaxation capacity), galactic phenomenology (dark matter effects correlated with local relaxation gradients), and fundamental-scale effects (environment-dependent variations in decay rates or couplings in extreme regimes). Future work will focus on the systematic derivation of the Standard Model spectrum as a hierarchy of topological frustration modes within the relaxation dynamics.

Part VI
Appendices

A Mathematical Foundations of Cosmochrony — Dynamics, Stability, and Analytical Solutions

This appendix provides a rigorous mathematical formulation of the χ-field dynamics. All results follow from the fundamental postulates without assuming a pre-existing spacetime metric. Geometric notions should be understood as effective, coarse-grained representations consistent with Appendix E.

A.1 Effective Lagrangian Description as a Hydrodynamic Limit

In regimes where χ varies smoothly, discrete relational couplings K_{ij} can be summarized by effective continuum quantities. Distances emerge as cumulative resistance to relaxation. The effective metric $g_{\mu\nu}$ encodes the coarse-grained density of correlations.

To reproduce the continuum evolution from the discrete rule (Eq. 160), one introduces a purely representational effective Lagrangian:

$$\mathcal{L}_{\text{eff}} = \frac{1}{16\pi G_{\text{eff}}} F(\chi)\, R - \Lambda_{\text{flow}}^4\, \chi + \cdots$$

where R is the Ricci scalar of the effective metric and $F(\chi)$ parametrizes how relaxation dynamics is encoded in the geometric description. Einstein-like field equations reflect the universality of geometric descriptions for slowly varying collective phenomena. Singularities signal only the limits of the hydrodynamic approximation. The effective Lagrangian has no ontological status and should not be quantized.

In projective regimes where the mapping Π is effectively injective, the existence of $S_{\text{eff}} = \int \mathcal{L}_{\text{eff}}\, \mathrm{d}^4x$ implies additional structural constraints. Admissible variations of underlying χ configurations that preserve projectability map to variations of the effective fields that leave S_{eff} invariant up to boundary terms. As a consequence, the effective description admits local continuity identities of Noether type. In particular, when $\mathcal{L}_{\text{eff}}$ is generally covariant with respect to the emergent metric $g_{\mu\nu}$, the associated effective stress tensor

$$T_{\text{eff}}^{\mu\nu} := \frac{2}{\sqrt{-g}} \frac{\delta S_{\text{eff}}}{\delta g_{\mu\nu}}$$

satisfies the local identity

$$\nabla_\mu T_{\text{eff}}^{\mu\nu} = 0$$

within the hydrodynamic domain.

From this perspective, local conservation is not a primitive postulate of the χ description but a stability condition of the projective regime. If relaxation approaches saturation and effective injectivity fails, the variational formulation may cease to be well-posed, and the above local identities need not remain strictly defined at the boundary of the saturated region. Global admissibility of the underlying χ dynamics is nonetheless preserved, and apparent non-local redistribution in the effective description is interpreted as deprojection followed by reprojection once projectability conditions are restored.

A.2 Stability Analysis of the χ-Field Dynamics

In the hydrodynamic regime, the effective relaxation dynamics reads $\partial_t \chi = c\sqrt{1 - |\nabla\chi|^2/c^2}$.

Around a homogeneous background $\chi_0(t) = ct + \chi_{0,0}$, a perturbation $\delta\chi$ satisfies $\partial_t \delta\chi = -(2c)^{-1}|\nabla\delta\chi|^2 + \mathcal{O}(|\nabla\delta\chi|^4)$. No linear term appears: the homogeneous solution is marginally stable at linear order. The leading nonlinear correction is strictly negative, so any spatial inhomogeneity reduces the local relaxation rate and is dynamically suppressed.

The diagnostic functional $E[\delta\chi] = \frac{1}{2}\int |\nabla\delta\chi|^2 \, d^3x$ is non-increasing. Planar perturbations are progressively flattened; spherical ones decay monotonically. The effective dynamics is dissipative and contractive, establishing nonlinear stability. This stability is inseparable from the monotonic character of relaxation: the same constraint defining the arrow of time precludes dynamical instabilities.

A.3 Analytical Solutions of the χ-Field Dynamics

Explicit solutions of the effective relaxation equation:

$$\partial_t \chi = c\sqrt{1 - \frac{|\nabla\chi|^2}{c^2}}. \tag{115}$$

Homogeneous relaxation.

$\nabla\chi = 0$ gives $\chi(t) = \chi_0 + ct$, underlying emergent cosmological expansion (Section 3.7).

Gradient-saturated profiles.

$|\partial_r \chi| = c$ yields $\partial_t \chi = 0$: local freezing of the ordering parameter. The profiles $\chi(r) = \chi_0 \pm cr$ model horizons and maximally constrained regions.

Linear relaxation fronts.

$\chi(x,t) = \chi_0 + ct \pm vx$ with $|v| < c$ satisfies Eq. (110) identically. These are kinematic boundaries, not propagating waves.

Absence of linear wave solutions.

Small perturbations around homogeneous configurations do not propagate as oscillatory modes (Section A.2). Apparent wave-like phenomena arise only at the effective level through collective excitations.

A.4 Coupling with Matter: Effective Source Term $S[\chi, \rho]$

In the emergent spacetime description:

$$\Box_{\text{eff}}\chi = S[\chi, \rho]. \tag{116}$$

$S[\chi, \rho]$ encodes the effective resistance of localized excitations to the global relaxation flow. It summarizes gravitational time dilation, inertial mass, and effective curvature.

Weak-field regime.

$$S[\chi, \rho] \simeq -\alpha\, \rho, \tag{117}$$

with $\alpha \sim G/c^2$. This reproduces the Poisson equation and the Schwarzschild solution at leading order.

Strong-field regime.

$$S[\chi, \rho] = -\alpha\, \rho\, F\left(\frac{\rho}{\rho_c},\, \chi\right), \tag{118}$$

where F is bounded and ρ_c denotes a characteristic density beyond which relaxation resistance saturates. These nonlinearities prevent unphysical halting of the relaxation flow and encode departures from classical gravity, signaling the breakdown of the hydrodynamic approximation.

A.5 Strong-Field Constitutive Coupling Near a Schwarzschild Black Hole

The effective constitutive relation:

$$K_{\text{eff}} = K_0 \exp\left(-\frac{(\Delta\chi)^2}{\chi_c^2}\right). \tag{119}$$

The operational lapse-like factor:

$$N(r) \equiv \frac{\mathcal{D}_{\text{loc}}\chi(r)}{\mathcal{D}_0\chi}, \quad 0 < N(r) \leq 1. \tag{120}$$

Matching to the Schwarzschild metric (purely effective):

$$ds^2 = -f(r)c^2dt^2 + f(r)^{-1}dr^2 + r^2d\Omega^2, \quad f(r) = 1 - \frac{r_s}{r}. \tag{121}$$

$$N(r)^2 = f(r) = 1 - \frac{r_s}{r}. \tag{122}$$

Minimal identification $K_{\text{eff}}(r)/K_0 \equiv N(r)^2$:

$$K_{\text{eff}}(r)/K_0 \equiv N(r)^2. \tag{123}$$

Yielding the strong-field profile:

$$K_{\text{eff}}(r) = K_0\left(1 - \frac{r_s}{r}\right), \quad r > r_s. \tag{124}$$

Inverting Eq. (114):

$$\frac{(\Delta\chi(r))^2}{\chi_c^2} = -\ln\left(1 - \frac{r_s}{r}\right). \tag{125}$$

As $r \to r_s^+$:

$$\Delta\chi(r) \sim \chi_c \sqrt{-\ln\Big(1 - \frac{r_s}{r}\Big)}. \tag{126}$$

This logarithmic divergence signals that the hydrodynamic parametrization exceeds its domain of validity near the effective horizon. A Schwarzschild horizon corresponds to vanishing relaxation conductivity ($K_{\text{eff}} \to 0$), not a fundamental spacetime singularity.

A.6 Minimal Kinematic Constraint

In its saturated form:

$$(\partial_t \chi)^2 + |\nabla\chi|^2 = c^2, \tag{127}$$

where ∂_t and ∇ denote effective variations introduced only once a projectable geometric regime is established. More generally, admissible configurations satisfy the corresponding inequality.

This constraint is imposed ab initio at the pre-geometric level and does not presuppose a spacetime metric, light cones, or Lorentzian structure. The constant c is the effective manifestation of the invariant structural bound c_χ (Section 2.11). Lorentz symmetry arises a posteriori as a property of saturated relaxation.

In homogeneous regimes, the constraint enforces $\partial_t \chi = c$, leading to linear growth and effective cosmic expansion. In inhomogeneous regimes, partial saturation manifests as local slowdown underlying gravitational time dilation. At scales near the Planck length, the continuum approximation breaks down and a fully discrete formulation is required.

A.7 Effective Evolution Equation

Once a stable geometric description has emerged, large-scale regularities of admissible projected configurations may be written as $\Box_{\text{eff}}\chi = S[\chi, \rho]$, where $\Box_{\text{eff}}$ is the d'Alembertian of the emergent metric and ρ represents the effective density of relaxation-resistant configurations. Neither the operator nor the source term is fundamental.

$S[\chi, \rho]$ encodes how localized patterns locally reduce the admissible relaxation rate. Gradients in the effective ordering parameter are reinterpreted as gravitational time dilation and spacetime curvature.

In weak-field regimes, $S[\chi, \rho] \simeq -\alpha\rho$ with $\alpha \sim G/c^2$, reproducing the Poisson equation and Schwarzschild-like solutions. Nonlinear corrections encode saturation effects inherited from the kinematic constraint $\partial_t \chi \leq c$ and signal the breakdown of the hydrodynamic approximation.

A.8 Relational Foundation and Emergent Geometry

The continuous representation of χ is a pragmatic strategy for contact with established formalisms, not an ontological commitment. At a more fundamental level, Cosmochrony can be formulated in purely relational terms where neither spacetime points, distances, nor a metric are assumed a priori. Temporal ordering arises from monotonic relaxation; spatial relations are reconstructed operationally from patterns of correlation and

connectivity. The metric appears only as a derived object. A concrete realization is developed in Appendix F.

B Step A: Admissible Injective Projections Have Trivial Holonomy

This appendix formalizes Step A announced in Section 5.6. We classify admissible projection maps $\Pi : \mathcal{C}_\chi \to \mathcal{M}$ by their fiber topology. We show that injective maps in this class have trivial holonomy. Since non-trivial holonomy is the minimal condition for a re-identification symmetry to arise as a descriptive invariance, injectivity structurally precludes emergent gravity under Hypothesis H and ontological uniqueness.

B.1 Setup: admissible projections as fibered structures

We work in the regime where $\mathcal{C}_\chi$ and $\mathcal{M}$ admit smooth structures (the continuum limit of Section E.1 and Appendix D.5). In this regime, the projection $\Pi : \mathcal{C}_\chi \to \mathcal{M}$ is required to be *admissible*.

Definition B.1 (Admissible projection)**.** A smooth surjective map $\Pi : \mathcal{C}_\chi \to \mathcal{M}$ is called admissible if:

(A1) Π is a fiber bundle map. For each $y \in \mathcal{M}$, the preimage $\Pi^{-1}(y) \subset \mathcal{C}_\chi$ is a smooth submanifold. Fibers are mutually diffeomorphic.
(A2) Π is compatible with the relaxation rule F. If $x, x' \in \mathcal{C}_\chi$ satisfy $\Pi(x) = \Pi(x')$, then $\Pi(F(x)) = \Pi(F(x'))$. Effective dynamics is therefore well-defined on $\mathcal{M}$.
(A3) Π supports a connection. There exists a smooth horizontal distribution $H \subset T\mathcal{C}_\chi$ complementary to the vertical, with the usual equivariance properties whenever a fiber group action is present.

Condition (A1) places Π in the category of fiber bundles over $\mathcal{M}$. In the principal bundle case, where G_Π acts freely and transitively on fibers, non-injectivity of Π corresponds to G_Π being non-trivial. For general fiber bundles where the fiber is not identified with the structure group, non-injectivity is the weaker condition $|\Pi^{-1}(y)| > 1$. The structure group may still be non-trivial even when fibers are discrete. The arguments below apply to the principal bundle case, which is the relevant one for Cosmochrony (Section 5.1, $\Pi \cong S^3$ with $G_\Pi \supseteq \mathrm{SU}(2) \times \mathrm{U}(1)$).

B.2 Holonomy as the obstruction to global re-identification

Let Π be an admissible projection equipped with a connection. In the principal case, the connection is a $\mathfrak{g}_\Pi$-valued one-form ω on $\mathcal{C}_\chi$. The holonomy group $\mathrm{Hol}(\omega, x_0)$ at $x_0 \in \mathcal{C}_\chi$ is the subgroup of G_Π generated by parallel transport along loops γ in $\mathcal{M}$ based at $y_0 = \Pi(x_0)$:

$$\mathrm{Hol}(\omega, x_0) = \left\{ P_\gamma \in G_\Pi \;\middle|\; \gamma : [0,1] \to \mathcal{M},\ \gamma(0) = \gamma(1) = y_0 \right\} \subseteq G_\Pi. \tag{128}$$

Holonomy measures the obstruction to globally consistent re-identification of fibers. It detects the failure of horizontal lifts of loops in $\mathcal{M}$ to close in $\mathcal{C}_\chi$.

Definition B.2 (Re-identification symmetry)**.** A *re-identification symmetry* of the projection Π is a transformation $\phi : \mathcal{C}_\chi \to \mathcal{C}_\chi$ that:

(i) preserves effective states: $\Pi(\phi(x)) = \Pi(x)$ for all x,
(ii) is non-trivial: $\phi \neq \mathrm{id}$ on a non-empty open set,
(iii) is locally implementable: ϕ acts fiberwise and continuously.

In the principal case, re-identification symmetries correspond to bundle automorphisms acting along fibers. Their global consistency is constrained by holonomy.

Proposition B.1 (Holonomy controls global re-identification consistency)**.** *Let Π be an admissible projection with connection ω. If $\mathrm{Hol}(\omega, x_0) = \{e\}$, the bundle admits a global flat section and re-identification symmetries are globally trivializable. If $\mathrm{Hol}(\omega, x_0)$ is a positive-dimensional Lie subgroup of G_Π, re-identification symmetries are intrinsic and cannot be globally trivialized. The converse, flat connection implies trivial holonomy, holds when $\mathcal{M}$ is simply connected, but not in general. The argument below does not rely on this converse.*

Proof Standard result in differential geometry (Ambrose–Singer theorem and its converse). The holonomy algebra $\mathfrak{hol}(\omega, x_0)$ equals the Lie algebra generated by curvature values $\Omega(u, v)$ for all horizontal vectors u, v at points reachable from x_0.

A flat connection ($\Omega = 0$) has holonomy group contained in a discrete subgroup of G_Π when $\mathcal{M}$ is simply connected. In the general case, the holonomy of a flat connection is a representation of $\pi_1(\mathcal{M})$ into G_Π, which may be non-trivial.

However, under injectivity $G_\Pi = \{e\}$ (Theorem B.1). So the holonomy group is trivial regardless of the topology of $\mathcal{M}$. The flat connection argument is therefore not the primary route here. It is superseded by the triviality of G_Π established directly from injectivity. □

B.3 The triviality theorem for injective admissible projections

Theorem B.1 (Injective admissible projections have trivial holonomy)**.** *Let $\Pi : \mathcal{C}_\chi \to \mathcal{M}$ be an admissible projection in the sense of Definition B.1. In the principal bundle case, where G_Π acts freely and transitively on fibers, non-injectivity of Π corresponds to G_Π being non-trivial. For general fiber bundles where the fiber is not identified with the structure group, non-injectivity is the weaker condition $|\Pi^{-1}(y)| > 1$. The structure group may still be non-trivial even when fibers are discrete. The arguments below apply to the principal bundle case, which is the relevant one for Cosmochrony (Section 5.1, $\Pi \cong S^3$ with $G_\Pi \supseteq \mathrm{SU}(2) \times \mathrm{U}(1)$). If Π is injective, then:*

(a) the fiber over every $y \in \mathcal{M}$ is a single point: $\Pi^{-1}(y) = \{x_y\}$,
(b) in the principal specialization, the structure group is trivial: $G_\Pi = \{e\}$,
(c) in that principal case, the holonomy group is trivial: $\mathrm{Hol}(\omega, x_0) = \{e\}$ for any connection ω and any basepoint x_0,

(d) no non-trivial re-identification symmetry exists in the sense of Definition B.2.

Proof Part (a) is immediate from injectivity. If $\Pi(x) = \Pi(x') = y$, then $x = x'$, hence $|\Pi^{-1}(y)| = 1$ for all y.

Part (b) is a principal-bundle statement. If fibers are singletons, the only group acting freely and transitively on a one-element set is $\{e\}$.

Part (c) follows from $\mathrm{Hol}(\omega, x_0) \subseteq G_\Pi$. If $G_\Pi = \{e\}$, then $\mathrm{Hol}(\omega, x_0) = \{e\}$.

Part (d) follows directly from injectivity. If $\Pi(\phi(x)) = \Pi(x)$ for all x, injectivity implies $\phi(x) = x$ for all x. Hence $\phi = \mathrm{id}$, contradicting non-triviality. □

B.4 From trivial holonomy to absence of emergent gauge structure

Corollary B.1 (No emergent gauge field from injective projection)**.** *Under the hypotheses of Theorem B.1 in the principal specialization, any connection is trivial in the sense that its curvature vanishes. No non-trivial gauge field can emerge from the projection structure alone.*

Proof With $G_\Pi = \{e\}$, the Lie algebra is $\{0\}$. Any connection is therefore $\omega = 0$, and $\Omega = d\omega + \omega \wedge \omega = 0$. A non-trivial gauge field would require an independent postulate at the level of $\mathcal{M}$, violating ontological uniqueness. □

Corollary B.2 (No emergent diffeomorphism invariance from injective projection)**.** *Under the hypotheses of Theorem B.1 and Hypothesis H, no diffeomorphism invariance as a descriptive invariance can arise from* Π *alone.*

Proof Diffeomorphism invariance as a descriptive invariance (D2) requires multiple representatives of the same effective state. That is, it requires $|\Pi^{-1}(y)| > 1$ on some region of $\mathcal{M}$. Under injectivity, $|\Pi^{-1}(y)| = 1$ everywhere. Therefore, the diffeomorphism group of $\mathcal{M}$ cannot arise as a re-identification symmetry induced by Π. Any such invariance would have to be postulated directly at the level of $\mathcal{M}$, contradicting emergence and ontological uniqueness. □

B.5 Closing the gap: from holonomy to gravitational curvature

The preceding results establish that injective projections cannot produce the structural prerequisites of emergent gravity, namely re-identification symmetry and descriptive invariance as consequences of the projection. We now connect fiber curvature to effective base curvature in the standard bundle-induced manner.

In the Cosmochrony framework, the effective metric on $\mathcal{M}$ is induced by the Hessian of the effective Lagrangian (Section A.12, Eq. (117)):

$$g^{\mathrm{eff}}_{\mu\nu} \propto \frac{\partial^2 \mathcal{L}_{\mathrm{eff}}}{\partial(\partial_\mu \chi)\, \partial(\partial_\nu \chi)}, \tag{129}$$

valid in projectable regimes.

Proposition B.2 (Fiber curvature contributes to base curvature)**.** *Let $\Pi : \mathcal{C}_\chi \to \mathcal{M}$ be an admissible principal G_Π-bundle with connection ω and curvature Ω. If g^{eff} is induced from the bundle geometry via Eq. (124), then the projection-induced contribution to the effective Ricci tensor contains a term of the form*

$$R^{\text{eff}}_{\mu\nu} \supset \operatorname{tr}_{\mathfrak{g}_\Pi}\big(\Omega_{\mu\alpha}\,\Omega_\nu{}^\alpha\big) + \dots, \tag{130}$$

where the trace runs over $\mathfrak{g}_\Pi$ and the ellipsis denotes additional terms fixed by the same induction scheme.

Flat connection ($\Omega = 0$, hence $G_\Pi = \{e\}$ under injectivity). The fiber-induced contribution to effective base curvature vanishes. The term $\operatorname{tr}_{\mathfrak{g}_\Pi}\big(\Omega_{\mu\alpha}\Omega_\nu{}^\alpha\big)$ in Eq. (125) is identically zero since $\Omega = 0$. The effective metric g^{eff} on $\mathcal{M}$ receives no curvature sourcing from the fiber geometry. Whether g^{eff} is globally flat depends on additional structure of $\mathcal{M}$. The claim here is only that no curvature is generated by the projection without an independent postulate at the effective level.

Proof In a principal bundle with non-flat connection, Ω is a horizontal adjoint-valued 2-form. Bundle-induced reductions yield quadratic curvature contributions of Yang–Mills type, which appear in the base Ricci tensor in the standard Kaluza–Klein reduction. If $G_\Pi = \{e\}$, then $\mathfrak{g}_\Pi = \{0\}$ and $\Omega = 0$, so the term vanishes identically. □

Remark.

$$\Pi \text{ injective} \Rightarrow G_\Pi = \{e\} \Rightarrow \Omega = 0 \Rightarrow \text{no fiber-induced curvature on } \mathcal{M} \Rightarrow R^{\text{eff}}_{\mu\nu\rho\sigma} \text{ receives no projective sourc} \tag{131}$$

Equation (126) shows that effective gravitational curvature on $\mathcal{M}$ receives no sourcing from the fiber geometry when Π is injective. Any non-zero curvature of g^{eff} would then require an independent postulate at the level of $\mathcal{M}$, violating ontological uniqueness. The chain is topological, not dynamical, and holds for any admissible projection in the sense of Definition B.1.

B.6 The minimal non-injective case: $G_\Pi = \mathrm{U}(1)$

As a consistency check and to connect to Section 5.1, we consider the minimal non-trivial case $G_\Pi = \mathrm{U}(1)$. A principal U(1)-bundle over $\mathcal{M}$ with connection ω has:

$$\operatorname{Hol}(\omega, x_0) \subseteq \mathrm{U}(1), \tag{132}$$

$$\Omega = d\omega \in \Omega^2(\mathcal{M}, i\mathbb{R}), \tag{133}$$

where Ω is interpreted as the electromagnetic field strength in the Cosmochrony setting (Section A.11). The first Chern class $c_1(\Pi) = [\Omega/2\pi i] \in H^2(\mathcal{M}, \mathbb{Z})$ is non-trivial if and only if the bundle is topologically non-trivial.

This matches the structure of Section 5.2. The electromagnetic U(1) gauge symmetry emerges because the projection fiber supports a non-trivial Hopf fibration $S^1 \hookrightarrow S^3 \to S^2$.

In the injective limit, where the fiber degenerates to a point, the bundle trivializes and the U(1) gauge structure disappears, consistent with Eq. (126).

B.7 Summary of Step A

The classification of admissible injective projections establishes the following hierarchy, completing Step A of Theorem 5.1.

Fiber type	Structure group G_Π	Emergent structure
Point ($\lvert\Pi^{-1}(y)\rvert = 1$, injective)	$G_\Pi = \{e\}$	No gauge, no projection-induced curvature, no
Circle (S^1, minimal non-injective)	$G_\Pi = \mathrm{U}(1)$	U(1) gauge field, electromagnetic curvature
Three-sphere (S^3, Cosmochrony setting)	$G_\Pi \supseteq \mathrm{SU}(2) \times \mathrm{U}(1)$	Gauge structure and projection-induced curvat

The injective case is the unique case in which no re-identification symmetry and no projection-induced curvature can arise without an independent postulate. Non-injectivity is therefore not merely sufficient but necessary for emergent gauge and gravitational structure under Hypothesis H and ontological uniqueness.

B.8 Infrared expansion of the coherence functional

To extract the dominant infrared behavior of S_{coh}, we expand $\mathcal{L}_{\mathrm{defect}}$ in powers of the curvature scale ℓ_c^{-2}, where ℓ_c is the characteristic scale of curvature variations. In the infrared regime $\ell_c \gg \ell_\chi$ (with $\ell_\chi = \hbar_\chi / c_\chi$ the microscopic capacity length), curvature is slowly varying and the expansion is controlled.

Step 1: metric from the operator symbol.

Following the derivation in [48] and Appendix A.12, the effective metric $g_{\mu\nu}$ is identified with the principal symbol of the effective continuum operator $\mathcal{L}_\Pi = \nabla^\mu(A^{\mu\nu}(x)\nabla_\nu)$:

$$g^{\mu\nu}(x) \propto A^{\mu\nu}(x), \tag{134}$$

where $A^{\mu\nu}$ encodes the local connectivity and stiffness of the relational substrate [48]. This is an emergent metric: it is not introduced as an independent variable but arises from the spectral structure of Π.

Step 2: from fiber curvature to effective Laplacian to Riemann tensor.

The curvature 2-form $\Omega_{\mu\nu}$ of the fiber connection acts on sections of the adjoint bundle $\mathrm{ad}\, P$ over $\mathcal{M}$. Its square $\|\Omega_{\mu\nu}\|^2_{\mathfrak{g}_\Pi}$, integrated over $\mathcal{M}$, defines a Yang–Mills-type functional on $\mathcal{M}$. In the Kaluza–Klein reduction from $\mathcal{C}_\chi$ to $\mathcal{M}$, the fiber curvature contributes to the effective operator $\mathcal{L}_\Pi$ through its symbol. Following [48], the principal symbol of $\mathcal{L}_\Pi$ is $\sigma_2(\mathcal{L}_\Pi)(x,k) = A^{\mu\nu}(x)k_\mu k_\nu$, which identifies $g^{\mu\nu} \propto A^{\mu\nu}$. The fiber curvature Ω modifies the sub-principal symbol of $\mathcal{L}_\Pi$ at order ℓ_c^{-2}, contributing a term proportional to $R_{\mu\nu}k^\mu k^\nu$ through the standard formula for the sub-principal symbol

of a connection Laplacian $\nabla^\mu \nabla_\mu$ acting on sections of a bundle with curvature Ω:

$$\sigma_1(\nabla^\mu \nabla_\mu) \supset \frac{1}{6} R \cdot \mathrm{id} + \mathcal{F}(\Omega),$$

where the first term is the Lichnerowicz correction and $\mathcal{F}(\Omega)$ encodes the fiber curvature contribution. It is this sub-principal symbol, not the Yang–Mills square $\|\Omega\|^2$ directly, that generates R at two-derivative order. The Yang–Mills square $\|\Omega\|^2 \sim R^2_{\mu\nu\rho\sigma}$ appears only at four-derivative order and is subdominant under (D3). The two-derivative IR term R arises from the sub-principal symbol of the connection Laplacian on the fiber bundle, via the Lichnerowicz–Weitzenböck identity. We summarize the infrared content of this statement as:

$$\sigma_1(\mathcal{L}_\Pi)\big|_{\text{fiber}} \supset \frac{1}{6} R + \mathcal{O}(\ell_c^{-4}), \tag{135}$$

yielding $\mathcal{L}^{\text{geom}}_{\text{defect}} \propto R$ at two-derivative order, with the four-derivative Yang–Mills term $\|\Omega\|^2$ entering only as a subleading correction.

However, conditions (D1)–(D4) impose additional constraints. In particular, (D3) (infrared dominance of a low-derivative action) requires that the action be organized by the number of derivatives, with the lowest-derivative terms dominating in the infrared.

Step 3: integration by parts and the Gauss–Bonnet identity.

In four dimensions, the Gauss–Bonnet combination $\mathcal{G} = R_{\mu\nu\rho\sigma} R^{\mu\nu\rho\sigma} - 4 R_{\mu\nu} R^{\mu\nu} + R^2$ is a total derivative and does not contribute to the equations of motion. Therefore, among all quadratic curvature invariants, only R^2 and $R_{\mu\nu} R^{\mu\nu}$ are independent at the level of the action, modulo boundary terms. But both are of order ℓ_c^{-4}, subdominant under (D3).

The leading IR contribution to the defect density from the geometric sector is therefore:

$$\mathcal{L}^{\text{geom}}_{\text{defect}} = \frac{c_\chi^3}{\hbar_\chi} \cdot \frac{1}{16\pi} \cdot R + \mathcal{O}(\ell_c^{-4}), \tag{136}$$

where the prefactor $c_\chi^3/\hbar_\chi$ matches the dimensions of the Einstein–Hilbert density up to the normalization fixed by the precise operator mapping. The normalization is tracked explicitly in Section B.10.

B.9 Saturation selects the Born–Infeld completion

The IR expansion (35) is valid only for $\ell_c \gg \ell_\chi$. In the ultraviolet regime $\ell_c \sim \ell_\chi$, higher-derivative corrections become comparable to the Einstein–Hilbert term, and the expansion breaks down. The saturation bound $|\partial_t \chi| \leq c_\chi$ provides the principle that selects among the possible UV completions.

As established in [48], the minimal conditions for a UV completion compatible with bounded flux propagation are:

(i) it reduces to a quadratic (Einstein–Hilbert-like) form in the IR ($\ell_c \gg \ell_\chi$),
(ii) it enforces a strict upper bound on admissible field invariants at $\ell_c \sim \ell_\chi$,
(iii) it introduces no additional microscopic scales beyond c_χ and $\hbar_\chi$.

Applied to the gravitational sector, a natural Born–Infeld-like completion takes the form:

$$S_{\rm coh}^{\rm full}[g,\psi] = \frac{c_\chi^4}{\hbar_\chi^2}\int_{\mathcal{M}}\left(\sqrt{-\det\left(g_{\mu\nu}+\frac{\hbar_\chi}{c_\chi^2}\mathcal{R}_{\mu\nu}\right)}-\sqrt{-g}\right)d^4x + S_{\rm matter}[g,\psi], \quad (137)$$

where $\mathcal{R}_{\mu\nu}$ is a symmetric curvature tensor. The precise identification of $\mathcal{R}_{\mu\nu}$ requires the tensorial extension of the operator-theoretic analysis of [48].

In the IR expansion $\hbar_\chi/c_\chi^2 \ll \ell_c^2$:

$$\sqrt{-\det\left(g_{\mu\nu}+\frac{\hbar_\chi}{c_\chi^2}\mathcal{R}_{\mu\nu}\right)} \approx \sqrt{-g}\left(1+\frac{\hbar_\chi}{2c_\chi^2}\mathcal{R}+\mathcal{O}\left(\frac{\hbar_\chi^2}{c_\chi^4}\mathcal{R}_{\mu\nu}\mathcal{R}^{\mu\nu}\right)\right), \quad (138)$$

so that:

$$S_{\rm coh}^{\rm full} \xrightarrow{\ell_c \gg \ell_\chi} \frac{c_\chi^2}{2\hbar_\chi}\int_{\mathcal{M}}\mathcal{R}\sqrt{-g}\,d^4x + S_{\rm matter} + \mathcal{O}(\ell_c^{-4}), \quad (139)$$

where $\mathcal{R} \equiv g^{\mu\nu}\mathcal{R}_{\mu\nu}$. If $\mathcal{R}_{\mu\nu} = R_{\mu\nu}$, then $\mathcal{R} = R$ and the leading term reproduces (35).

Proposition B.3 (Born–Infeld structure as gravitational UV completion)**.** *Under conditions (i)–(iii) and ontological uniqueness, the UV completion of the Einstein–Hilbert term in $S_{\rm coh}$ belongs to the class of Eddington-inspired Born–Infeld actions of the form (132). This structure is the unique diffeomorphism-invariant extension of the scalar Born–Infeld form satisfying (i)–(iii) under the ansatz that the completion depends on the metric and its curvature only through a single symmetric rank-2 tensor. The tensorial extension of the uniqueness argument from the scalar case to the gravitational case remains an open step requiring the full operator analysis.*

Proof The scalar and vector cases are established in [48]. The extension to the gravitational sector follows by the same argument under the ansatz that the completion depends on $g_{\mu\nu}$ and $\mathcal{R}_{\mu\nu}$ only through their determinant combination, which is the minimal diffeomorphism-invariant structure satisfying (i)–(iii). The identification $\mathcal{R}_{\mu\nu} = R_{\mu\nu}$ is natural but not uniquely forced at this level. Alternatives such as $\mathcal{R}_{\mu\nu} = R_{\mu\nu} - \frac{1}{4}g_{\mu\nu}R$ are also compatible with (i)–(iii) and would modify the IR expansion only at subleading order. This residual ambiguity is the primary open point of the gravitational Born–Infeld completion within the present framework. □

B.10 Prediction: $G_{\rm eff}$ in terms of c_χ and $\hbar_\chi$

Comparing (134) with the standard Einstein–Hilbert normalization $\frac{c^4}{16\pi G}\int R\sqrt{-g}\,d^4x$ and using $c = c_\chi$, the identification requires:

$$\frac{c_\chi^4}{16\pi G_{\rm eff}} = \frac{c_\chi^2}{2\hbar_\chi}.$$

Formally, this gives:

$$G_{\text{eff}} = \frac{c_\chi^2 \hbar_\chi}{8\pi}. \tag{140}$$

A dimensional check in SI units yields $[c_\chi^2 \hbar_\chi] = \mathrm{kg\,m^4\,s^{-3}}$, while $[G] = \mathrm{m^3\,kg^{-1}\,s^{-2}}$. These do not match, which signals that the prefactor $c_\chi^4/\hbar_\chi^2$ in Eq. (132) must carry the residual dimensions. The dimensional consistency of Eq. (135) depends on the precise normalization of the Born–Infeld gravitational action, which requires the full tensorial derivation noted in Section B.9 as an open step. The structural prediction $G_{\text{eff}} = G(c_\chi, \hbar_\chi)$ is robust. The precise numerical prefactor and dimensional matching are left as a quantitative step contingent on the tensorial completion.

B.11 Energy and Curvature

Energy emerges as a diagnostic of constrained relaxation. At the effective level:

$$\mathcal{E}_\chi^{\text{eff}} = \tfrac{1}{2}\big[(\partial_t \chi)^2 + (\nabla \chi)^2\big].$$

This functional has no Hamiltonian or variational status. Regions of large $\mathcal{E}_\chi^{\text{eff}}$ correspond to strong internal gradients and are identified with particle-like excitations.

The apparent ordering of atomic orbitals by increasing energy reflects the structural cost of sustaining extended oscillatory configurations. An outer orbital constrains relaxation over a wider region, increasing total resistance independently of the geometric visibility discussed in Appendix B.12.

Curvature characterizes internal deformation of projected χ configurations and how they modulate the propagation of relaxation. Effective spacetime curvature arises secondarily as a macroscopic descriptor. Stable solitonic configurations emerge when nonlinear self-interaction balances dispersive gradients, providing a dynamical origin for long-lived particle-like excitations.

B.12 Level Sets, Projections, and Apparent Orbital Geometry

For a continuous scalar field $\phi : \mathbb{R}^3 \to \mathbb{R}$, the level set $\mathcal{L}_c = \{\mathbf{x} \mid \phi(\mathbf{x}) = c\}$ is generically a two-dimensional surface, possibly with disconnected components.

Projecting the thresholded set $P_c = \{z \mid \exists (x, y)\ \phi(x, y, z) \geq c\}$ generically produces disjoint intervals even when ϕ is continuous. This fragmentation is a purely geometric consequence of thresholding followed by projection: no discontinuity of ϕ is involved.

The envelope $f(z) = \max_{x,y} \phi(x, y, z)$ is continuous, but the condition $f(z) \geq c$ selects disconnected regions whose appearance and disappearance as c varies reflect visibility changes, not structural changes. The inverse reconstruction of ϕ from P_c is underdetermined.

Orbital-like patterns, nodal structures, and probabilistic visibility regions are therefore emergent manifestations of an underlying continuous field. Their apparent discreteness reflects projection and detection criteria.

B.13 Emergent Electrodynamics from χ Dynamics

In the weak-gradient regime, $\nabla\chi$ decomposes as $\nabla\chi = -\nabla\phi + \mathbf{A}_\mathrm{T}$ with $\nabla \cdot \mathbf{A}_\mathrm{T} = 0$, induced by the topology of localized excitations.

Charge as Transverse Torsion

The bounded canonical current $\mathbf{J}_\chi \propto \nabla\chi/\sqrt{1 - |\nabla\chi|^2/c^2}$ saturates as $|\nabla\chi| \to c$. An effective charge invariant is $q = \kappa \oint_\gamma \mathbf{A}_\mathrm{T} \cdot d\boldsymbol{\ell}$, whose sign reflects the chirality of the transverse torsion. The magnetic field is $\mathbf{B} = \nabla \times \mathbf{A}_\mathrm{T}$.

Emergent Electromagnetic Fields

Electric and magnetic fields:

$$\mathbf{E} = -\nabla\phi - \frac{1}{c}\frac{\partial \mathbf{A}_\mathrm{T}}{\partial t}, \quad \mathbf{B} = \nabla \times \mathbf{A}_\mathrm{T}.$$

These satisfy a closed system of Maxwell-like relations. Gauge invariance under $\phi \to \phi - c^{-1}\partial_t\Lambda$, $\mathbf{A}_\mathrm{T} \to \mathbf{A}_\mathrm{T} + \nabla\Lambda$ reflects the relational nature of χ (Section A.8).

Electromagnetism appears as a geometric and topological manifestation of the χ substrate, not an independent interaction mediated by elementary gauge fields.

B.14 Relational Consistency of the Effective Lagrangian

Step 1: Relational Constraint

$$\mathcal{C}_i[\chi] \equiv \sum_j K_{ij}(\chi_i - \chi_j)^2 \leq \chi_c^2. \tag{141}$$

Step 2: Variational Formulation

Constrained action with KKT conditions:

$$S[\{\chi_i\}, \{\mu_i\}] = \int d\lambda \left[\sum_i \tfrac{1}{2}(d\chi_i/d\lambda)^2 - U[\{\chi_i\}] - \sum_i \mu_i(\mathcal{C}_i - \chi_c^2) \right]. \tag{142}$$

Step 3: Continuum Limit and Canonical Form

In projectable regimes:

$$|\nabla\chi|^2 \leq c^2, \tag{143}$$

with $c^2 \equiv a^2\chi_c^2/K_0$. The canonical representation satisfying boundedness, monotonicity, and regularity:

$$f(x) = -c^2\sqrt{1 - x}, \tag{144}$$

yielding the Born–Infeld-like Lagrangian:

$$\mathcal{L}_\mathrm{eff} = -c^2\sqrt{1 - \frac{|\nabla\chi|^2}{c^2}} + \partial_t\chi. \tag{145}$$

Step 4: Role of $U[\{\chi_i\}]$

In the continuum limit, $U[\{\chi_i\}] \to \int d^3x\, V(\chi)$, connected to the main text's $V(\chi)$ via coarse-graining.

Step 5: Connection to Emergent Geometry

The effective metric is defined via the Hessian:

$$g_{\mu\nu}^{\text{eff}} \propto \frac{\partial^2 \mathcal{L}_{\text{eff}}}{\partial(\partial_\mu \chi)\, \partial(\partial_\nu \chi)}, \tag{146}$$

valid in projectable regimes (Section E.5).

Continuum Limit: Laplace–Beltrami Operator

In the dense limit ($N \to \infty$), the discrete graph Laplacian converges to the Laplace–Beltrami operator on an emergent Riemannian manifold. No background geometry is assumed: g_{ab} arises as the continuum encoding of microscopic connectivity.

Necessity of the Born–Infeld Structure

A quadratic action permits unbounded gradients and instantaneous propagation, contradicting the maximal relaxation speed c_χ. The Born–Infeld form is the minimal non-polynomial functional enforcing strict saturation, causal consistency, and self-regularization. The saturation constant b represents the substrate's upper relaxation bound; the speed of light c is a derived parameter with $c \leq b$.

C Conceptual Extensions of Cosmochrony — Particles, Quantum Phenomena, and Classical Limits

This appendix illustrates how familiar particle, quantum, and classical structures may emerge once the χ field admits localized and stable configurations. These developments serve as a conceptual bridge between the mathematical foundations (Appendix A) and the cosmological considerations (Appendix D). None are required for the logical coherence of the framework.

C.1 Interpretative Status of the χ Field

χ encodes a non-energetic relational scale of relaxation from which duration, distance, and causal ordering are reconstructed. The notation $\chi(x^\mu)$ is representational: spacetime coordinates serve as labels for relational information in regimes where a stable geometric description has emerged. χ should not be interpreted as a matter field on spacetime, a scalar coupled to a pre-existing metric, or a hidden-variable replacement for the wavefunction. Spacetime is an emergent bookkeeping structure *for* χ, not a container *of* χ.

C.2 Topological Configurations of the χ Field: Solitons as Particles

Solitonic configurations are effective geometric representations illustrating how particle-like properties arise from stable, localized configurations of χ_{eff} once a smooth geometric projection applies (Appendix F).

Charge as Oriented Relaxation Asymmetry

A localized configuration deforms χ_{eff} relative to the background $\chi_{\text{eff},0}$: excess (positive charge) or deficit (negative charge). The magnitude is diagnosed by a Gauss-like flux integral $q_{\text{eff}} \propto \oint_\Sigma \nabla\chi_{\text{eff}} \cdot d\mathbf{S}$. Coulomb-like interactions emerge from frustration minimization of the Dirichlet functional $\mathcal{F}[\chi_{\text{eff}}] = \frac{1}{2}\int |\nabla\chi_{\text{eff}}|^2\, d^3x$.

Vortical Configurations and Integer-Spin Excitations

An effective winding number $n = (2\pi)^{-1} \oint \nabla \arg(\chi_{\text{eff}}) \cdot d\mathbf{l}$ characterizes charge orientation, topological robustness, and integer spin.

Skyrmion-Like Configurations and Spin-$\frac{1}{2}$ Excitations

Configurations with topological index $Q = \pm 1$ exhibit 4π-periodicity under rotations, providing a geometric origin for spin-$\frac{1}{2}$ behavior and fermionic statistics.

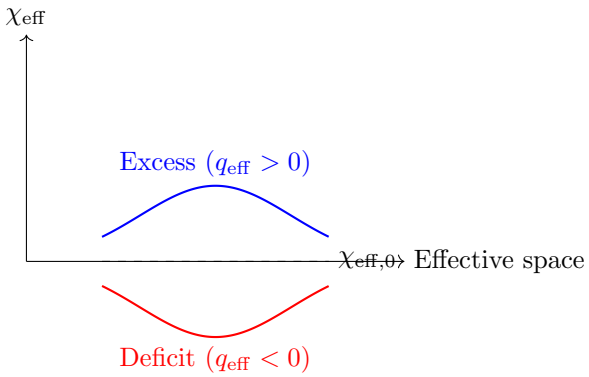

Fig. 15 Oriented deformations of χ_{eff} defining effective charge polarity.

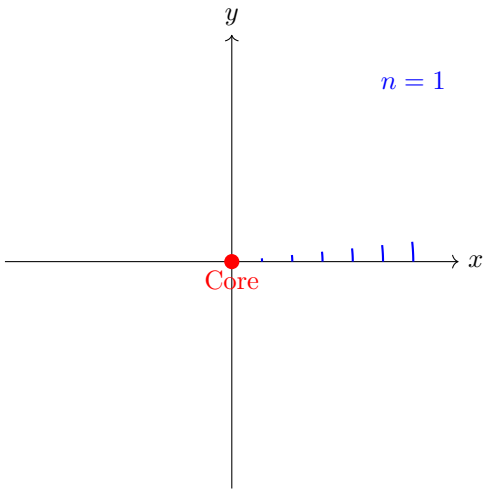

Fig. 16 Vortical configuration with winding $n = 1$ (integer spin).

Table 2 Effective solitonic configurations and emergent particle properties.

Configuration	**Index**	χ_{eff} **asymmetry**	**Properties**
Vortical	n	Excess/deficit	Charge $\propto n$, int. spin
Skyrmion	$Q = \pm 1$	Oriented deformation	Charge $\propto Q$, spin-$\frac{1}{2}$

Summary: Topology, Charge, and Spin

C.3 Soliton Energy and Structural Mass Scaling

Mass is interpreted as total resistance to relaxation. In the effective geometric regime:

$$M_{\text{eff}} \propto \int_{\mathcal{V}} \left[\mathcal{T}(\nabla\chi_{\text{eff}}) + \mathcal{U}(\chi_{\text{eff}})\right] d^3x.$$

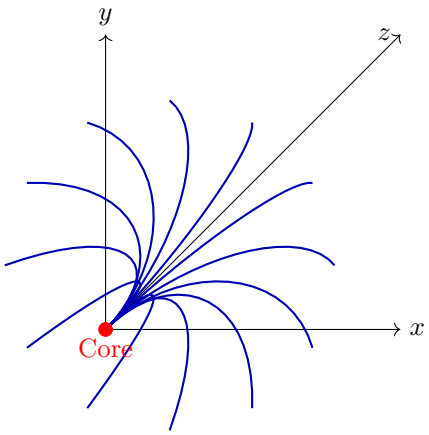

Fig. 17 Skyrmion-like configuration of χ_{eff} (spin-$\frac{1}{2}$).

For kink-like configurations, a balance between gradient resistance and nonlinear stabilization fixes the soliton width ξ, yielding $M_{\text{eff}} \sim \sqrt{\lambda_{\text{eff}}}\,\xi\,\chi_c^2$. Configurations with higher winding or linking indices involve increased gradients, so $M_{n+1} > M_n$, establishing mass hierarchies structurally. From a spectral viewpoint, $M_{\text{eff}} \sim \lambda_{\min}^{-1}$, where $\lambda_{\min}$ is the smallest positive eigenvalue of the linearized relaxation operator.

C.4 Example: 4π-Periodic Soliton and Spinorial Behavior

An illustrative construction supporting the topological interpretation of spin (Section 8.12).

In the projectable regime, certain localized excitations admit an effective internal phase θ. A complex-valued proxy (the underlying field remains real): $\chi_{\text{eff}}(x) = \eta \tanh(\kappa x)\, e^{i\theta(x)}$. Choosing $\theta(\alpha) = \alpha/2$:

$$\psi(\alpha) \equiv \psi_0\, e^{i\alpha/2}. \tag{147}$$

A 2π cycle inverts the sign:

$$\psi(\alpha + 2\pi) = -\psi(\alpha). \tag{148}$$

A 4π cycle restores identity:

$$\psi(\alpha + 4\pi) = \psi(\alpha). \tag{149}$$

Schematically:

$$\begin{aligned} &\alpha : 0 \to 2\pi \Rightarrow \text{nontrivial loop } (\mathbb{Z}_2) \Rightarrow \psi \mapsto -\psi, \\ &\alpha : 0 \to 4\pi \Rightarrow \text{trivial loop} \Rightarrow \psi \mapsto \psi. \end{aligned} \tag{150}$$

This 4π-periodicity mirrors the double-cover $\mathrm{SU}(2) \to \mathrm{SO}(3)$ and provides a geometric basis for fermion-like transformation behavior without fundamental spinor fields. The sign change is an effective encoding of the $\mathbb{Z}_2$ obstruction (Section C.6: $\pi_1(\mathcal{C}_{\text{eff}}) = \mathbb{Z}_2$).

C.5 Relation to Classical Limits

Classical behavior corresponds to a dynamical regime where χ_{eff} varies slowly, localized excitations are dilute, and topological constraints are suppressed. Perturbations propagate as weak disturbances on an effectively flat background, recovering superposition and approximate locality. In the nonlinear regime, large gradients induce effective curvature and horizon-like behavior. The classical limit is defined not by $\hbar \to 0$ but by the stability of a particular relaxation regime of the underlying χ field.

C.6 Status of the Formulation

The framework is minimal yet structurally complete at the conceptual level. A fully covariant action principle and systematic quantization remain open technical extensions, not conceptual deficiencies. GR and QFT emerge as effective, coarse-grained descriptions within specific dynamical regimes of χ_{eff}. Cosmochrony should be viewed as a foundational framework clarifying what is fundamental and how known structures arise, rather than as a closed effective field theory.

C.7 Soliton and Particle Solutions

Elementary particles are stable localized configurations arising in the projectable regime. While the fundamental field is scalar, certain configurations possess nontrivial internal organization requiring a double-valued representation under effective rotations. The Dirac equation appears as the minimal effective dynamics compatible with approximate locality, relativistic covariance, and 4π-periodic topology. Spin, fermionic statistics, and exclusion behavior arise as consequences of the nontrivial configuration space. The effective self-interaction functional must support localized configurations with finite mass, dynamical stability, and topologically inequivalent sectors.

C.8 Perspectives: Towards a Derivation of the Proton-to-Electron Mass Ratio

Normal modes of the stability operator $\mathcal{L}_{\text{sol}}\psi_n = \lambda_n \psi_n$ encode intrinsic stiffness scales. The effective mass scaling is $m_n \propto \sqrt{\lambda_n}\,\chi_c$, and energy levels satisfy $E_n \sim \lambda_n \chi_c^2$.

The proton is modeled as a composite three-soliton bound state ($Q = 3$, motivated by topological phase locking [49, 50]), with

$$\frac{m_p}{m_e} \approx \sqrt{\frac{\lambda_{\text{bind}}}{\lambda_e}}, \quad \frac{\lambda_{\text{bind}}}{\lambda_e} \sim 3.4 \times 10^6.$$

The spectral packing fraction $\alpha \equiv \lambda_e/\lambda_{\text{bind}} \sim 3 \times 10^{-7}$ measures spectral compression from topological binding. Heuristically, $\lambda_{\text{bind}}/\lambda_e \sim \chi_c^2$ gives $\chi_c \approx 8.3$.

Working Ansatz for $V(\chi)$

A minimal two-scale effective potential:

$$V(\chi) = \frac{\lambda}{4}(\chi^2 - \eta^2)^2 + \varepsilon\,\eta^4 \left[1 - \cos\left(\frac{\chi}{\eta}\right)\right], \tag{151}$$

with $\varepsilon \ll 1$.

Linking (λ, η) to Observables

Dimensionless control combinations:

$$g \equiv \lambda\,\chi_c^2\,\eta^2, \quad u \equiv \varepsilon. \tag{152}$$

Matching strategy.

The feasibility condition:

$$\exists\,(g,u) \text{ s.t.} \quad \frac{\lambda_{\rm bind}(Q{=}3;\,g,u)}{\lambda_e(g,u)} \approx 3.4 \times 10^6, \tag{153}$$

while remaining stable under small (g, u) variations.

Numerical Program

The pipeline tests whether bounded relaxation plus $V(\chi)$ admits stable sectors with $\lambda_{\rm bind}/\lambda_e \sim 10^6$ without fine-tuning: dynamics and formation, soliton harvesting by topological classification, stability operator extraction, spectral ratio test, and fine-structure diagnostics.

C.9 Spectral Scaling and the Projection Ontology

Inertial mass is a spectral signature of projection visibility. The non-injective projection Π implies that each effective particle corresponds to a large equivalence class of micro-configurations whose stability eigenvalues measure the fiber weight. The ratio $m_p/m_e \approx \sqrt{\lambda_p/\lambda_e}$ is independent of the absolute action scale $\hbar_\chi$ and is therefore a structurally protected invariant.

C.10 Spectral Characterization of Mass and the Secondary Role of $V(\chi)$

Particle masses emerge as eigenmodes of an effective relaxation operator $\Delta_G^{(0)}\psi_n = -\lambda_n\psi_n$, with $m_n c^2 \propto \sqrt{\lambda_n}\,\chi_c$. This is analogous to bounded elastic systems where vibrational frequencies arise from geometry and connectivity.

Three conceptual levels are distinguished: the background-independent spectral operator (fundamental), coarse-grained $\chi_{\rm eff}$ geometry (emergent), and interaction-induced redistributions (dynamical). $V(\chi)$ plays a secondary role, providing local

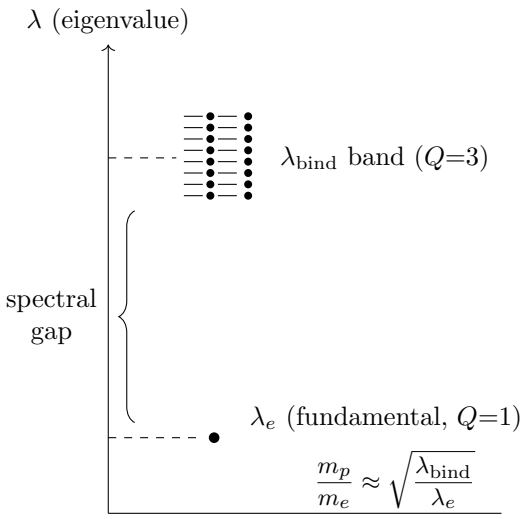

Fig. 18 Spectral gap in the stability spectrum of $\mathcal{L}_{\text{sol}}$: elementary mode λ_e separated from binding-mode band λ_{bind}.

stabilization and fine splittings without setting the overall mass scale. Its admissible form is constrained by compatibility with the pre-existing spectral structure. Potential-induced corrections shift eigenvalues as $\lambda_n \to \lambda_n^{(0)} + \Delta\lambda_n^{(V)}$, affecting small splittings (e.g. neutron–proton) while leaving topologically dominated ratios largely invariant.

C.11 Spectral Stability and the Emergence of $\hbar_{\text{eff}}$

From the fundamental scales K_0 (stiffness), χ_c (correlation length), and c (maximal speed), a natural action unit is $\hbar_\chi \equiv c^3/(K_0\chi_c)$. Here K_0 and χ_c denote bare substrate parameters.

For a solitonic mode with eigenvalue λ_n, identifying the rest energy $E_n = \hbar_{\text{eff}}\,\nu_n$ yields $\hbar_{\text{eff}}$ as a geometric and spectral quantity. At microscopic scales ($\ell \sim \chi_c$), $\hbar_{\text{eff}} \approx \hbar_\chi \approx \hbar$. At macroscopic scales, $\hbar_{\text{eff}} \approx \hbar_\chi(\chi_c/\ell_{\text{spacetime}})^2$, suppressing quantum effects through reduced spectral accessibility rather than decoherence. Reproducing particle-scale behavior requires $K_0\chi_c^2 \sim \hbar$.

C.12 Renormalization of Substrate Parameters

Bare parameters (K_0, χ_c) are universal substrate invariants; effective parameters (K_{eff}, χ_{eff}) emerge through coarse-graining (Appendix E). The universality of $\hbar$ and the spectral invariant α_{spec} stems from their dependence on bare ratios, invariant under projective scaling within a given relaxation epoch. Dimensionless couplings such as α_{EM} inherit no arbitrariness from substrate parameters: the electric charge is a geometric invariant of the soliton's spectral embedding relative to Π, so the dependence on K_0 cancels in dimensionless ratios.

C.13 Structural Origin of Quantum Correlations and Non-Locality

The non-injective projection Π provides a structural reinterpretation: what appear as two spatially separated particles may correspond to a single relational configuration in χ. Entanglement is the manifestation of a single χ-source through multiple non-injective projective images. Spin correlations arise from torsional conservation: a local stabilization at A structurally constrains admissible projective states at B originating from the same source. Bell inequality violations are attributed to the use of emergent metric locality in a context where correlations are established prior to spacetime separation. The framework remains ontologically realist at the substrate level but structurally non-local with respect to the emergent spacetime.

C.14 Metastability, Decay Channels, and Exponential Lifetimes

Diagnostic Structural Functional

$E_{\text{struct}}[\chi_{\text{eff}}] \sim \int_{\mathcal{V}} (|\nabla \chi_{\text{eff}}|^2 + \mu^2 |\chi_{\text{eff}}|^2)\, d^3x$ quantifies resistance to relaxation.

Admissible Factorization Channels

A decay channel is an admissible factorization preserving topological invariants: $Q(\chi_{\text{eff},A}) = \sum_i Q(\chi_{\text{eff},i})$. Kinematic accessibility requires $\Delta E_{\text{struct}} > 0$. The survival probability is $P(\tau) = \exp(-\Gamma\tau)$ with $\Gamma = \sum_c \Gamma_c$.

Different interaction classes correspond to different degrees of constraint: strong decays involve direct topological reorganization, electromagnetic decays preserve core topology, and weak decays require deep reconfiguration through rarer paths.

Non-Injective Projection and Structural Factorization

Entanglement: a single χ_0 admits a non-factorizable projection. Decay: the projection becomes unstable and admissibility is recovered through factorization $\Pi(\chi_0) \to \Pi(\chi_1) \oplus \Pi(\chi_2) \oplus \cdots$. The distinction is not at the substrate level but in the stability properties of the projected description.

C.15 Measurement, Temporal Ordering, and Antiparticle Emergence

Measurement corresponds to the stabilization of a single projected description $\Pi_{\alpha^*}(\chi_0)$ under interaction with an environment. A partial ordering $\prec$ on admissible projected configurations induces an effective arrow of time without a fundamental temporal parameter.

Antiparticles emerge when admissible factorization of a configuration with $Q(\chi_A) = 0$ produces paired contributions with opposite signs: $Q(\chi_i) = +q$, $Q(\chi_j) = -q$. This reflects the necessity of preserving signed structural invariants under non-injective projection.

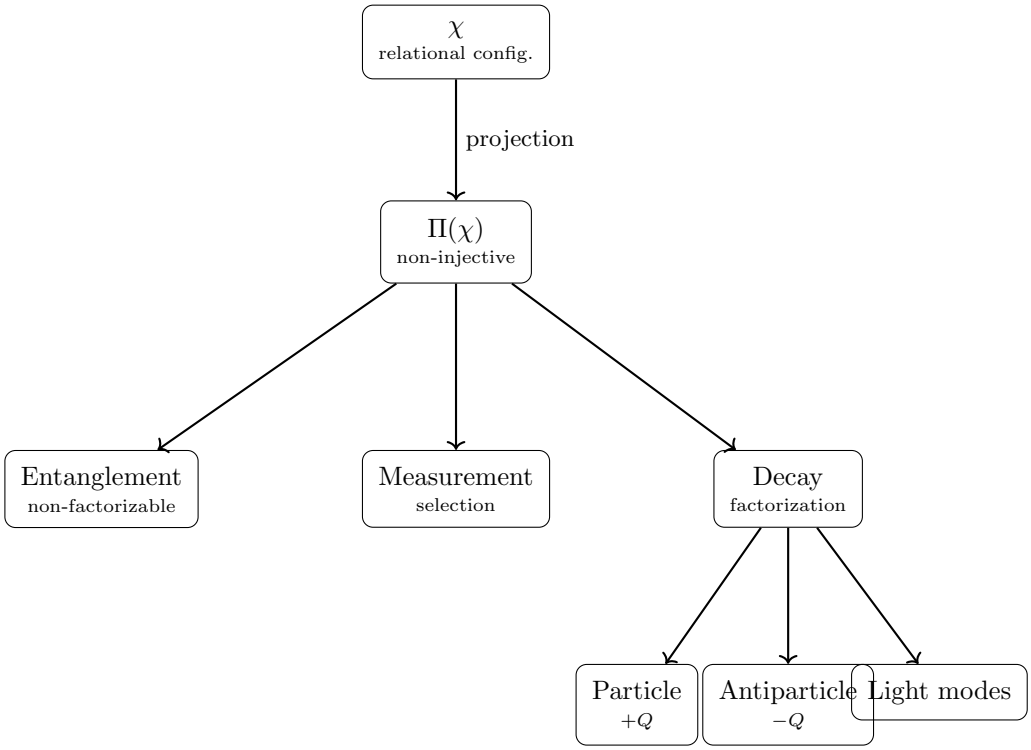

Fig. 19 Unified structural interpretation: entanglement, measurement, and decay all originate from Π. Antiparticles emerge when signed invariants are redistributed.

C.16 Structural Interpretation of CPT Symmetry

The combined transformation $(Q, \tau, \mathbf{x}) \to (-Q, -\tau, -\mathbf{x})$ leaves admissibility conditions invariant. Under factorization, conservation of signed invariants enforces particle–antiparticle pairs. CPT symmetry emerges as an invariance of the admissible projection structure.

C.17 CP Asymmetry and Chiral Selection

CPT versus CP as Admissibility Symmetries

Let projected configurations carry a set of signed structural invariants $\{Q_i\}$, associated with orientation, chirality, or phase winding. The admissibility conditions are invariant under the combined transformation

$$(Q_i,\ \tau,\ \mathbf{x}) \to (-Q_i,\ -\tau,\ -\mathbf{x}),$$

which defines an effective CPT symmetry at the level of the projected description.

In contrast, CP acts only on a subset of the invariants $\{Q_i\}$ and does not reverse the effective ordering parameter. CP is therefore not, in general, an invariance of

admissibility. Effective CP violation may arise without violating CPT invariance, reflecting a structural asymmetry of the projection rather than a breakdown of the relational substrate.

Structural Bias and Statistical Asymmetry

Assume that admissible projected configurations exhibit a slight asymmetry in relaxation efficiency with respect to the sign of a structural invariant Q. Let $\Gamma(Q)$ denote the effective stabilization rate.

If

$$\Gamma(Q) \neq \Gamma(-Q),$$

then configurations carrying one orientation are statistically favored during relaxation. Matter–antimatter asymmetry may therefore emerge as a dynamical bias in the projective selection process, without requiring explicit symmetry breaking at the fundamental level.

This statistical asymmetry provides the ontological background within which the more specific spectral structure of flavor mixing, reconstructed in Section 10.4, can operate.

Spectral Structure and the Jarlskog Invariant

In the Standard Model, CP violation in the quark sector is characterized by the Jarlskog invariant [51], which vanishes if any two fermion masses within a given sector are degenerate or if the mixing matrix is reducible to a two-generation form.

Within Cosmochrony, this structure is interpreted in terms of the spectral properties of the projection fiber Π. Let $\{\lambda_{u,i}\}$ and $\{\lambda_{d,i}\}$ denote the effective spectral eigenvalues associated with the up-type and down-type relaxation modes, respectively. These eigenvalues determine the inertial masses via Eq. (24) and encode the relaxation resistance of the corresponding projected configurations.

Degeneracy of eigenvalues within either sector,

$$\lambda_{u,i} = \lambda_{u,j} \quad \text{or} \quad \lambda_{d,i} = \lambda_{d,j},$$

restores rotational freedom within the corresponding subspace, allowing phase redefinitions that eliminate any CP-odd invariant.

The presence of three spectrally distinct generations ($n \geq 3$) is therefore the minimal condition under which an irreducible phase can arise. This threshold signals that the projective holonomy of the flavor manifold cannot be embedded in a two-dimensional spectral subspace.

Sectorial Misalignment and Cubic Commutator Structure

The full CP-violating structure depends not only on spectral non-degeneracy within a single sector, but on the incompatibility between the up-type and down-type spectral bases.

Let Π_u and Π_d denote the sectorial restrictions of the global non-injective mapping Π associated with these two relaxation channels. Because the projected state U has

finite descriptive capacity (bounded by the projective bandwidth b_χ), these operators cannot in general be simultaneously diagonalized. Their non-commutativity reflects an irreducible misalignment of spectral anchors within the same fiber.

Following the algebraic structure identified by Jarlskog [51], the CP-odd invariant can be expressed in terms of the imaginary part of the trace

D Cosmological and Observational Implications of Cosmochrony

This appendix examines cosmological and observational implications of Cosmochrony. All results arise from the same scalar relaxation dynamics governing the χ field; no additional cosmological degrees of freedom are introduced.

D.1 Low-ℓ CMB Power Suppression from Global χ Relaxation

The lowest CMB multipoles probe global properties of χ_{eff} rather than independent local perturbations (Sections 7.6, 7.11). Because the finite relaxation capacity of χ limits how globally coherent configurations can deviate from the relaxed background, the lowest ℓ-modes are systematically attenuated.

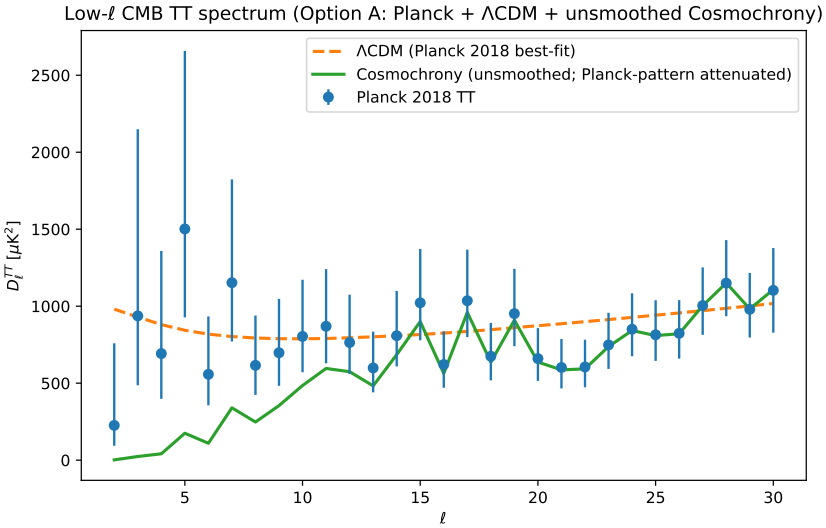

Fig. 20 Observed CMB temperature power spectrum at low multipoles. The shaded region illustrates a qualitative attenuation envelope from global relaxation constraints.

Significance of the unsmoothed comparison.

Figure 20 is not intended as a precision fit, but as a structural diagnostic. Unlike a sharp infrared cutoff or a purely statistical suppression, the attenuation mechanism preserves the relative multipole-to-multipole variations observed in the Planck data. As $\ell \to 0$, the same increasing and decreasing trends are reproduced, albeit with a progressively reduced amplitude.

This behavior is non-trivial. In ΛCDM, the lowest multipoles are treated as cosmic-variance–dominated outliers, with no underlying mechanism constraining their relative structure. Here, the correlated attenuation emerges from a single global constraint: the finite relational coherence capacity of χ_{eff}.

Phenomenological parametrization.

$$C_\ell^{\mathrm{CC}} = C_\ell^{\Lambda\mathrm{CDM}} \left[1 - \alpha \exp\left(-\frac{\ell}{\ell_0}\right)\right], \quad \alpha \in [0,1],\ \ell_0 > 0. \tag{154}$$

Graph-theoretic admissibility filter.

The weighted Laplacian $L_G(t)$ of the relational connectivity graph sets a minimal nonzero eigenvalue $\lambda_2(t)$ characterizing global connectivity. The primordial power spectrum is modulated by

$$\mathcal{A}(k,t) = \exp\left[-\left(\frac{\lambda_2(t)}{k^2}\right)^{p/2}\right],$$

reflecting the inability of an insufficiently connected relational graph to support large-scale coherent modes.

D.2 Resolution of the Horizon and Flatness Problems Without Inflation

Horizon problem: pre-geometric connectivity.

Large-scale correlations originate from the global connectivity of χ prior to the emergence of any effective spacetime description. Regions that later appear causally disconnected share correlated configurations inherited from earlier relaxation phases.

Flatness problem: relaxation toward geometric uniformity.

Effective spatial curvature reflects large-scale gradients in the relaxation rate of χ_{eff}. Configurations with large curvature gradients are dynamically disfavored, so near-flat spatial geometry emerges as a natural attractor of the relaxation dynamics, without exponential expansion or fine-tuning.

Implications for primordial correlations.

Because large-scale coherence arises from global organization of χ rather than amplification of quantum vacuum fluctuations, exact scale invariance is not expected at the largest wavelengths. Deviations at the lowest CMB multipoles motivate the analysis in Section D.1.

D.3 Evolution of the Hubble Parameter and the Hubble Tension

At the homogeneous background level, $a(t) \propto \chi(t)$ and $H(t) = \dot{\chi}/\chi$. In the idealized limit $\dot{\chi} = c$, one obtains $H(t) = c/\chi(t)$.

Illustrative $H(z)$ profile.

Using $1 + z = \chi(t_0)/\chi(t)$, the simplest background closure gives

$$H_\chi(z) = H_0\,(1+z)\,\sqrt{1-\Omega_\chi} \quad \text{(illustrative)}, \tag{155}$$

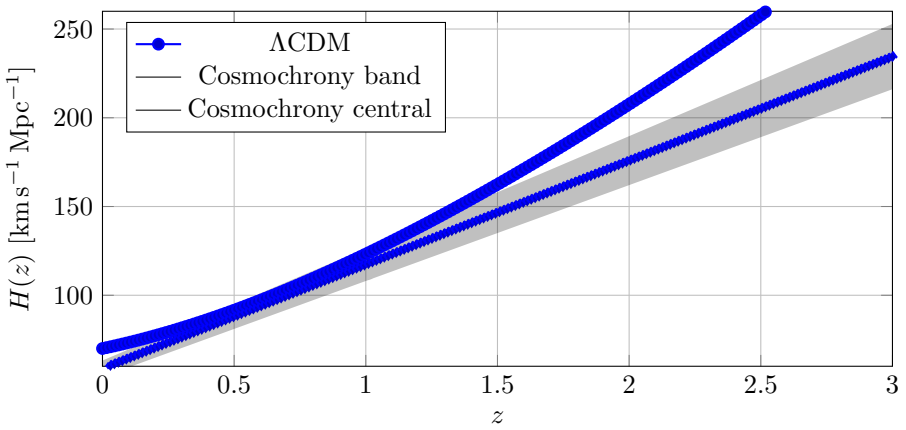

Fig. 21 Illustrative comparison of $H(z)$. The Cosmochrony band uses $H_\chi = H_0(1+z)\sqrt{1-\Omega_\chi}$ with (H_0, Ω_χ) variations.

to be compared with

$$H_{\Lambda\mathrm{CDM}}(z) = H_0\sqrt{\Omega_m(1+z)^3 + \Omega_r(1+z)^4 + \Omega_\Lambda}. \tag{156}$$

Relaxation budget.

The dimensionless parameter

$$\Omega_\chi \equiv \langle\beta^2\rangle, \quad \beta \equiv \frac{|\nabla\chi|}{c}, \tag{157}$$

measures the fraction of relaxation capacity stored in spatial gradients. The effective global expansion rate is then $\bar{H} = (c/\chi)\sqrt{1-\Omega_\chi}$.

Local expansion and the Hubble tension.

For a region with density contrast δ, a minimal mean-field closure gives

$$H_{\mathrm{loc}} = \bar{H}\sqrt{\frac{1-\Omega_\chi(1+\delta)}{1-\Omega_\chi}}. \tag{158}$$

For $\Omega_\chi \approx 0.3$ and a KBC-void underdensity $\delta \approx -0.4$, one finds $H_{\mathrm{loc}}/\bar{H} \approx 1.08$, comparable to the observed tension. Structural consistency imposes $\Delta H/H \in [3.5\%, 9.5\%]$ at $z \sim 1$.

Parameter degeneracies.

The effective gravitational coupling constrains

$$K_0\,\chi_c^2 \sim \frac{c^4}{16\pi G}, \tag{159}$$

so that K_0 and χ_c cannot be fixed independently without additional input.

D.4 Relation to Observational Units and Numerical Estimates

Normalization of the χ Field

$\chi(t_0)$ is identified with the characteristic geometric scale governing large-scale expansion, via $a(t) \propto \chi(t)$.

Emergent Gravitational Coupling

G emerges from the constitutive relation: $K_0 \chi_c^2 \sim c^4/(16\pi G)$.

Hubble Constant

In the homogeneous limit, $H_0 \simeq c/\chi(t_0)$ yields $\chi(t_0) \sim 4 \times 10^{26}$ m, of order the Hubble radius.

Age of the Universe

With $\dot{\chi} \simeq c$, $t_0 \simeq \chi(t_0)/c \sim 4 \times 10^{17}$ s (≈ 13.8 Gyr).

Redshift Interpretation

$1 + z = \chi(t_{\text{obs}})/\chi(t_{\text{emit}})$.

CMB Scale

At recombination ($z_{\text{rec}} \simeq 1100$), $\chi(t_{\text{rec}}) \simeq \chi(t_0)/(1 + z_{\text{rec}})$.

Orders of Magnitude and Robustness

All estimates rely solely on observed quantities and bounded relaxation dynamics. No fine-tuning or additional degrees of freedom are assumed.

Summary

Cosmochrony reproduces key cosmological scales without introducing new fundamental parameters.

D.5 Phenomenological Implications

Gravitational perturbation speed.

Linearizing the kinematic constraint around $\chi_0(t) = ct$ yields

$$\left(\frac{1}{c^2} \partial_t^2 - \nabla^2 \right) \delta\chi = 0, \tag{160}$$

so gravitational perturbations propagate at exactly c, consistent with GW170817.

Emergent acceleration scale.

The kinematic constraint $(\partial_t \chi)^2 + |\nabla \chi|^2 = c^2$ enforces a residual spatial gradient even in the absence of matter. This defines an effective acceleration scale $a_0(t) \sim c\, H(t)$. At large radii the effective acceleration approaches $g_{\text{eff}} \simeq \sqrt{g_N\, a_0}$, recovering deep-MOND scaling without interpolation functions or dark matter particles.

Gravitational lensing.

Near a localized mass, an effective refractive index $n(r) \simeq 1 + GM/(c^2 r)$ yields a deflection angle $\alpha = 4GM/(bc^2)$, reproducing the GR prediction from the nonlinear structure of χ relaxation dynamics.

D.6 Toy-Model of Spectral Gravitational Susceptibility

The local relaxation field strength is $\mathbf{E}_\chi = -\nabla \Phi_\chi$, governed by

$$\nabla \cdot [\epsilon_{\text{spec}}(\mathbf{E}_\chi)\, \mathbf{E}_\chi] = 4\pi G_0\, \rho_b,$$

with spectral permittivity $\epsilon_{\text{spec}} = 1 + \phi(\mathbf{E}_\chi)$. The spectral susceptibility interpolates between $\phi = 0$ ($|\mathbf{E}_\chi| \gg \mathcal{K}_c$, Newtonian) and $\phi = \mathcal{K}_c/|\mathbf{E}_\chi|$ ($|\mathbf{E}_\chi| \ll \mathcal{K}_c$, saturation).

In the low-field limit, $g_{\text{eff}} \approx \sqrt{G_0 M \mathcal{K}_c}/r$, yielding $v^4 = G_0 M \mathcal{K}_c$ (Baryonic Tully–Fisher Relation).

Feature	**MOND**	**Cosmochrony**
Origin	Modified inertia/force	Non-linear substrate susceptibility
Threshold	Universal a_0	Local stiffness $\mathcal{K}_c$
Bullet Cluster	Requires additional DM	Relaxation hysteresis (wake)
GR relation	Requires TeVeS	GR is the linear-response limit

Table 3 MOND vs. Cosmochrony substrate response.

Cosmochrony predicts **spectral echoes**: residual curvature in regions where matter has recently passed, distinguishing it from WIMP-based models.

D.7 Substrate Origin of the Effective Galactic Potential

Localized excitations influence large scales via a relaxation flux $\Phi_\chi(r) \sim |\nabla \chi|/K(r)$, where effective stiffness $K(r)$ increases with distance from excitations. A critical stiffness K_c separates the unsaturated Newtonian regime ($K \ll K_c$) from the saturated non-injective regime ($K \gtrsim K_c$), manifesting as a threshold $g_N(r) \simeq a_0(t)$.

The cosmological origin is $a_0(t) \sim c\, H(t)$, predicting slow evolution of the effective acceleration scale. In the saturated regime, scale-invariant relaxation flux implies $g_{\text{eff}} \propto 1/r$ and a logarithmic effective potential $\Phi_{\text{eff}}(r) \propto \ln r$, directly accounting for flat rotation curves.

D.8 Spectral Interpretation of the Galactic Saturation Regime

In projectable regimes, the collective response is characterized by an effective elliptic operator $\mathcal{L}_{\text{eff}}$ with spectrum λ_n. Beyond a critical scale, the smallest eigenvalue approaches a saturation threshold λ_c, corresponding to the stiffness threshold K_c of Appendix D.7. The effective acceleration scale satisfies $a_0 \sim \lambda_c/\tau_\chi^2$. When the spectrum becomes marginally scale-invariant near λ_c, the Green function behaves as $G(r) \propto \ln r$, providing a spectral explanation for flat rotation curves. At scales where $\lambda_{\min} \ll \lambda_c$, the dense spectrum recovers the familiar $1/r$ Newtonian behavior.

D.9 Cosmological Role of Neutrino-Like Excitations

Neutrino-like excitations occupy an intermediate regime between particle-like solitons and radiative modes, with minimal structural energy and weak localization. Their free streaming implements a non-local relaxation channel that transports residual structural mismatch without efficient thermalization. This suppresses growth of small-scale projected structures and contributes to the emergence of a cosmological arrow of time as an ordering of admissible projected configurations.

D.10 Neutrino-Mediated Structural Smoothing and Cosmological Inference

The effective Hubble rate encodes both geometric expansion and cumulative structural relaxation. Early-time observables (CMB anisotropies) are sensitive to the integrated neutrino-mediated smoothing; parameter inference assuming purely geometric expansion may systematically underestimate the late-time expansion rate. The lowest CMB multipoles may reflect anisotropic relaxation during the neutrino-dominated smoothing phase.

D.11 Cosmic Voids as Observational Tests of Maximal Substrate Relaxation

Voids probe the regime of near-maximal relaxation, where departures from ΛCDM are most pronounced. Observables are modeled as a ΛCDM baseline plus a Born–Infeld-like saturating correction:

$$\kappa_{\text{obs}}(R) = \kappa_{\Lambda\text{CDM}}(R)\left[1 + \beta_{\text{void}}\,\mathcal{S}\big(\mathcal{A}(R)\big)\right], \tag{161}$$

$$v_{\text{obs}}(r) = v_{\Lambda\text{CDM}}(r)\left[1 + \beta_{\text{void}}\,\mathcal{S}\big(\mathcal{B}(r)\big)\right], \tag{162}$$

with saturation function $\mathcal{S}(x) = x/\sqrt{1+x^2}$. Key predictions: more negative void lensing than ΛCDM with non-linear saturation, enhanced peculiar velocity outflows at void boundaries, and cross-consistency between lensing and velocities through a single β_{void}. Enhanced void outflows predict a correlation between negative void-lensing strength, boundary outflows, and elevated local H_0 estimates.

E Numerical Methods and Technical Supplements

This appendix collects numerical methods, technical constructions, and auxiliary derivations. All methods operate within regimes where χ admits an effective, discretized, or coarse-grained representation. Auxiliary representations (graphs, lattices, finite-difference schemes) are introduced solely for calculational convenience and carry no ontological significance.

The simulation code is archived on Zenodo: 10.5281/zenodo.18292335.

E.1 Collective Gravitational Coupling and Operational Geometry

Localized excitations act as persistent resistances to global relaxation. Their collective influence is summarized by a response operator K_{ij}, the dressed counterpart of the bare connectivity $K_{0,\mathrm{bare}}$ (Section E.6).

In the weak-structure regime, the effective potential satisfies

$$\nabla^2 \Phi_{\mathrm{eff}} \approx 4\pi G_{\mathrm{eff}}\, \rho, \tag{163}$$

with

$$G_{\mathrm{eff}} \approx \frac{c^4}{K_{0,\mathrm{eff}}\, \chi_{c,\mathrm{eff}}^2}. \tag{164}$$

Spatial geometry is defined operationally: configurations are close if perturbations propagate efficiently between them. Gravity is recovered as a macroscopic manifestation of relaxation resistance.

E.2 Estimates of χ-Field Parameters

Effective parameters characterize the projected relaxation operator and do not represent fundamental degrees of freedom. We distinguish bare parameters ($K_{0,\mathrm{bare}}$, $\chi_{c,\mathrm{bare}}$), which are universal substrate invariants, from effective parameters ($K_{0,\mathrm{eff}}$, $\chi_{c,\mathrm{eff}}$) encoding the local density of relaxation constraints (Section E.6).

The emergent gravitational constant is driven by the ratio $K_{0,\mathrm{eff}}/\chi_{c,\mathrm{eff}}^2$. Two illustrative normalizations highlight the scale-dependency: Planck-scale identification ($\chi_c \sim \ell_P$) yields $K_0 \sim 10^{93}\,\mathrm{m}^{-2}$; cosmological-scale identification ($\chi_c \sim c/H_0$) yields $K_0 \sim 10^{-52}\,\mathrm{m}^{-2}$. Both are internally consistent, suggesting the dynamics are spectrally self-similar: G remains constant across observational scales provided the ratio of effective stiffness to correlation length is preserved.

E.3 Order-of-Magnitude Consistency Checks

1. **Electron mass scale.** The lowest stability eigenvalue must satisfy $\lambda_1 \sim (m_e c^2/\hbar_{\mathrm{eff}})^2 \sim 10^{41}\,\mathrm{s}^{-2}$, implying $K_0 \sim 10^{31}\,\mathrm{m}^{-2}$ for $a \sim 10^{-15}\,\mathrm{m}$.
2. **Correlation scale.** Electroweak compatibility requires $\chi_c \lesssim \hbar c/v \sim 10^{-18}\,\mathrm{m}$.
3. **Absence of fine-tuning.** Viable regimes are defined by $K_0 a^2 \gg 1$, $\chi_c \lesssim 10^{-18}\,\mathrm{m}$, and $K_0 \lesssim c^2/a^2$.

Algorithm 1 Bounded χ-relaxation with diagnostics

Require: $\chi_i^{(0)}$, K_{ij}, bound c, tolerances $\varepsilon_\chi, \varepsilon_S$
Ensure: Relaxed $\chi^\star$ and diagnostics
$n \leftarrow 0$, $\chi \leftarrow \chi^{(0)}$
while $n < N_{\max}$ **do**
  for each i **do**
    $S_i \leftarrow \frac{1}{c^2} \sum_j K_{ij}(\chi_i - \chi_j)^2$
    $S_i \leftarrow \min(S_i, 1)$
    $v_i \leftarrow c\sqrt{1 - S_i}$
  end for
  Choose $\Delta\lambda$ adaptively
  $\chi_i \leftarrow \chi_i + \Delta\lambda\, v_i$
  if $\max_i |\Delta\chi_i| < \varepsilon_\chi$ **then break**
  end if
  $n \leftarrow n + 1$
end while

Summary and Status

Quantity	Indicative scale	Interpretation
$K_0(\ell_{\rm cg})$	10^{-52}–$10^{93}\,\mathrm{m}^{-2}$	Effective stiffness at coarse-graining scale $\ell_{\rm cg}$
χ_c	ℓ_P–c/H_0	Characteristic χ-scale for structure-induced slowdown
$\hbar_{\rm eff}$	$\approx \hbar$ (microscopic)	Effective quantization scale
$a_0(t)$	$\sim cH(t)$	Emergent acceleration scale

Table 4 Indicative consistency windows for effective χ-field parameters.

E.4 Simulation Algorithms for χ-Field Dynamics

Numerical simulations implement finite-dimensional approximations of the continuous relaxation dynamics. Any apparent graph-like structure reflects the choice of numerical basis, not a physical discretization.

Relaxation update rule.

$$\frac{d\chi_i}{d\lambda} = c\sqrt{1 - \frac{1}{c^2}\sum_j K_{ij}(\chi_i - \chi_j)^2}. \tag{165}$$

This enforces strict monotonicity, a universal upper bound on local relaxation rate, and suppression of gradient-driven instabilities.

Reference pseudocode.

Chiral–torsional charge invariant.

For closed loops γ in the numerical representation:

$$Q_\gamma \equiv \frac{1}{2\pi} \sum_{(i,j)\in\gamma} \Delta\theta_{ij}. \tag{166}$$

Localized configurations.

Simulations robustly exhibit spontaneous emergence of stable localized configurations that resist global relaxation, interpreted as numerical counterparts of solitonic excitations (Section 4).

Effective entanglement observable.

$$E_{\text{eff}}(\mathcal{C}) \equiv \Delta_\Pi(\mathcal{C}) \left(1 - \mathcal{C}^\nu\right), \quad \nu > 0, \tag{167}$$

where Δ_Π quantifies spectral non-injectivity and $(1 - \mathcal{C}^\nu)$ encodes the loss of projective mobility near Born–Infeld saturation. Entanglement emerges only during discrete spectral reorganization events—a structural prediction of Cosmochrony.

Projectability threshold Θ_p.

Monitored through spectral gap stability ($(\lambda_2 - \lambda_1)/\mathrm{Tr}(L) > \epsilon_p$) and topological coherence ($\mathcal{E}_{\text{proj}} < \mathcal{E}_{\max}$). Crossing Θ_p marks the transition from ontological poverty to complex solitonic structures. The natural order of magnitude of ϵ_p is set by the emergence scale of $\hbar$; in continuum terms the Planck length is understood as the effective manifestation of a nonzero projection threshold.

E.5 Numerical Validation of the $\chi \to \chi_{\text{eff}}$ Transition

Discrete model.

On a cubic lattice with periodic boundaries, the local slope and bounded relaxation rate are

$$S_i(\chi) \equiv \frac{1}{c^2} \sum_{j\in\mathcal{N}(i)} K_{ij}(\chi_i - \chi_j)^2, \quad K_{ij} = \frac{K_0}{1 + (\chi_i - \chi_j)^2/\chi_c^2}, \tag{168}$$

$$R_i \equiv c\sqrt{\max(0,\, 1 - S_i)}. \tag{169}$$

The explicit update is

$$\chi_i(t + \Delta t) = \chi_i(t) + \Delta t\big(R_i(t) + \kappa\,(\Delta_G\chi)_i(t)\big). \tag{170}$$

Coarse-graining.

$$\chi_{\text{eff}}(t) \equiv \mathrm{CG}\big(\chi(t)\big). \tag{171}$$

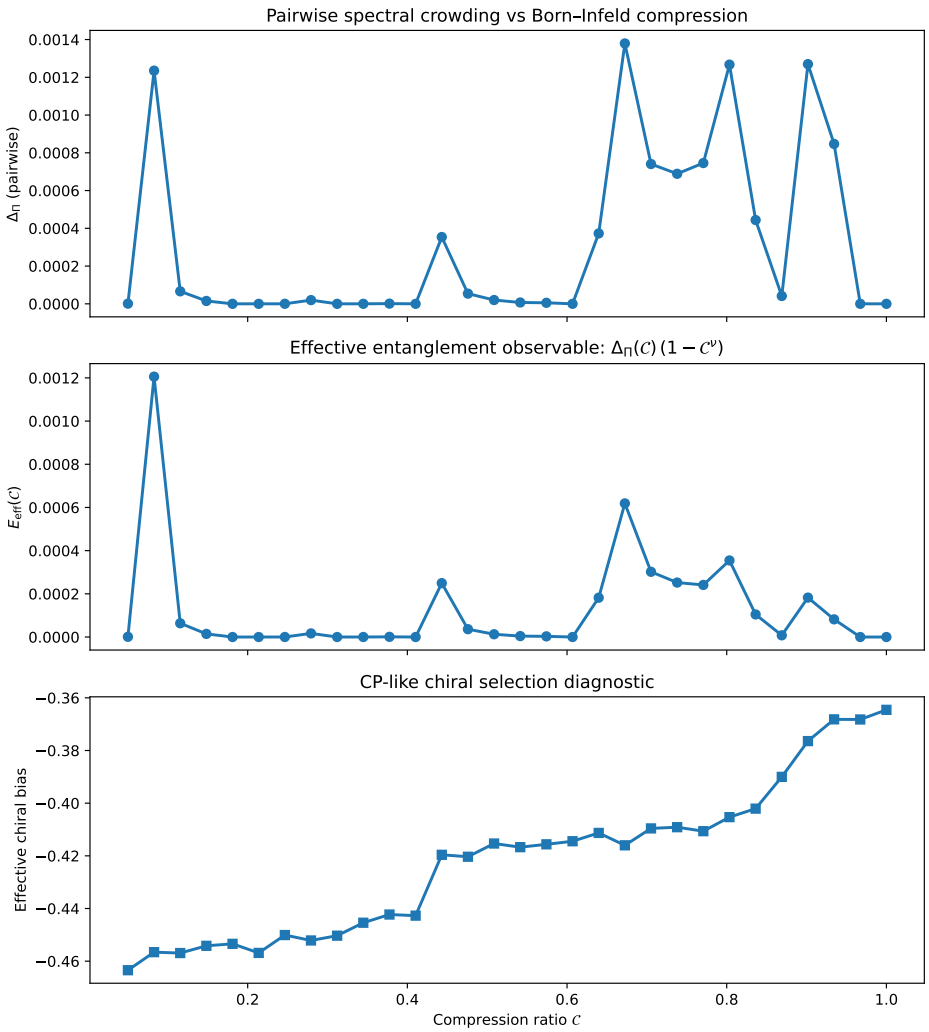

Fig. 22 Effective entanglement and chiral bias vs. compression $\mathcal{C}$. Top: spectral non-injectivity Δ_Π. Middle: E_{eff} showing intermittent activation. Bottom: chiral (CP) bias, monotonic and robust.

Validation target.

Because coarse-graining does not commute with the nonlinear dynamics, the target is the coarse-grained micro-dynamics:

$$\partial_t \chi_{\text{eff}} \approx \mathrm{CG}\Big(c\sqrt{\max(0, 1 - S(\chi))} + \kappa\, \Delta_G \chi\Big). \tag{172}$$

Residual metric.

$$\varepsilon(t) \equiv \frac{\big\|\partial_t \chi_{\text{eff}} - \mathcal{R}_{\text{eff}}\big\|}{\big\|\partial_t \chi_{\text{eff}}\big\|}. \tag{173}$$

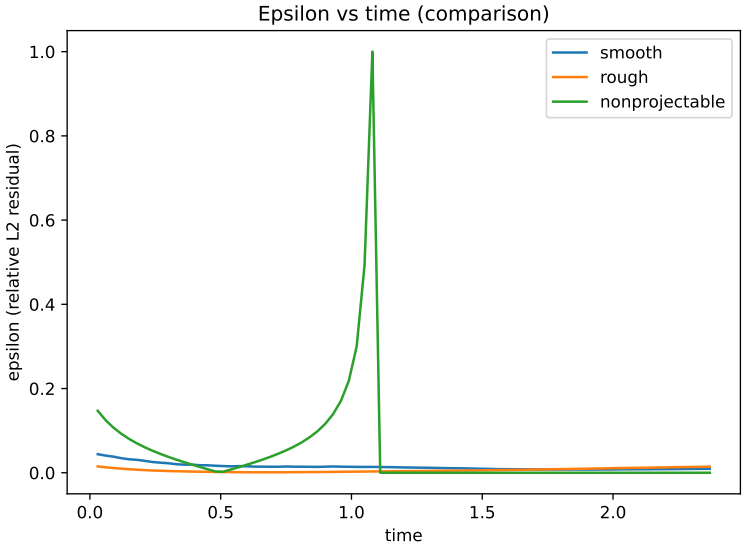

Fig. 23 Residual $\varepsilon(t)$ for smooth and rough runs, converging to $\sim 10^{-2}$.

Results.

For $N = 32$, $\ell_0 = 4$, $\Delta t = 0.03$: smooth run $\varepsilon_{L^2} \approx 9.3 \times 10^{-3}$; rough run $\varepsilon_{L^2} \approx 1.45 \times 10^{-2}$. The same order of magnitude persists at $N = 48$, confirming the small-residual regime is not a resolution artifact.

Limitations.

Numerical stability ($\varepsilon \ll 1$) does not imply projectability. Fully saturated configurations ($S_i > 1$ everywhere) yield trivially small residuals without faithful geometric interpretation.

E.6 Renormalization and the Universality of $\hbar$

We distinguish bare substrate parameters from their effective counterparts:

$$\hbar_\chi \equiv \frac{c^3}{K_{0,\mathrm{bare}}\, \chi_{c,\mathrm{bare}}}. \tag{174}$$

Effective parameters ($K_{0,\mathrm{eff}}$, $\chi_{c,\mathrm{eff}}$) incorporate the local density of relaxation constraints. No observable variation of $\hbar$ arises within a fixed relaxation epoch, since bare parameters remain invariant. The perceived universality of $\hbar$ stems from its exclusive dependence on the ratio of bare quantities, invariant under projective scaling.

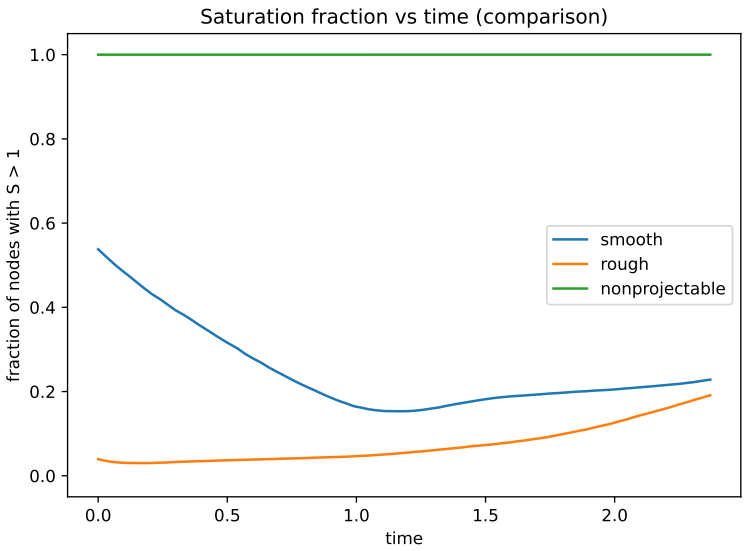

Fig. 24 Saturation fraction vs. time. The nonprojectable run rapidly reaches $f_{\mathrm{sat}} \simeq 1$.

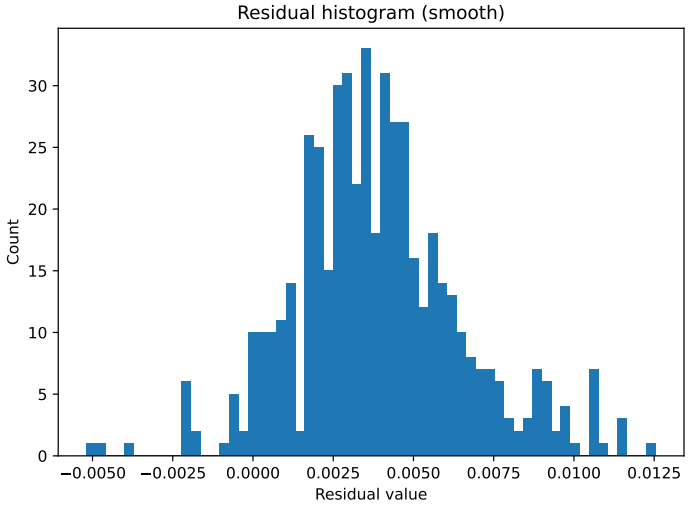

Fig. 25 Pointwise residual distribution (smooth run), centered around zero.

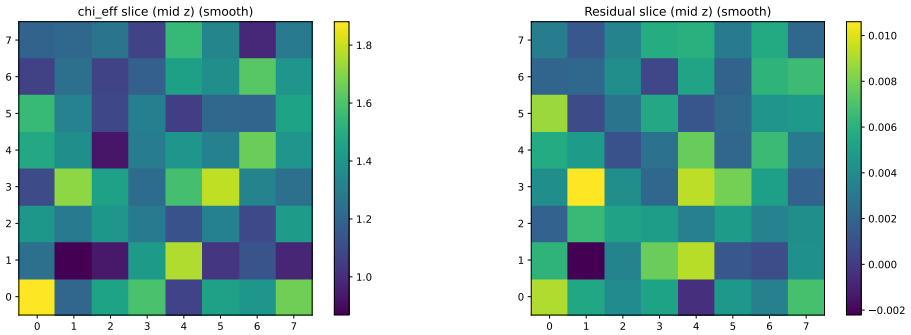

Fig. 26 Spatial slices: χ_{eff} (left, smooth) and residual (right, no coherent long-wavelength structure).

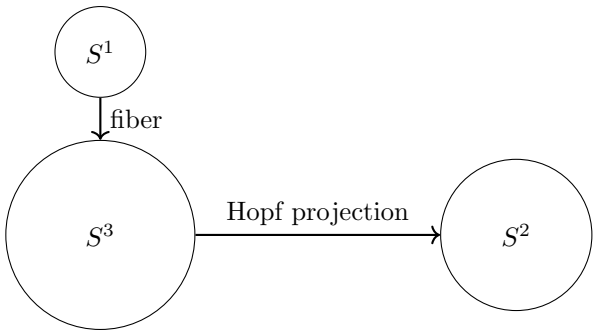

Fig. 27 Hopf fibration $S^1 \hookrightarrow S^3 \to S^2$.

E.7 Numerical Derivation of the Spectral Ratio $\lambda_2/\lambda_1 = 8/3$

Discrete Laplacian on a Representative Graph

An anisotropic kernel on a k-NN graph sampled from S^3:

$$K_\alpha(i,j) = \exp\left(-\frac{d^2_{\text{base}}(i,j) + a(\alpha)\, d^2_{\text{fiber}}(i,j)}{2\sigma^2}\right), \tag{175}$$

with $a(\alpha) = \exp(-\max(\alpha, 0))$.

Spectral Observable

$$R(\alpha) = \frac{E_{\text{fiber}}(\alpha)}{E_{\text{base}}(\alpha)}. \tag{176}$$

Both Monte–Carlo and spectral evaluations converge to the same value.

Emergence of the 8/3 Ratio

In the isotropic regime, $R_0 \simeq 0.876$. As α increases, the normalized fiber energy converges to $8/3$ independently from both estimators.

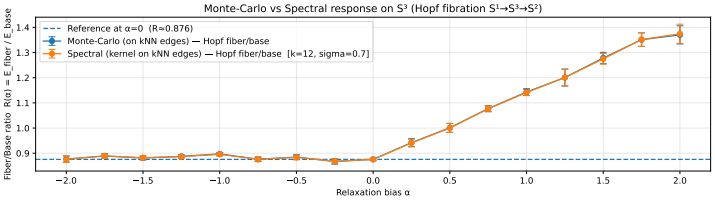

Fig. 28 Fiber and base energies vs. α.

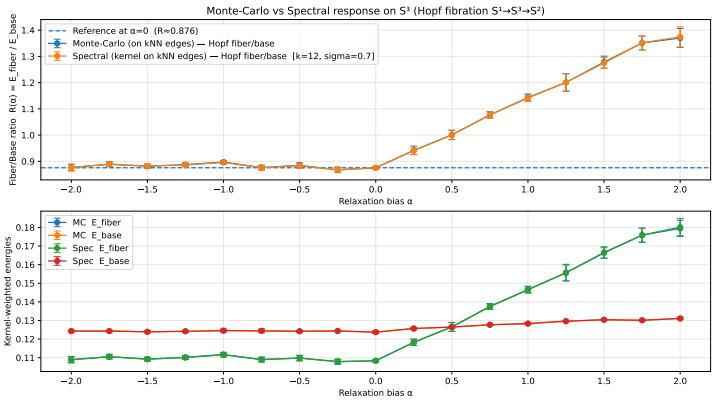

Fig. 29 Monte–Carlo vs. spectral $R(\alpha)$.

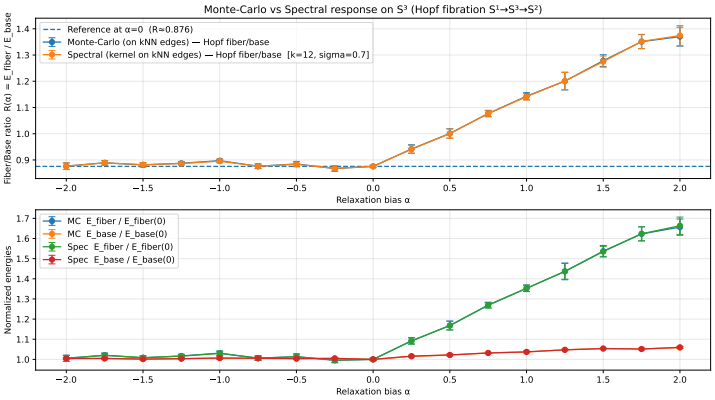

Fig. 30 Normalized energies; fiber energy $\to 8/3$.

Analytical Foundation

For a relaxation vector sampled uniformly on $S^3 \subset \mathbb{R}^4$, $\mathbb{E}[v_i^2] = 1/4$. The fiber moment is $\propto 1/4$, the base moment $\propto 3/4$. With a stiffness amplification factor of 8 for the fiber mode:

$$R_\infty = \frac{8 \cdot (1/4)}{3/4} = \frac{8}{3}. \tag{177}$$

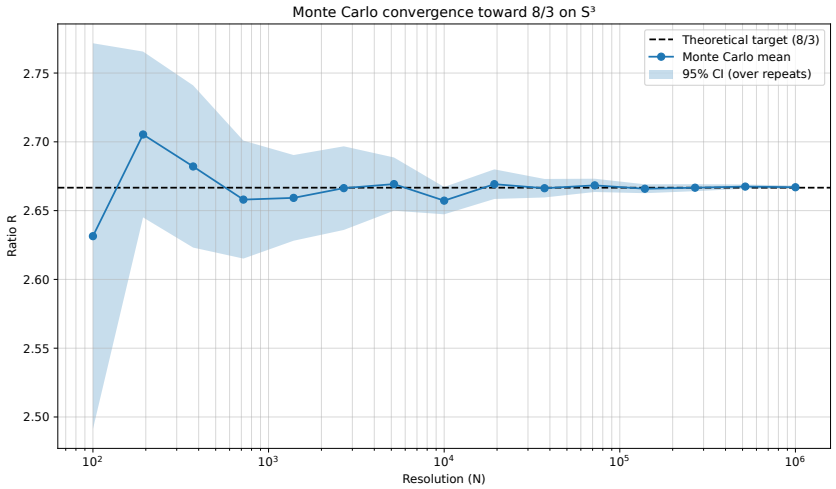

Fig. 31 Monte–Carlo convergence of R toward $8/3$ on S^3.

Numerical Convergence

Nodes (N)	Observed R	Rel. error
10^2	2.5651	3.81%
10^4	2.6994	1.23%
10^6	**2.6664**	**0.01%**
Limit	**2.6667**	—

Table 5 Convergence of spectral ratio on S^3.

Computational Protocol

Uniform sampling on S^3 via normalized Gaussian 4-vectors; fiber-base decomposition relative to a reference axis; stiffness estimation from statistical moments.

Equivalence between Grids and Statistical Integration

On periodic relational grids, $\Lambda_2/\Lambda_1 \approx 2.6617$, confirming $8/3$ as a universal spectral attractor:

$$\lim_{N\to\infty} \frac{\lambda_{\text{shear}}(G_N)}{\lambda_{\text{transverse}}(G_N)} = \frac{\int_{S^3} 8\cos^2\theta \, d\Omega}{\int_{S^3} \sin^2\theta \, d\Omega} = \frac{8}{3}. \tag{178}$$

Interpretation

The ratio $\lambda_2/\lambda_1 = 8/3$ emerges dynamically as a spectral invariant, supporting the central claim that mass and excitation hierarchies originate from topological and spectral constraints rather than tunable couplings.

E.8 Galactic Rotation Curves as Tests of Saturation Dynamics

Rotation curve data for NGC 3198, NGC 2403, and NGC 5055 are taken from SPARC-like analyses with fixed distances and inclinations. The effective acceleration is

$$g_{\rm eff}(r) = \sqrt{g_N(r)^2 + a_0(t)\, g_N(r)}, \tag{179}$$

with $a_0(t_0) = \eta\, cH_0$ ($\eta = 0.15$, fixed universally). The sole free parameter per galaxy is the stellar mass-to-light ratio $\Upsilon_\star$. No dark matter halo is introduced.

The hypothesis would be falsified if a single $\Upsilon_\star$ fails to reproduce inner and outer regions simultaneously, if systematic overshooting occurs in declining rotation curves, or if flat curves require galaxy-dependent acceleration scales.

F Relational Formulation of χ Dynamics

This appendix develops a fully relational and explicitly non-geometric formulation of χ dynamics. It clarifies how particle-like properties, topological stability, and quantum correlations arise from the intrinsic relational structure of χ, prior to the emergence of geometry.

The relational formulation does not assume a background spacetime or metric, spatial localization, a tensorial or spinorial fundamental ontology, or an underlying Hilbert space structure. Particle-like excitations are identified with internally stable relational configurations whose apparent properties—mass, charge, spin, statistics—emerge from topological and organizational features once a projectable regime applies.

F.1 Relational Configurations of χ

The substrate χ is defined as a relational structure whose admissible configurations are characterized by adjacency relations rather than by embedding in a pre-existing spacetime manifold. Two configurations are considered adjacent if they can be connected through an admissible elementary relaxation update.

A minimal structural requirement of the framework is that the relational adjacency structure of χ be connected. That is, for any two admissible configurations, there exists a finite relational chain of admissible updates linking them at the χ level. This connectedness condition applies to the pre-geometric relational network itself (or to its continuum limit), not to the emergent spacetime description.

Connectedness of χ does not imply persistent effective coupling between all projected regions. Because the projection Π is generally non-injective and subject to saturation, its image $\Pi(\Omega)$ may decompose into multiple disjoint effective domains. Such disjointness reflects a loss of mutual projectability rather than the existence of ontologically independent substrates.

This distinction is essential. While effective domains may become mutually inaccessible within the emergent geometric description, the underlying χ-structure remains a single connected system supporting a global relaxation ordering. The uniqueness of this ordering ensures the universality of structural invariants such as the effective bounds associated with c and $\hbar$.

The connectedness condition can also be formulated spectrally. Let Δ_χ denote the relational Laplacian associated with the adjacency structure of χ. Connectedness requires that Δ_χ admit a single zero mode on the admissible sector. Multiple zero modes would correspond to independent relational components, which are excluded by the assumption of a single substrate. Effective "islands" may nonetheless arise as spectrally weakly coupled sectors under projection, without implying ontological multiplicity.

F.2 Non-Factorization and Entanglement

Factorization—decomposition preserving internal relaxation structure while isolating disjoint subsets of relations—is not fundamental but emerges only in restricted regimes. Quantum entanglement arises as a direct manifestation of persistent non-factorization: when a non-factorizable relational configuration admits an effective projection onto spatially separated degrees of freedom, its components remain relationally inseparable.

Projection-induced non-factorization.

Because the projection $\Pi : \mathcal{C}_\chi \to \mathcal{C}_{\text{eff}}$ is generically non-injective, a single effective configuration y corresponds to an equivalence class

$$\Pi^{-1}(y) \subset \mathcal{C}_\chi. \tag{180}$$

Entanglement arises when this fiber contains globally constrained configurations that do not admit decomposition into independent substructures compatible with the effective subsystem decomposition. No conditioning on underlying relational degrees of freedom can restore a product structure for joint outcome statistics.

Compression and limits of entanglement.

Entanglement persists only in an intermediate regime where projection preserves sufficient global relational structure to prevent factorization, while still allowing stable decomposition into effective subsystems. If projection is effectively injective, fibers collapse to single elements and factorization is recovered; if excessively coarse-grained, relational constraints are erased and descriptions become fully factorized.

F.3 Locality, Causality, and the Role of the Bound c

Correlations between configurations of χ may extend across arbitrarily large effective distances once a geometric description applies. However, all modifications of relational configurations are constrained by a universal kinematic bound c.

F.4 Relational Distance as a Minimal Path Functional

Two distances operate at different descriptive levels:

1. **Combinatorial distance** d_{ij}^C (pre-geometric): $d_{ij}^C = \min_{\gamma_{ij}} \sum_{(u,v)\in\gamma_{ij}} 1$, counting graph steps only, independent of field values.
2. **Weighted distance** d_{ij}^W (emergent): $d_{ij}^W = \min_{\gamma_{ij}} \sum_{(u,v)\in\gamma_{ij}} w_{uv}$, encoding effective relational stiffness.

Weights are parametrized by

$$w_{uv}(\bar{\chi}) = \frac{1}{K_0}\left[1 + \left(\frac{\bar{\chi}_u - \bar{\chi}_v}{\chi_c}\right)^2\right], \quad K_{uv}(\bar{\chi}) = \frac{1}{w_{uv}(\bar{\chi})}. \tag{181}$$

F.5 Derivation of χ_{eff} from Relational Observables

A two-level construction avoids circularity. First, define $\bar{\chi}$ using only the combinatorial distance:

$$N_i = \left\{ j \,\middle|\, d_{ij}^C \le \ell_0 \right\}, \tag{182}$$

$$\bar{\chi}_i = \frac{1}{|N_i|} \sum_{j\in N_i} \chi_j. \tag{183}$$

Then define the weighted distance from $\bar{\chi}$:

$$d_{ij}^{W} = \min_{\gamma_{ij}} \sum_{(u,v)\in\gamma_{ij}} w_{uv}(\bar{\chi}). \tag{184}$$

Finally, χ_{eff} is obtained by coarse-graining over weighted neighborhoods:

$$V_{\ell_0}(i) = \left\{ j \,\middle|\, d_{ij}^{W} \le \ell_0 \right\}, \tag{185}$$

$$\chi_{\text{eff}}(i) = \frac{1}{|V_{\ell_0}(i)|} \sum_{j\in V_{\ell_0}(i)} \chi_j. \tag{186}$$

The dependency chain is explicitly non-circular: $d^C \Rightarrow \bar{\chi} \Rightarrow w(\bar{\chi}), K(\bar{\chi}) \Rightarrow d^W \Rightarrow \chi_{\text{eff}}$.

F.6 Relation to the Effective Geometric Description

Effective geometric structures (metric fields, spatial gradients, Poisson-type equations) arise as coarse-grained summaries of relational configurations once a projectable regime applies. They carry no independent ontological status.

F.7 Emergent Coordinates via Manifold Reconstruction

When the relational distance matrix $D = \{d_{ij}\}$ admits a low-dimensional embedding, coordinates can be reconstructed using multidimensional scaling. The centered Gram matrix is

$$G_{ij} = -\tfrac{1}{2}\Big(d_{ij}^2 - d_{i\cdot}^2 - d_{\cdot j}^2 + d_{\cdot\cdot}^2\Big), \tag{187}$$

yielding eigenpairs (λ_k, v_k) and an embedding

$$x_i^{(a)} = \sqrt{\lambda_a}\,(v_a)_i, \quad a = 1, \ldots, d. \tag{188}$$

The intrinsic dimension d is selected by the eigenvalue gap:

$$\Delta\lambda_{d+1} > \eta\,\lambda_1, \tag{189}$$

with $\eta \sim 0.1$. For smooth large-scale configurations, a stable $d = 4$ embedding is expected.

Failure of the reconstruction (non-local connectivity or no clear spectral gap) signals a transition to a pre-geometric regime where a smooth manifold is not an adequate description. The effective metric is defined implicitly through propagation properties and carries only a restricted subset of the relational information. Poisson-type and wave-like equations arise from linearizing relaxation dynamics around quasi-homogeneous configurations; they are regime-dependent approximations, not fundamental laws.

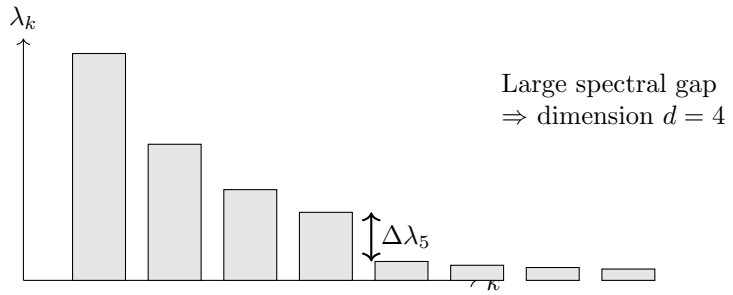

Fig. 32 Schematic eigenvalue spectrum for intrinsic dimension selection. A clear gap after four modes indicates a robust $d = 4$ projectable regime.

F.8 Topological Stability of Relational χ Configurations

Particle-like excitations are identified with nontrivial relational patterns whose stability is guaranteed by intrinsic topological constraints in configuration space (Section 4.2). Topology here characterizes inequivalent classes of χ configurations that cannot be continuously transformed into one another without violating relaxation constraints.

Stability arises from topological obstructions to global relaxation: certain configurations cannot relax continuously to the homogeneous vacuum without passing through forbidden regions. This does not rely on conserved charges imposed by symmetry principles.

Geometric metaphors (knots, twists, vortices) provide intuition when configurations admit effective geometric projection but should not be taken literally at the relational level. A paradigmatic example: configurations exhibiting intrinsic 4π-periodic internal structure cannot be unwound and, when projected, exhibit spinorial transformation properties. Distinct particle species correspond to inequivalent topological sectors; the energetic cost of deformation provides a unified origin for mass, stability, and spectral separation.

F.9 Topological Origin of Fermionic and Bosonic Statistics

The distinction between fermionic and bosonic behavior originates from the internal topological structure of χ configurations in configuration space.

Fermionic behavior.

Configurations with intrinsic 4π-periodicity are double-valued under 2π reorientation. When projected, they exhibit fermion-like behavior: sign change under 2π rotations, restoration only after 4π, and spin-$\frac{1}{2}$ transformation properties—without introducing fundamental spinors.

Bosonic behavior.

Topologically orientable configurations return to an equivalent state after 2π reorientation, yielding integer-spin transformation properties.

Topological mass ratios (heuristic).

The mass ratios between particles emerge from knot-like configurations: an electron corresponds to a twisted unknot ($Q_e = 1$) with fiber volume $\propto \chi_c$; a proton to a trefoil knot ($Q_p = 3$) with fiber volume $\propto \chi_c^3$. The observed ratio is

$$\frac{m_p}{m_e} = \frac{\mathrm{Vol}(\Pi^{-1}(\text{proton}))}{\mathrm{Vol}(\Pi^{-1}(\text{electron}))} \approx 27\,\chi_c^2.$$

For $\chi_c \approx 8.3$, this reproduces $m_p/m_e \approx 1836$, providing a topological explanation independent of ad hoc parameters.

Spin–statistics connection.

The relational-topological distinction between 4π- and 2π-periodic configurations provides a natural qualitative explanation of the spin–statistics connection, demonstrating that the observed dichotomy can arise from internal organization of χ prior to any effective quantum description.

F.10 Vacuum Energy versus Relaxation Capacity of the χ Field

No fundamental vacuum energy density is postulated. Phenomena commonly attributed to vacuum energy are reinterpreted as manifestations of the *relaxation capacity* of χ: the ability of a relational configuration to undergo further structural reorganization under bounded constraints. Relaxation capacity is contextual and non-extensive; it cannot be meaningfully assigned to spacetime points.

Observable vacuum effects arise only when relational constraints restrict admissible configurations. The Casimir effect, for instance, results from a differential in relaxation capacity between constrained and unconstrained configurations, not from an absolute vacuum energy density.

Because relaxation capacity is non-extensive, it does not enter gravitational dynamics as a uniform source term. This provides a natural conceptual resolution of the cosmological constant problem: the enormous vacuum energy inferred from zero-point counting is not a physically meaningful quantity in the Cosmochrony ontology.

F.11 Conceptual Positioning with Respect to Existing Frameworks

Aspect	**QM / QFT**	**GR and extensions**	**Cosmochrony**
Primary ontology	Quantum states, operator fields	Spacetime geometry, metric	Relational substrate χ
Status of spacetime	Fixed background	Fundamental dynamical entity	Emergent, projective
Nature of time	External parameter	Coordinate-dependent	Ordering via relaxation
Gravitation	Introduced externally	Metric curvature	Collective relaxation slowdown
Quantum behavior	Postulated	Added via quantization	Emergent from χ
Vacuum structure	Zero-point energy	Geometric ground state	Contextual relaxation capacity
Particle ontology	Fundamental entities	Field excitations	Topologically stable configurations
Empirical status	Highly successful	Highly successful	Exploratory

Table 6 Conceptual positioning of the relational χ framework with respect to quantum and geometric approaches.

Aspect	**Cosmochrony**	**ΛCDM**	**LQG**
Fundamental ontology	Single substrate χ	$g_{\mu\nu}$ + matter + Λ	Quantum geometry
Status of spacetime	Emergent, projected	Fundamental (classical)	Quantized but assumed
Nature of time	Emergent from relaxation	External parameter	Problematic / relational
Dark energy	Not required	Explicit Λ term	No consensus
Inflation	Not required	Required (inflaton)	Alternative scenarios
Origin of mass	Spectral inhibition	Higgs mechanism	Not intrinsic
Testable predictions	$H(z)$, CMB low-ℓ, drift	H_0, w, growth	Planck-scale signatures

Table 7 Cosmological and gravitational comparison between Cosmochrony, ΛCDM, and Loop Quantum Gravity.

G Glossary of Core Quantities and Notation

This appendix summarizes the meaning, role, and ontological status of the main quantities used throughout the Cosmochrony framework. It is intended strictly as a reference guide and does not introduce new assumptions, dynamics, or physical postulates.

G.1 Fundamental Quantities

χ ***(Chi substrate).***

The unique fundamental entity of the Cosmochrony framework. χ is a pre-geometric, relational substrate not defined on a pre-existing spacetime manifold. Its irreversible relaxation supplies a continuous flux of relational configurations. χ does not encode a prescriptive set of admissible physical states; admissibility arises only through projection under finite resolution and compatibility constraints. Localized, topologically stable configurations of χ correspond to particle-like excitations upon projection.

χ_i ***(Local configuration).***

Discrete local degrees of freedom of the χ substrate, associated with vertices of the relaxation network. They encode the microscopic relational state prior to any geometric projection.

χ_c ***(Critical relaxation threshold).***

A fundamental structural bound limiting local variations of χ. It constrains the projection and update process by enforcing causal consistency, and underlies all effective speed and action bounds. This threshold does not prescribe physical laws, but limits the capacity of admissible projected updates.

τ ***(Operational time).***

An effective ordering parameter defined from the monotonic succession of distinguishable projected configurations, constructed from the effective descriptor χ_{eff}. Operational time τ is not a fundamental temporal coordinate and does not exist at the level of the χ substrate. It emerges only in projectable regimes as an operational measure of duration, defined through the ordered differentiation of admissible effective states. A perfectly stationary projection would correspond to $\Delta\tau = 0$ and is therefore excluded by the requirement of projective continuity.

c_χ ***(Fundamental relaxation speed).***

The maximal propagation speed of relaxation disturbances within the χ substrate. It represents the fundamental causal bound of the theory, from which the effective speed of light emerges. The maximal propagation speed of relaxation disturbances within the χ substrate. It represents the kinematic manifestation of the invariant relaxation bound b_χ in transport-limited regimes. The effective speed of light c emerges as its geometric projection.

G.2 Effective and Projected Quantities

χ_{eff} ***(Effective projected field).***

A coarse-grained scalar field arising from the non-injective projection of χ onto an emergent spacetime description. χ_{eff} provides an effective field-theoretic representation without fundamental status.

Fiber (of the projection).

For a given effective configuration χ_{eff}, the fiber is the set of underlying χ configurations mapped to it by the projection π. Elements of a fiber are operationally indistinguishable at the spacetime level. Non-trivial fibers reflect the structural non-injectivity of the projection.

Operational projection (contextual access).

A measurement-context-dependent map that specifies how the effective description χ_{eff} is accessed and turned into operational observables. It introduces no additional ontology: it formalizes the contextual readout of χ_{eff} (e.g., choice of apparatus, coarse-graining, relational query).

Phase stiffness (superconducting coherence stiffness). ρ_s denotes the effective stiffness associated with spatial variations of the coherent $U(1)$ fiber phase. It is an operational proxy for the collective relaxation capacity of the projected description in the coherent regime. In Section 5.7, ρ_s controls the energetic cost of phase gradients and enters the London-type gradient term through $F_{\text{grad}} \propto (\nabla\theta - (2e/\hbar)A)^2$. ρ_s is not a fundamental constant of the χ substrate. It is a regime-dependent effective quantity, vanishing when coherence is lost and recovering normal-state behavior.

π ***(Projection).***

An operational projection correspondence relating configurations of χ to effective descriptions χ_{eff} in projectable regimes. The projection is generally non-injective and does not define a single-valued function: distinct underlying configurations of χ may correspond to the same effective state, defining equivalence classes (fibers).

π^{-1} ***(Deprojection).***

The inverse reconstruction problem of identifying classes of χ configurations compatible with a given effective state. Deprojection is not unique and does not destroy structural information.

$V(\chi)$ ***(Effective potential).***

An effective, coarse-grained description used to model localization and stability properties of χ configurations. $V(\chi)$ is not fundamental and is secondary to the spectral characterization of mass and inertia.

ℓ ***(Descriptive resolution scale).***

A scale characterizing the local spectral resolution of the projected state U. It measures the minimal relational differentiation that can be operationally resolved within the effective description. Variations of ℓ across scales modulate the apparent saturation threshold $a_\star$ without altering the underlying bound b_χ.

Observable.

A stable, projectable quantity defined on χ_{eff} through an interpretative framework. Observables do not correspond to additional ontological entities, but to operational readings of the same effective physical reality.

Physical reality.

In the Cosmochrony framework, physical reality is identified with the effective level χ_{eff}. The substrate χ is ontologically real but does not constitute a physical universe until projected into a projectable regime.

t_{proj} ***(Projected time).***

Operational time measured within the emergent spacetime description. It arises from the local rate of χ relaxation and reproduces relativistic time dilation effects.

Universe.

The physically real domain described at the χ_{eff} level, where spacetime structure, causality, and physical observables are well-defined. The Universe does not refer to the fundamental substrate χ, which is ontologically prior to any notion of universe.

G.3 Relaxation Network and Operators

$G(V, E)$ ***(Relaxation network).***

A discrete graph representing the underlying relational structure on which the χ substrate is defined. Vertices correspond to elementary degrees of freedom and edges encode relaxation couplings.

K_{ij} ***(Relaxation coupling).***

Edge-dependent coupling coefficients defined on the relaxation network. They quantify the resistance to relative variations of χ between neighboring nodes and encode geometric and topological information. K_{ij} are structural parameters of the pre-geometric substrate and do not represent dynamical interaction constants.

Δ_G ***(Graph Laplacian / relaxation operator).***

The discrete Laplace–Beltrami operator associated with the network $G(V, E)$ and the couplings K_{ij}. Its spectral properties govern the stability, localization, and inertial behavior of χ configurations.

$D_{\mathrm{loc}}\chi$ ***(Local relaxation operator).***
A local relational operator governing the evolution of χ at the microscopic level. It replaces differential operators defined on continuous manifolds.

G.4 Spectral and Inertial Quantities

Projective stability gap of a composite fiber class. Δ_Π is defined as the lowest positive eigenvalue of the effective relaxation operator restricted to the fiber sector around a composite winding configuration (notably $w = 2$), $\Delta_\Pi \equiv \lambda_{\min}(L_\Pi|_{w=2})$. Operationally, it measures the minimal excitation cost required to destabilize the composite class, either by separation into lower-winding excitations or by inducing a local phase defect. Δ_Π is a spectral stability quantity associated with admissibility of coherent composite sectors, and it may admit distinct amplitude and phase-controlled manifestations depending on the regime.

Amplitude (formation) scale associated with composite stability. $\Delta_\Pi^{\mathrm{ampl}}$ denotes the amplitude scale governing local composite formation in strongly constrained regimes. In the strongly correlated case discussed in Section 5.7, it is controlled by the dominant frustration or exchange scale, written schematically as $\Delta_\Pi^{\mathrm{ampl}} \sim J$. This quantity should be distinguished from the phase ordering scale controlled by ρ_s.

λ_n ***(Spectral eigenvalues).***
Eigenvalues of the linearized relaxation or stability operator acting on small perturbations of a localized χ configuration. They determine inertial mass scales in the effective description.

ψ_n ***(Spectral modes).***
Eigenmodes associated with the operator Δ_G. They encode the internal structure and stability of particle-like configurations.

m_{eff} ***(Effective mass).***
An emergent invariant determined by the spectral stability of localized χ configurations under projection. Operationally, effective mass measures the self-consistency overhead associated with maintaining a coherent projected description under local updates. Mass is not a fundamental parameter nor a coupling constant.

Q ***(Topological charge).***
An integer-valued invariant characterizing the topology of a stable χ configuration. Different values of Q correspond to distinct particle families.

$\Omega^{\pm}$ ***(Chiral topological sectors).***
Opposite chiral configurations of topological χ structures. They are related by orientation reversal and need not be energetically equivalent.

G.5 Dimensionless Parameters

*S **(Gradient saturation parameter).***

A dimensionless quantity defined as

$$S \equiv \frac{1}{c^2} \sum_{j \sim i} K_{ij} (\chi_i - \chi_j)^2, \tag{190}$$

measuring the local density of projected χ gradients. The bound $S \leq 1$ enforces causal consistency in the emergent spacetime description. The constant c appearing here is the effective geometric projection of the invariant transport bound b_χ.

*Ω_χ **(Relaxation budget parameter).***

A dimensionless global quantity characterizing the fraction of total χ relaxation stored in spatial gradients. In cosmological regimes, it plays a role analogous to a density parameter.

Frustration density (operational proxy). F denotes a dimensionless proxy for the density of incompatible local raccordement constraints in the fiber sector. It is introduced as an operational quantity, grounded in independently measurable correlators in the relevant materials. In the strongly correlated regime, F parametrizes the strength of staggered frustration and enters the qualitative selection of the low-cost composite coherence channel. F is not an additional fundamental field or a new ontological variable. It summarizes environmental and material constraints within an effective description.

Relative frustration ratio. $r_F$is a dimensionless ratio encoding the relative amplitude of the dominant frustration sector across material families. It is used to compare coherence channel selection across systems with different lattice constraints and correlation structure. In particular, r_F organizes the expected transition between distinct symmetry channels in the superconducting regime.

G.6 Constants and Emergent Limits

*$a_\star$ **(Operational saturation threshold).***

An effective acceleration proxy marking the onset of saturated response in the projected description. It scales inversely with the local descriptive resolution ℓ according to

$$a_\star \sim \kappa \frac{b_\chi}{\ell},$$

where κ is a dimensionless normalization factor. $a_\star$ is not a fundamental constant but a regime-dependent manifestation of the invariant transport bound b_χ.

b_χ ***(Invariant relaxation bound).***

The fundamental bound on admissible relaxation transport within the χ substrate. It limits the maximal rate at which relational configurations can be updated while preserving operational closure under projection. All effective saturation phenomena are manifestations of this invariant bound under different dimensional projections.

c ***(Effective speed of light).***

The maximal signal propagation speed in emergent spacetime. c is not fundamental: it is the geometric projection of the substrate transport bound b_χ through the relaxation speed c_χ in projectable regimes.

$\hbar$ ***(Effective Planck constant).***

An emergent quantum of action associated with projection thresholds and spectral granularity. It is not fundamental at the level of χ.

G ***(Newtonian gravitational constant).***

An emergent coupling constant arising from large-scale collective relaxation dynamics of χ. Its value reflects structural properties rather than fundamental interaction strengths.

Λ_{eff} ***(Effective cosmological constant).***

A residual large-scale relaxation effect associated with incomplete equilibration of the χ substrate.

G.7 Key Conceptual Terms

Energy.

Energy is an effective quantity measuring the operational cost associated with modifying a projected configuration while preserving coherence under admissible updates. This cost reflects the mobilization of the underlying relaxation capacity of the χ substrate under projection, but energy itself is not a fundamental property of χ. Standard conservation laws remain valid at the effective level.

Fluctuations.

Local stochastic modulations of χ configurations that affect event timing and localization without altering underlying topological constraints.

Matter.

Stable topological configurations of χ whose persistence gives rise to particle-like behavior and inertial properties.

Measurement.

A localized interaction that selects a specific effective realization within a non-injective projection. Measurement does not induce a fundamental collapse, but resolves an equivalence class of projected configurations into a stable operational outcome.

Probability.

An emergent descriptor reflecting the multiplicity of projected realizations compatible with a given relational configuration and effective state. Probability is projective rather than fundamental, and does not correspond to intrinsic randomness of the substrate.

Relaxation (of the χ field).

The intrinsic irreversible reorganization of relational configurations of χ under internal coupling constraints. Relaxation supplies the flux of candidate configurations required for successive projected updates. It is pre-thermodynamic and does not correspond to dissipation.

Spacetime.

An emergent relational structure arising from large-scale configurations of the χ substrate. Its metric description remains valid within its domain of applicability.

Time.

An effective parameter associated with the local rate of χ relaxation. Operational and relativistic notions of time are recovered without modification.

Relaxation transmittance (gauge interpretation).

An effective, context-dependent measure of how efficiently relaxation flux (or ordering capacity) is transmitted through a given projected configuration. In Cosmochrony, gauge structure can be interpreted as a parametrization of transmittance variations across the projection fiber, rather than as a fundamental interaction field.

Wavefunction.

An effective statistical representation of the dynamics and topology of the χ substrate. It has no fundamental ontological status.

Wave–Particle Duality.

A manifestation of interaction-induced changes in the local configuration of χ, producing localized particle-like behavior from an underlying wave-like substrate.

Winding number (fiber topological class). w labels the winding class of a configuration in the projected $U(1)$ fiber sector. A $w = 1$ configuration corresponds to an elementary charged excitation in the effective description. A $w = 2$ configuration denotes a composite topological class supporting a collective phase degree of freedom. The winding number is a topological invariant of the projected description and does not constitute a new dynamical postulate. It is used to classify admissible coherent regimes and their stability properties.

Acknowledgements. The author acknowledges the use of large language models as a supportive tool for refining language, structure, and internal consistency during the development of this manuscript. All conceptual contributions, theoretical choices, and interpretations remain the sole responsibility of the author.

References

[1] Dirac, P.A.M.: The Principles of Quantum Mechanics. Oxford University Press, Oxford (1930)

[2] Einstein, A.: Die feldgleichungen der gravitation. Sitzungsberichte der Preussischen Akademie der Wissenschaften, 844–847 (1915)

[3] Misner, C.W., Thorne, K.S., Wheeler, J.A.: Gravitation. W. H. Freeman and Company, San Francisco (1973)

[4] Weinberg, S.: Gravitation and Cosmology: Principles and Applications of the General Theory of Relativity. John Wiley & Sons, New York (1972)

[5] Rovelli, C.: Quantum Gravity. Cambridge University Press, Cambridge (2004). Foundational text on spin networks and background independence.

[6] Born, M.: Zur quantenmechanik der stoßvorgänge. Zeitschrift für Physik **37**, 863–867 (1926)

[7] Penrose, R.: The Emperor's New Mind: Concerning Computers, Minds, and the Laws of Physics. Oxford University Press, Oxford (1989)

[8] Prigogine, I.: The End of Certainty: Time, Chaos, and the New Laws of Nature. Free Press, New York (1997)

[9] Peebles, P.J.E.: Principles of Physical Cosmology. Princeton University Press, Princeton (1993)

[10] Logan Nye: On spacetime geometry and gravitational dynamics. Preprint (2024). Explores emergent spacetime geometry and gravitational dynamics from underlying geometric principles

[11] Singh, N.: A field-theoretic framework for emergent spacetime (2025)

[12] Strominger, A.: Lectures on the infrared structure of gravity and gauge theory. Princeton University Press (2018) arXiv:1703.05448 [hep-th]

[13] McKinley, J.C.W.: Photon Out of Time: Why Light Experiences No Time and What That Means for Physics. Preprint introducing the Timeless Light Model (TLM) (2025)

[14] Rovelli, C.: Time in quantum gravity: An hypothesis. Physical Review D **43**(2),

442–456 (1991)

[15] Rovelli, C.: Relational quantum mechanics. International Journal of Theoretical Physics **35**(8), 1637–1678 (1996)

[16] Aristotle: Categories. In: Barnes, J. (ed.) The Complete Works of Aristotle. Princeton University Press, ??? (1984)

[17] Shields, C.: Aristotle. Stanford Encyclopedia of Philosophy (2016). https://plato.stanford.edu/entries/aristotle/

[18] Rovelli, C.: The Order of Time. Penguin, London (2018)

[19] Born, M., Infeld, L.: Foundations of the new field theory. Proceedings of the Royal Society A **144**, 425–451 (1934) https://doi.org/10.1098/rspa.1934.0059

[20] Deser, S., Gibbons, G.W.: Born–infeld–einstein actions? Classical and Quantum Gravity **15**, 35–39 (1998) https://doi.org/10.1088/0264-9381/15/5/002

[21] Milgrom, M.: Mond—a pedagogical review. New Astronomy Reviews **46**, 741–753 (2002) https://doi.org/10.1016/S1387-6473(02)00184-5

[22] Famaey, B., McGaugh, S.S.: Modified newtonian dynamics (mond): Observational phenomenology and relativistic extensions. Living Reviews in Relativity **15**(10) (2012) https://doi.org/10.12942/lrr-2012-10

[23] Rajaraman, R.: Solitons and Instantons: An Introduction to Solitons and Instantons in Quantum Field Theory. North-Holland, ??? (1982)

[24] Beau, J.: Relational Reconstruction of Spacetime Geometry from Graph Laplacians. Cosmochrony companion paper A (2026). https://doi.org/10.5281/zenodo.18356037

[25] Pauli, W.: Über den Zusammenhang des Abschlusses der Elektronengruppen im Atom mit einer nichtklassifizierbaren Eigenschaft der Elektrons. Zeitschrift für Physik **31**, 765–783 (1925) https://doi.org/10.1007/BF02980749

[26] Dirac, P.A.M.: The Quantum Theory of the Electron. Proceedings of the Royal Society of London. Series A **117**, 610–624 (1928) https://doi.org/10.1098/rspa.1928.0023

[27] Hawking, S.W.: Breakdown of predictability in gravitational collapse. Physical Review D **14**(10), 2460–2473 (1976) https://doi.org/10.1103/PhysRevD.14.2460

[28] Guth, A.H.: Inflationary universe: A possible solution to the horizon and flatness problems. Physical Review D **23**, 347–356 (1981) https://doi.org/10.1103/PhysRevD.23.347

[29] Linde, A.D.: A new inflationary universe scenario: A possible solution of the horizon, flatness, homogeneity, isotropy and primordial monopole problems. Physics Letters B **108**, 389–393 (1982) https://doi.org/10.1016/0370-2693(82)91219-9

[30] Friedmann, A.: Über die krümmung des raumes. Zeitschrift für Physik **10**(1), 377–386 (1922)

[31] Hubble, E.: A relation between distance and radial velocity among extra-galactic nebulae. Proceedings of the National Academy of Sciences **15**(3), 168–173 (1929) https://doi.org/10.1073/pnas.15.3.168

[32] Hogg, D.W.: Distance measures in cosmology. arXiv:astro-ph/9905116 (1999)

[33] Sachs, R.K., Wolfe, A.M.: Perturbations of a cosmological model and angular variations of the microwave background. Astrophysical Journal **147**, 73–90 (1967) https://doi.org/10.1086/148982

[34] Hu, W., White, M.: The damping tail of cosmic microwave background anisotropies. Astrophysical Journal **479**, 568–579 (1997) https://doi.org/10.1086/303888

[35] Collaboration, P.: Planck 2018 results. vi. cosmological parameters. Astronomy & Astrophysics **641**, 6 (2020)

[36] Riess, A.G.e.a.: Large magellanic cloud cepheid standards provide a 1% foundation for the determination of the hubble constant. The Astrophysical Journal **876**(1), 85 (2019)

[37] Riess, A.G., Yuan, W., Macri, L.M., Scolnic, D., Brout, D., Casertano, S., Jones, D., Murdoch, T., Pelliccia, E., Schommer, R.: A Comprehensive Measurement of the Hubble Constant and Constraints on Errors in the Standard Cosmological Model. The Astrophysical Journal Letters **934**, 7 (2022) https://doi.org/10.3847/2041-8213/ac756e 2112.04510

[38] Di Valentino, E., Handley, W., Herbig, T., Linder, E.V.: The Hubble tension: a global perspective. Classical and Quantum Gravity **39**, 163001 (2022) https://doi.org/10.1088/1361-6382/ac7639 2112.00843

[39] Collaboration, P.: Planck 2018 results. VI. Cosmological parameters. Astronomy & Astrophysics **641**, 6 (2020) https://doi.org/10.1051/0004-6361/201833910 arXiv:1807.06209

[40] Bell, J.S.: On the einstein podolsky rosen paradox. Physics Physique Fizika **1**(3), 195 (1964)

[41] Gorlach, A., Heuser, S., Drescher, M., Pfeifer, T.: Attosecond-resolved emergence of quantum correlations. Phys. Rev. Lett. **133**, 163201 (2024) https://doi.org/10.1103/PhysRevLett.133.163201

[42] Zurek, W.H.: Decoherence, einselection, and the quantum origins of the classical. Reviews of Modern Physics **75**, 715–775 (2003) https://doi.org/10.1103/RevModPhys.75.715 arXiv:quant-ph/0105127

[43] Aghanim, N., *et al.*: Planck 2018 results. vi. cosmological parameters. Astronomy & Astrophysics **641**, 6 (2020) https://doi.org/10.1051/0004-6361/201833910 arXiv:1807.06209 [astro-ph.CO]

[44] Peskin, M.E., Schroeder, D.V.: An Introduction to Quantum Field Theory. Westview Press, Boulder (1995)

[45] Shifman, M.: Understanding the qcd vacuum. Progress in Particle and Nuclear Physics **59**, 1–161 (2007) https://doi.org/10.1016/j.ppnp.2007.03.001 arXiv:hep-ph/0701083

[46] Planck Collaboration, *et al.*: Planck 2018 results. vi. cosmological parameters. Astronomy and Astrophysics **641**, 6 (2020)

[47] Rovelli, C.: Halfway through the woods: Contemporary research on space and time. Studies in History and Philosophy of Modern Physics **28**, 249–267 (1997)

[48] Beau, J.: Bell-Inequality Violations from Non-Injective Projection. Cosmochrony companion paper B (2026). https://doi.org/10.5281/zenodo.18371173

[49] Battye, P.M., Sutcliffe, P.M.: Skyrmion solutions and baryon structure. Annual Review of Nuclear and Particle Science **72**, 1–26 (2022) https://doi.org/10.1146/annurev-nucl-111919-092432

[50] Manton, N.S., Sutcliffe, P.M.: Topological Solitons. Cambridge University Press, Cambridge (2004)

[51] Jarlskog, C.: Commutator of the quark mass matrices in the standard electroweak model and a measure of maximal cp violation. Physical Review Letters **55**(10), 1039–1042 (1985) https://doi.org/10.1103/PhysRevLett.55.1039